BERICHTE
aus dem Fachbereich Geowissenschaften
der Universität Bremen

No. 286

Kopf, A., M. Belke-Brea, G. Ferentinos, T. Fleischmann, M. Geraga,
S. Kufner, S. Schlenzek, A. Steiner, M. Tryon, G. Wiemer

REPORT AND PRELIMINARY RESULTS OF RV POSEIDON CRUISE P429. MEDFLUIDS: Slope Stability, Mud volcanism, Faulting and Fluid Flow in the Eastern Mediterranean Sea (Cretan Sea, Mediterranean Ridge) and Ligurian Margin (Nice slope), Heraklion / Greece, 22.03.2012 – La Seyne sur Mer / France, 06.04.2012.

Berichte, Fachbereich Geowissenschaften, Universität Bremen, No. 286, 80 pages,
Bremen 2012

ISSN 0931-0800

The "Berichte aus dem Fachbereich Geowissenschaften" are produced at irregular intervals by the Department of Geosciences, Bremen University and by MARUM.

They serve for the publication of cruise reports, PhD-theses, experimental works, and scientific contributions made by members of the department.

Reports can be ordered from:

Monika Bachur

DFG-Forschungszentrum MARUM

Universität Bremen

Postfach 330 440

D 28334 BREMEN

Phone: (49) 421 218-65516

Fax: (49) 421 218-65515

e-mail: MBachur@uni-bremen.de

Citation:
Kopf, A. and cruise participants
Report and preliminary results of RV POSEIDON Cruise P429. MEDFLUIDS: Slope Stability, Mud volcanism, Faulting and Fluid Flow in the Eastern Mediterranean Sea (Cretan Sea, Mediterranean Ridge) and Ligurian Margin (Nice slope), Heraklion / Greece, 22.03.2012 – La Seyne sur Mer / France, 06.04.2012.
Berichte, Fachbereich Geowissenschaften, Universität Bremen, No. 286, 80 pages. Bremen, 2012.

ISSN 0931-0800

Table of Contents

Personnel aboard R/V *Poseidon*

1.	Kopf, Achim	MARUM Univ. HB
2.	Belke-Brea, Maria	Univ. HB
3.	Ferentinos, Georgios	Univ. Patras, Greece
4.	Fleischmann, Timo	MARUM Univ. HB
5.	Geraga, Maria	Univ. Patras, Greece
6.	Kufner, Sofia	Univ. HB
7.	Schlenzek, Sebastian	Univ. HB
8.	Steiner, Alois	MARUM Univ. HB
9.	Tryon, Mike	SCRIPPS, USA
10.	Wiemer, Gauvain	MARUM Univ. HB

Participating institutions

DFG-Centre of Excellence MARUM
University Bremen
Leobener Strasse
28359 Bremen --- GERMANY

University of Bremen
Dept. of Geosciences
Klagenfurter Strasse
28359 Bremen --- GERMANY

SCRIPPS Institution of Oceanography
University of California, San Diego
9500 Gilman Drive
92093 La Jolla --- USA

University of Patras
Geology Department
26504 Patras --- GREECE

Abstract

The expedition P429 *MEDFLUIDS* is associated with three earlier RV *Poseidon* cruises, i.e. P336 in the Cretan Sea (Kopf et al., 2006), P386 in the Ligurian Sea (Kopf et al., 2009) and P410 on the Mediterranean Ridge accretionary complex (Kopf et al., 2012). The earlier work as well a steh P429 objectives have in common that they investigate complex geodynamic settings with rapid sedimentary processes (mud volcanism, landslides) and fluid flow processes (mud volcanoes, deep-seated faults, groundwater seeps). Objectives included:

- Study slope stability in the Cretan Sea north of Crete with complementary gravity coring and geotechnical in situ measurements;
- Recover long-term flowmeter instruments from mud volcanoes in the Hellenic Subduction Zone (deployed during cruise P410) and get additional samples and *in situ* data; and
- Recover an osmo-driven long-term insztrument and carry out additional sampling and in situ measurements at the Nice Airport landslide.

Among the methods utilised during *Poseidon* Leg P429 were multibeam site surveys to complement existing bathymetric charts, *in situ* measurements to characterise the natural state of the materials near the backstop, seafloor sampling, and recovery of long-term instruments to study sedimentological and geochemical phenomena.

In the Cretan Sea, off NW Crete, a profile from the Spatha Ridge shelf to an adjacent salt dome was studied. Geophysical data suggest slumping and sliding of sediment, partly as coherent blocks, takes place in an eastward direction. Gravity cores and CPTu measurements support this interpretation and attested that the slide plane material is water-rich.

In the landward Mediterrnean Ridge accretionary prism and its backstop, the Inner Ridge, all 5 flowmeters deployed 12 months ago during cruise P410 were successfully recovered. Additional *in situ* temperature measurements confirm the elevated gradients observed at Milano MV a year ago (exceeding 1000°C/km in places). By comparison, Napoli MV shows signifiantly lower values, indicating lesser activity at present. Further north, three gravity cores sampled material from the contact between Inner Ridge and Cretan margin. The lithologies show eveidence for grey (likely deep-seated) mud and intense sediment deformation. Mass wasting deposits are found regularly in those cores, spanning from debrites with angular clasts of various composition to turbidites.

Offshore Nice, gravity coring and CPTu deployments aimed at reconnaissance and recovery of whoel round core for laboratory experiments. Cores were not opened and described. An osmo-sampler in the 1979 landslide scar was recovered and equipped with new pumps and tubings for another year of operation. Scuba divers assisted the seafloor operations.

2. Introduction

Given the diversity in study areas, this chapter is separated into three sections, each being kept rather brief because of the referencing to our earlier cruises. In Sections 2.1 and 2.2, the Eastern Mediterranean Sea with the Hellenic Subduction Zone setting is introduced. It comprises the Cretan Sea where extensional faulting and uplift of Crete dominate the tectonic situation (Ch. 2.1.) as well as the incipient collission of Africa and Eurasia with the mature accretionary complex, Mediterranean Ridge, which is peppered with deep-seated mud volcanoes and faults (Ch. 2.2.). Chapter 2.3 introduces the Ligurian Margin landslides and research offshore Nice, Southern France.

3. Regional geology

3.1. Cretan Sea slope stability

In addition to seismogenesis along faults representing a severe geohazard (e.g. megathrust earthquakes, subsequent landslides and tsunamis), which is documented by the area around Greece as the one with the highest seismicity in Europe, subduction zones are the loci of very important mass balance processes. While the downgoing plate is dewatered and altered by increasing pressure (P) and temperature (T), other constituents may be desorbed from clay, released during diagenetic and metamorphic reactions and mineral transformations, or finally melted at greater depth. Even at shallow levels, significant transfer is taking place between the hydrosphere and lithosphere (often summarised as fluid-rock interaction as well as compaction-driven fluid release). At depth, partial melting, devolatilisation and associated processes may cause either ascent of the material towards the volcanic arc, recycling of the material in the mantle, or a combination of the two. As a consequence, this so-called big loop in the subduction factory involves the atmosphere (through volcanic degassing), lithosphere (through magma production at the colcanic arc and back-arc, as well as the asthenosphere (mantle recycling) into the mass transfer processes. The subduction zone hence provides an idiosyncratic chemical filter between surface and deep Earth reservoirs, which preferentially allows or disallows deep subduction of volatile and non-volatile components. Although there exist estimates regarding the masses and composition of downgoing materials (i.e. sediment, pore fluid, altered oceanic crust), the chemical fluxes resulting as a function of PT increase down the slab are poorly understood and rarely constrained quantitatively. In the vicinity of Crete, steep faults and extensional tectonics allow fluid migration and strain localisation, and may result in slope instability.

The evolution of the backstop setting near Crete was summarised by Thomson et al. (1998) and Robertson and Kopf (1998), and is revisited here only very briefly. After closure of the Mesozoic

Pindos Ocean to the north, sedimentary units underwent rapid subduction to approximately 35 km depth, followed by HP/LT metamorphism, and then exhumation (Thomson et al., 1998). After slab breakoff, buoyant sedimentary units underthrust the nappe pile of Crete along a shallow-dipping detachment fault, associated with tectonic uplift and formation of a forearc high which then acted as an initial 'rigid' backstop to sediment being offscraped from the Neotethyan seafloor. Plate kinematic reconstruction suggests trench "roll-back" and accretion of a wide accretionary prism at the leading edge of the Eurasian Plate, whilst the forearc of Crete underwent extensional deformation during the Neogene (e.g. Meier et al., 2007). This very forearc allowed accretion to be initiated some 19 Ma before present (Kopf et al., 2003a). At some stage during the Pliocene, the proto-MedRidge had undergone considerable dewatering, and this, in turn, acted as the second phase backstop ('deformable' backstop, c.f. the 'rigid', initial backstop of Cretan nappes) to the present-day accretionary prism. Accretion was possibly accentuated after the early Miocene, in conjunction with southward "roll-back" of the Aegean arc and regional back-arc extension (e.g. Kastens, 1991). In the late Miocene (Messinian), the deep Mediterranean was overlain by thick evaporites (e.g. Ryan et al., 1973), while topographic highs between Lybia and Crete apparently remained free of salt (Chaumillon and Mascle, 1997). From the Messinian to present, the MedRidge is being thrust over its Cretan backstop domain due to incipient continental collision (Figs. 1 and 2). In the process, Crete is extending in both N-S- and E-W-direction, and mass wasting and fluid flow occur along active normal faults, backthrusts and out-of-sequence-thrusts (OOSTs).

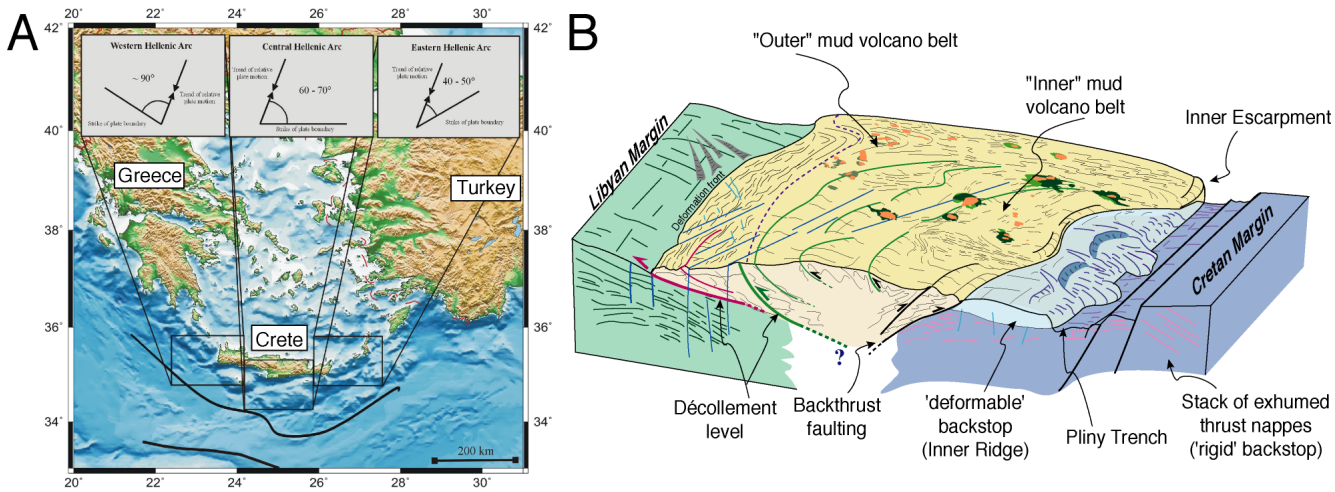

Figure 1: **a**) Location map showing the Hellenic subduction zone (HSZ) in the Eastern Mediterranean, including plate convergence vector and stress regimes along strike. **b**) Schematic block diagram of the MedRidge bordered by the Lybian margin in the south (left) and the Cretan Margin in the north (right). Green and orange pie-shaped features illustrate the occurrence of mud volcanoes. Note deep-seated faults beneath the prism and backstop.

The main features of a N-S traverse of the MedRidge and its backstop to the N are shown in Figure 1, from the North African passive margin, over a broad accretionary complex (ca. 100-120 km) and its backstop (ca. 80 km), across the forearc (Crete and adjacent islands), and the arc (e.g. Santorini), to the Aegean Sea back-arc basin. The MedRidge backstop domain is located 100-170 km behind the deformation front, and shows an increasing northward increase in the thickness of the overriding

forearc wedge/butress (4 - >7km bsf). From MCS data, the intensity of deformation and compaction increase considerably at the transition from prism (ca. 100 km) to the Inner Ridge (ca. 150 km) behind the deformation front. Further north in the continental Cretan backstop, reverse, out-of-sequence thrusting is observed.

When regarding the even deeper part of the HSZ, there has been growing evidence that the processes governing both "roll back" of the subduction system as well as uplift of the island of Crete are driven by sub-crustal dehydration (e.g. Meier et al., 2007). Based on recent geodetic, geophysical and structural data, the devolatising mantle wedge is believed to favour material transfer through the subduction channel up-dip along the plate boundary thrust (Fig. 2). This ascent of serpentinised peridotite/dunite or eclogite is likely responsible for the present-day uplift rates observed on Crete, which cause both N-S- and E-W-extension and hence decoupling of the landward forearc and the underlying downgoing slab, not dissimilar to that from the Mariana's forearc (see ODP Leg 195 drilling results; Shipboard Scientific Party 2002). Both seismological investigation and numerical simulation favour a model where return flow along a corridor of hydrated material atop of the subducting slab reaches crustal levels or even shallower (see Fig. 2, and Gerya et al., 2002; Meier et al., 2007). Along the subduction channel, partially hydrated oceanic lithosphere and trailing mantle wedge material have ascended along the wake of exhumed HP/LT units and account for both present-day uplift in the landward forearc and may have rendered extension in the Cretan Sea (north of Crete) ineffective. Given that recent work in that area has lacked any evidence for fluid expulsion or gas seepage (e.g. Chronis et al., 2000; Giresse et al., 2003; Kopf et al., 2006), one of the key questions is how certain areas around Crete accommodate for the significant deformation and dewatering and still behave non-catastrophic.

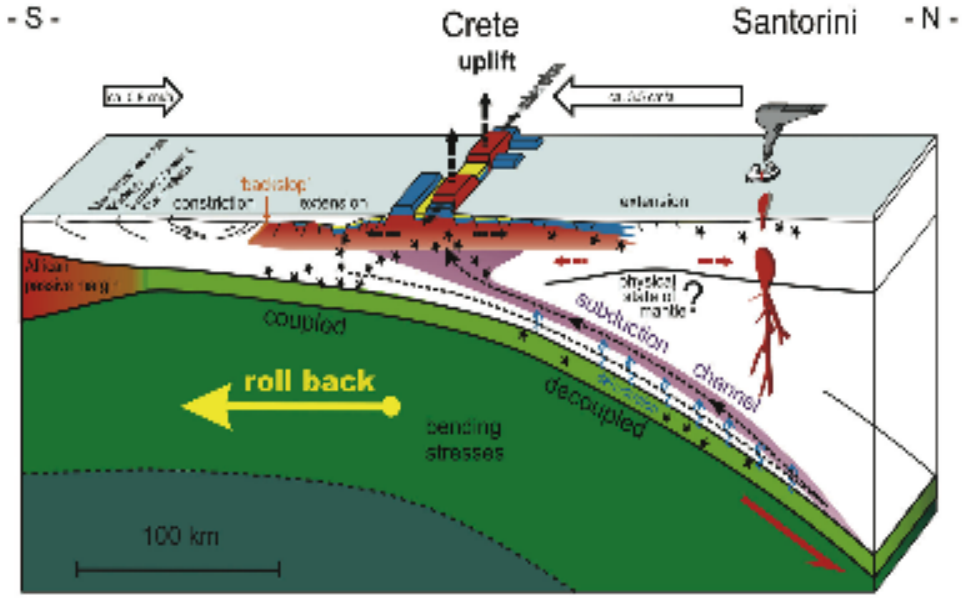

Figure 2: Schematic 3D drawing of the HSZ including the proposed pathway of hydrated mantle material, which accounts for the current uplift of Crete (see Meier et al., 2007 for details) and also which further favours migration of deep-seated fluids into the area of proposed drilling at the backstop.

Expedition P336 into the Cretan Sea gathered data from a number of landslide complexes with repeated Mass Transfer Deposits (MTDs), and used techniques such as multibeam mapping, seismic reflection, garvitry coring and geotechnical in situ measuremenst such as heat flow and cone penetration testing (Kopf et al., 2006). In the Malia basin, two submarine landslides with a total volume of approximately 4.6 km^3 and an area of about 135 km^2 show different geometry, internal deformations and transport structures (Strozyk et al., 2009). The older and stratigraphic lower MTD is interpreted as a debrite that fills a large part of the Malia Basin, while the second, younger MTD, with an age of at least 12.6 cal. ka B.P., indicates a thick, lens-shaped, partially translational landslide. This MTD comprises multiple slide masses with internal structure varying from highly deformed to nearly undeformed, suggesting a source area of the younger MTD in multiple headwalls at the slope-basin-transition in 450 m water depth. The possible triggers for slope failure and mass wasting include (i) seismicity and (ii) movement of the uplifting island of Crete from neotectonics of the Hellenic subduction zone, and (iii) slip of clay-mineral-rich or ash-bearing layers during fluid involvement (Strozyk et al., 2010).

Upon review of slope instability indications futher west, near the Spatha Ridge, evidence for landslides is scarce. The western end of the Outer Hellenic Arc extends over a length of about 150km from the southern tip of Peloponessos to western Crete (Fig. 3). In the Peloponissos the configuration of the shelf and slope is controlled by NW-SE and NNW-SSE trending active normal faults, whilst in western Crete the configuration is controlled by N-S and NNE-SSW sinistral oblique-normal and steep dipping faults (Kokkalas et al., 2006, Ferentinos et al., in press) (Fig. 3c). The former set is responsible for the formation of the NNW trending Messinian, Laconian and Argolikos Gulfs and Maleas-Kythera ridge in the southern Peloponessos, and the latter set is responsible for the formation of N-S trending basins and ridges: the Granvousa basin, Gramvousa Ridge, Kissanos basin, and Spatha Ridge in Crete (Ferentinos et al accepted for publication). The faulting activity started during the late Miocene and has been active since then. The area is characterised by high seismicity (McKenzie 1972, Papazachos and Papazachou 1977), which causes many and large submarine landslides (Ferentinos 1992, Ferentinos et al., in press).

The detailed study area is located in the offshore extension of the Spatha Peninsula, which extends northwards as a submarine ridge for about 20km. (Ferentinos and Papatheodorou 1989) (Fig. 1c) The Spatha ridge has a length of about 15km and a width of about 5km. The eastern and western flanks of the ridge are fault controlled. The faults trend in a N-S and NE-SW direction (Ferentinos and Papatheodorou 1989) (Fig. 1c). The ridge is characterised by a narrow shelf. The shelf has a width of about 2km and dips northwards at a gradient of about 2^o. The shelf break is at the 120m 1sobath. The slope extends from the 120m isobath to the 800m isobath with an average of about 5^o. The slope at a depth of about 450m is crossed by an elongated ridge structure trending in a WNW-ESE direction

(Ferentinos and Papatheodorou 1989). The ridge has a height of about 180m from the surrounding floor. The study of the seismic profiles has shown that the seafloor in the Spatha Ridge is affected by variety of sediment instability features and processes associated with sliding, slumping, creep and intra-stratal (Ferentinos and Papatheodorou 1989) (Fig. 4).

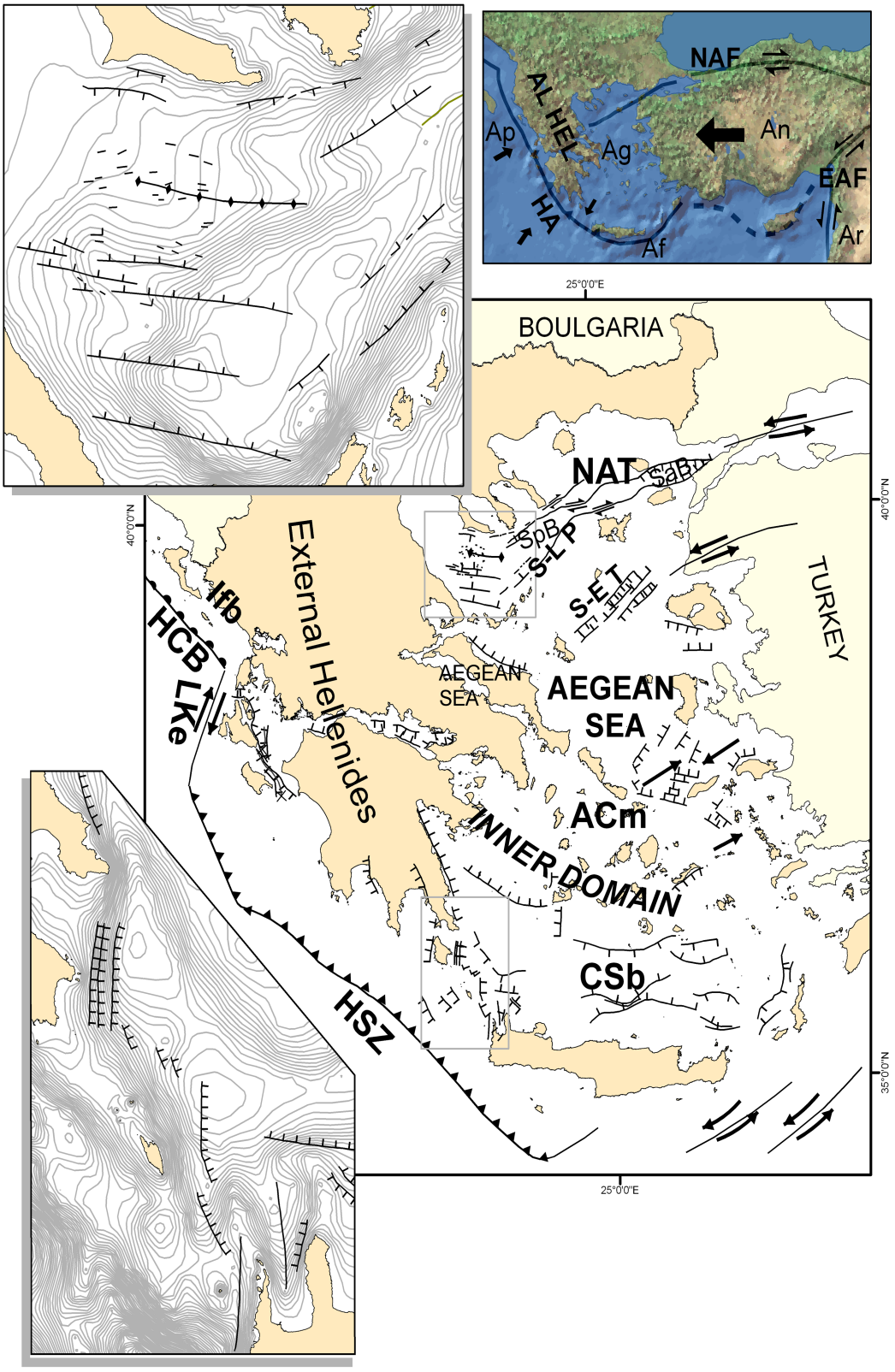

Figure 3: Map showing the major tectonic features of the Hellenic Arc System and the active Quaternary faults. The studied area is shown in the bottom inset. (from Ferentinos et al., in press).

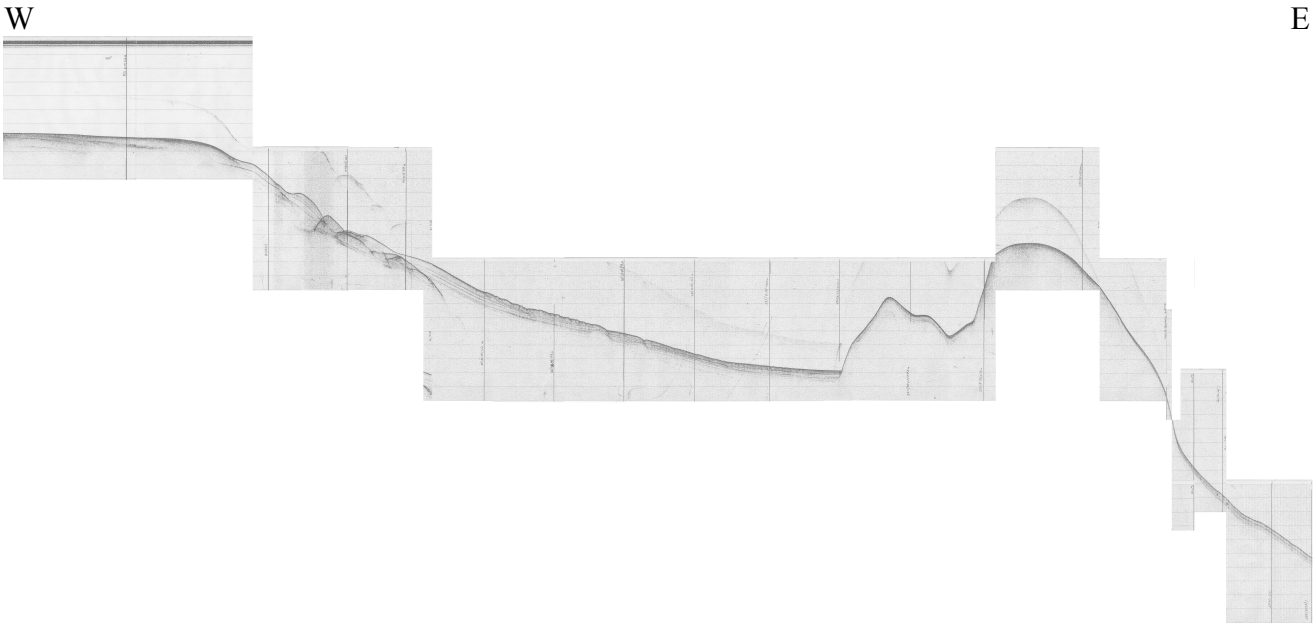

Figure 4: Main seismic profile (3.5 kHz) trending W-E from the shelf of the Spatha Peninsula towards the Spatha Ridge further E. Note slumped and slid material on the western slope as well as updoming underneath the ridge in the E.

3.2. Mediterranean Ridge mud volcanism, faulting and fluid flow

Approximately half of the sediment currently overlying the Earth's oceanic crust is traveling towards active convergent margins, part of which enters the subduction zone, is underthrust and eventually gets involved in diagenetic, metamorphic, and magma generation processes. Sediment has been shown to re-emerge in arc volcanoes based on typical geochemical signatures such as Be isotope values or depletion of high field strength elements (HFSE) relative to light rare earth elements (LREE) and large ion lithophile elements (LILE) at the volcanic arc (e.g. Tera et al., 1986; Morris et al., 1990; Brenan et al., 1995; Plank and Langmuir, 1998; Elliot et al., 1997). Afterwards, part of the sediment residue continues to sink into the mantle and becomes one of the potential sources of mantle plumes and/or heterogeneities (e.g., Kogiso et al., 1997; Kamber and Collerson, 2000). Despite the improvements of geophysical investigation techniques and numerous DSDP and ODP expeditions, there is a clear lack of understanding of the physico-chemical processes attendant to the subduction of sediment. This is particularly true for the mechanical processes controlling the the location and frictional behaviour of the plate boundary fault, but also regarding processes of fluid-rock interaction, mineral transformation, and devolatilisation that affect chemical cycling as well as effective strength of these materials (e.g. Dia et al., 1995; Johnson & Plank, 1999; Bebout et al., 1999). In the so-called subduction factory, there is a fundamental difference between the inputs (i.e. incoming sediment and crust as well as material from frontal and basal subduction erosion) and outputs, most importantly accretion, underplating, fluid release, and arc and back-arc magmatism (Fig. 5). In this proposal, we suggest to regard mostly the fault-driven fluid release originating from the frontal and intermediate loop (Fig. 5), which will be quantified *in situ* using CAT fluxmeter systems (Tryon et al., 2001). Five

of those systems were placed in key location in the northern part of the MedRidge during expedition P410 (Kopf et al., 2012) and are to be recovered during the cruise proposed here. The locations chosen were either surface outcrops of deep-seated faults or mud volcanoes believed to be actively emitting fuids from depth.

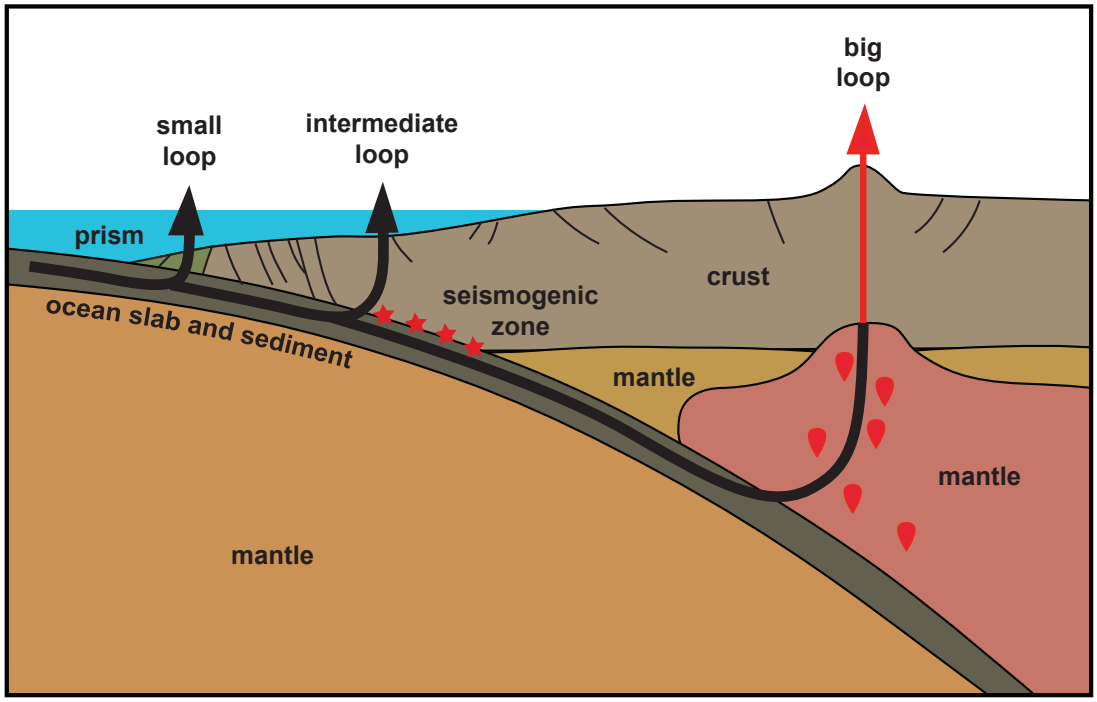

Figure 5: Schematic diagram of subduction zone devolitilisation in the frontal (short loop) as well as landward part of the forearc (intermediate loop) as well as the volcanic arc (big loop).

Physico-chemical processes and hydrology driving fault strength

The interaction between solid sediment particles and trapped pore water has profound physical and chemical repercussions and starts immediately after deposition on the seafloor. Consolidation may only occur if the fluid pressure from the pores can dissipate; otherwise pore pressures build up and counteract cohesion and reduce the mechanical strength of the sediment. This has first been described by Hubbert & Rubey (1959) and ever since has been a matter of controversial debate (see e.g. Byerlee [1978] vs. Rice [1992]). In addition to the physical properties, chemistry of the solids and fluids is also affected after deposition (in particular the ad-/desorption processes on clay minerals). Both mechanical pore space reduction and diagenetic reactions cause a decrease in permeability. Processes active include clay mineral dehydration, alteration of biogenic opal, zeolite formation, dissolution of metastable mineral phases, to name just a few (see summary in Moore & Saffer, 2001). Such diagenetic to low-grade metamorphic processes may mobilise major (such as K, Na, Ca, Mg, Fe, S, and Si) and minor components (e.g. Cl, Ba, B, Sr, Cs, Li, Rb) as well as many other trace elements as a result of dissolution and mineral transformation processes (see summary in Guangzhi, 1996). The resulting supersaturated pore fluids may cause precipitation and hence significantly modify the fabric (Kawamura & Ogawa, 2004) as well as the strength and permeability of the sediment (Bjorlykke &

Hoeg, 1997; Dewhurst et al., 1999), its mineralogy, and chemical composition of the pore fluid residue.

Mud volcanism, fluid budgets and geochemical cycling

Mud volcanism has been demonstrated to be a global phenomenon, which is commonly associated with compressional tectonics and sediment accretion at convergent margins (see review by Kopf, 2002). Mud domes and diapirs frequently occur in marine subduction zones at the plate boundary near the toe of accretionary prisms (Henry et al., 1996), further landward in the forearc (Mascle et al., 1999), but also on land where collisional processes and deformation are more accentuated (Lavrushin et al., 1996). Irrespective of the tectonic compression, the main driving force of mud extrusion is the negative buoyancy of the clay-rich material at depth. Fluids may either be trapped as a result of high sedimentation rates or lateral influx into clay-bearing sediments, or may be generated *in situ* owing to processes such as mineral dehydration reactions and hydrocarbon generation at greater depth (e.g. Hedberg, 1974). Quiescent as well as catastrophic emission of greenhouse gases (mostly methane) accompanies extrusion and may contribute significantly to climate change (Higgins & Saunders, 1974; Kopf, 2002).

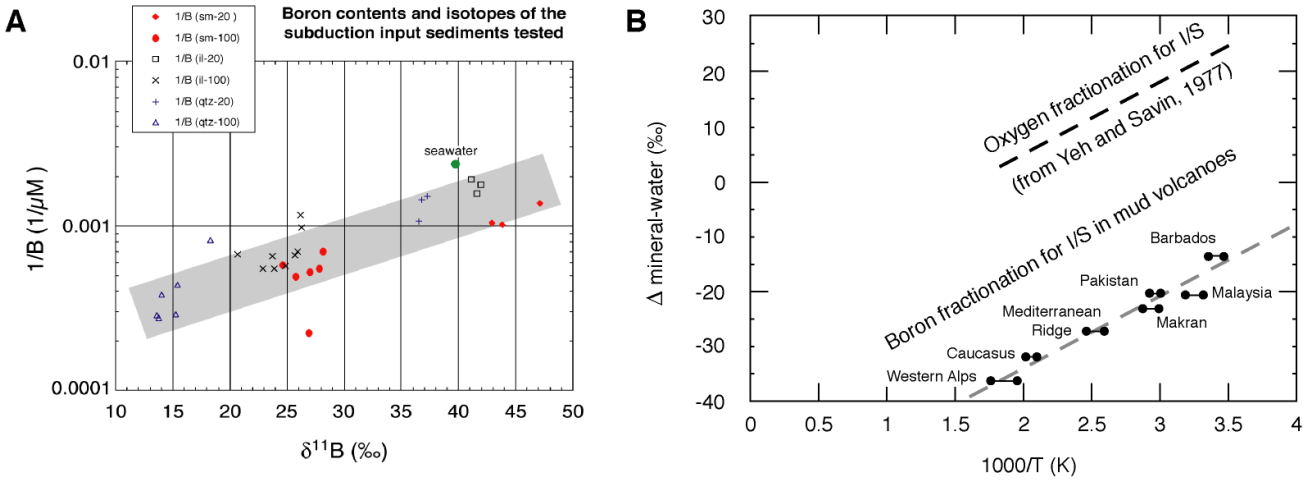

Figure 6: **a**) Results from B analysis on fluids and solid particles from hydrothermal deformation tests of smectite (sm)-, illite (il)- and quartz (qtz)-rich endmember sediments off Japan (from Kopf et al., 2002); b) Data compilation from MV study using B fractionation and paleo-T to estimate the depth of mud- and fluid mobilisation (from Kopf & Deyhle, 2002).

The Mediterranean Ridge is one of the areas where mud volcanism is most common globally (e.g. Kopf et al., 1998a, 2001), with estimated dewatering rates exceeding that at the frontal toe of the prism. Together with the enigmatic fluid chemistry of such fluids (Deyhle & Kopf, 2001; Dählmann & De Lange, 2003), this attests a profound influence on geochemical cycling and fluid budgets in subduction zones (Kopf et al., 2001). Ascent of the mud may be rather rapid in the MedRidge area (Kopf & Behrmann, 2000), and hence allows the preservation of chemical (and biological) signatures over time. Extrusive activity has been shown to be episodic from ODP Leg 160 drilling (Emeis et al., 1996), and may be coupled to deep-seated processes (e.g. seismicity in the HSZ, realease of brines

from Messinian formations containing evaporites, etc.), as was confirmed during cruise P410 (Kopf et al., 2012).

When returning to the subduction factory cycles (Fig. 5), mud volcanism and deep-seated faults may help illuminate the intermediate loop. Numerous authors have used the mobile element Boron and its stable isotope ratio ($\delta^{11}B$) to illuminate processes in the moderate T window of subduction zones (Spivack et al., 1987; You et al., 1993, 1996; Kopf et al., 2000; Deyhle & Kopf, 2001, 2002). These studies on natural samples and from hydrothermal experiments suggest that B is a powerful proxy with a wide variety of $\delta^{11}B$ values for different subduction inputs and related diagenetic reactions. Examples of the proponent's evolvement in these studies are given in Figure 6 and have been wrapped up in various publications (oral and as manuscripts; see Kopf & Deyhle, 2002; Deyhle & Kopf, 2001, 2002, 2005). The work attested that there are well-defined trends for B processes in selected silica systems such as clay-dominated ones (Kopf & Deyhle, 2002), but not in all of them (Deyhle & Kopf, 2005).

3.3. The Nice Airport landslide

The Ligurian Margin in the Western Mediterranean Sea has a number of similarities to the HSZ, Eastern Mediterranean Sea. It is located in a complex tectonic setting with collisional processes such as the Alpine orogeny and formation of the Appenines, and an Upper Oligocene-Miocene drifting-rifting episode behind the Apulian subduction zone (Rehault et al., 1984; Burrus et al. 1987; Rollet et al; 2002). During the late Miocene (Messinian), evaporation resulted in erosion surfaces cutting into the margin. In the central portion of the modern Ligurian basin, the sediment fill reaches 5-8 km at water depths around 2500 m. The Quaternary uplift of the Alps and associated erosion supply large volumes of sediment. The Var Canyon system represents the offshore extension of the Var River, one of the major rivers entering the Ligurian Basin west of Nice.

Figure 7: Location and transport pathway of the Nice Airport Landslide (NAIL) on Oct 16, 1979. a) The trace and velocity of the mobilised material running down the Nice Slope southward into the Var Canyon, and then redirected towards the West and then South again (data from Dan, 2007). Panels (b) and (c) are newspaper clipping from the Nice Matin the day after the event, illustrating the damage to the airport , here inspected by airport police (b) and the effect the tsunami had in the village of Antibes (c). In the course of detailed mapping of the seafloor in 1986, ROV dives discovered blocks having originated from the fill used for the failed harbor construction that got transported to the deeper part of the slope (d). Positions for panels b through d is given in Fig. a.

The Ligurian margin has a very narrow (or absent) continental shelf of ~2-3km width and a steep continental slope with a mean gradient of ca. 11° (Cochonat et al., 1993). From the 1960s onwards, land gaining activities caused the shoreline to migrate southward, and large volumes of fill were loaded onto the already rapidly deposited sediments of the Var delta (e.g. Dan, 2007). In fall 1979, construction of an embankment south of Nice Airport put additional point loads onto these deposits, and after a period of heavy rain the embankment collapsed and a major landslide caused damage to the airport, destroyed the new construction as well as part of the narrowe shelf, and initiated a 2-3 m high tsunami with several casualties and significant damage to the coast of Antibes and adjacent regions (Gennesseaux et al., 1980; Assier-Rzadkiewicz et al., 2000) (Fig. 7).

The exact cause(s) of the 1979 catastrophe are still controversely debated, however, the Nice Slope represents one of the few examples on the planet where a suite of different mechanisms that govern slope stability can be studied in an affordable manner (because of the shallow water locality of appx. 30 mbsl). These include, in order of assumed importance:

1. rapid sediment deposition in the Var delta deposits,
2. hydraulic communication between the Var river bed and submarine strata through (presumed) Pliocene substratum and permeable Holocene sand/gravel. The Var river discharge and aquifers charging are cyclic with maxima in November (rainfall) and April-May (rain fall and snowmelt),
3. gently dipping layers of weak sensitive clay, presumably influenced by fluids of reduced salinity migrating in interbedded sand and gravel,
4. seismicity owing to tectonic activity in the Western Alps and the marine realm,

additional vertical loading from human land reclaim (e.g. Nice airport peninsula) or construction (harbour embankment) a few decades ago.

During two cruises led by the proponent (M73 and Pos386; Kopf et al., 2008, 2009) plus two cruises with Bremen participants on expeditions organised by French colleagues at IFREMER in 2007 (Prisme) and 2011 (STEP), a large data set exists already (e.g. Sultan et al. 2008). Those data attest that the 1979 Nice Airport landslide most likely resulted from a combination of rapid sediment loading owing to construction plus groundwater flux in the material underlying the airport, which was pronounced after a period of heavy rain in October 1979 (e.g. Dan, 2007). In order to assess the current risk of slope failure, a comprehensive monitoring programme is underway. Measurements include coring, heat flow, CPTu (cone penetration testing with pore pressure) and geochemical sampling during the cruises and scuba dives, but also long-term measurements with piezoprobes, osmosamplers and strainmeters (Stegmann et al., 2012).

The latter approach of a combined array of probes that tap into the shallow (5-8 mbsf) sub-seafloor is promising given that the former Holocene delta sediments are highly inhomogeneous and show muddy laminates being interbedded with sand or gravel beds. The resulting contrasts in hydraulic properties of those sediments make the Nice slope an ideal natural laboratory for sloep stability research. Consequently, long-term instruments need maintenance in order to function reliably and provide the basis for a more comprehensive understanding of the governing factors. One of the main goals of cruise P429 was hence to replace parts of the osmo-sampling lance in the 1979 landslide failre scar where fresh water was seen occasionally (Kopf et al., 2010, and Fig. 8).

A

B

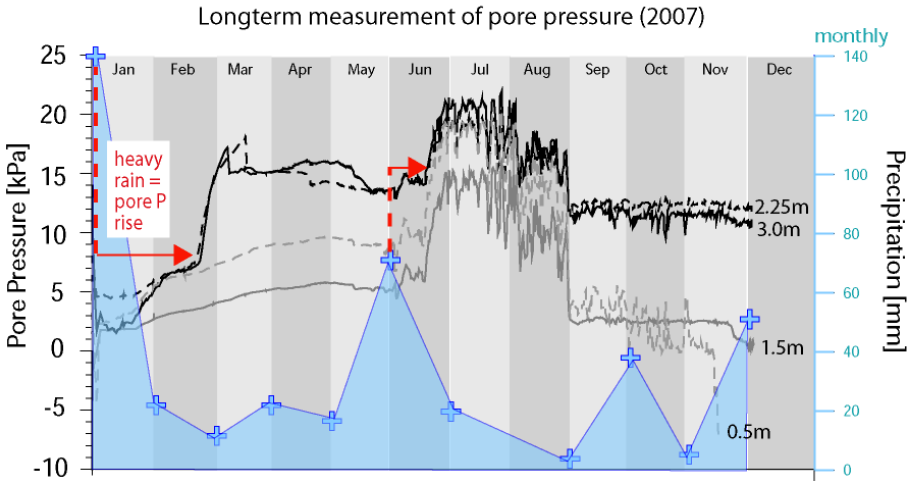

Figure 8: a) Satellite view and projected bathymetric map (IFREMER) around the Var estuary/Nice international airport (from Kopf et al., 2010). The star marks the location of the long-term piezometer v1; b) Long-term piezometer data covering the period from Nov 2006 – Nov 2007, showing distinct (but delayed) changes in pore pressure as a function of precipitation (after Stegmann et al., 2011, 2012). Such changes may also be recorded in the fluid sample's salinity from the osmo-lance to be recovered during cruise P429 with RV *Poseidon*.

4. Narrative of the cruise

(A. Kopf)

Given the different research goals and the distance between the regional targets in the Eastern and Western Mediterranean, cruise P429 had almost as much transit days as it had days for research work. The vessel headed out from Heraklion, Greece on 22 March 2012 and and dedicated the first couple of days to the Spatha Ridge area, northwestern Crete. Owing to severe engine problems and a small storm, only 2 working days with multibeam mapping, gravity coring and SW CPTu deployments were possible until the area was left on 27 March.

RV Poseidon surrounded the island of Crete in clockwise direction and a technician and three scientists left the ship near Plakias at the southern coast (28 March 2012). Submarine trials by the Greek navy disabled any further research south of Crete until 29 March, when we started to run multibeam again on the Mediterranean Ridge. Work there also included heat flow measurements in two mud volcanoes, DW-CPTu deployments, recovery of CAT flowmeter systems (deployed during expedition P410 a year ealier) and gravity coring at the border between the Inner Ridge and Cretan margin.

On 30 March 2012 in the late afternoon, the transit towards the Western mediterranean Sea was started. We went through the Messina Strait in the morning of 2 April, passed Mt. Stromboli during the day, and arrived in the research area south of Nice on 4 April 2012 in the evening.

Work there included SW-CPTu deployments, gravity coring and the exchange of once scientist with two journalists. We also collaborated with TLO, the scuba diving company in Nice, who assisted with the attempted recovery and re-deployment of an osmo-sampling unit in one of the long-term probes situated in the 1979 landslide scar south of Nice international airport.

The ship was returned in La Seyne sur Mer on 6 April 2012 at 10:00.

5. Methods

5.1. Seafloor surveys

(S. Kufner)

During cruise P429, a site survey was carried out in Area 1 (Cretan Sea) as well as Area 2 (Mediterranean Ridge). For this purpose, the multibeam sonar system *Multibeam 3050* from *L-3 Communications ELAC Nautik* (1) was used. This system has been installed on RV *Poseidon* in October 2010 and was still in the testing phase.

To determine the structure and depth of the sea floor, a short pulse of sound (ping) is generated by a projector. The created signal travels as compressional wave through the water. The local speed of sound depends on salinity, pressure and temperature. As the wave front is interrupted by the sea bottom, a certain factor of the energy is reflected. This reflected signal (echo) has the same frequency than the source wave and is recorded by hydrophones which measure the oscillations in pressure as the pressure front of a sound wave passes. Knowing the travel time and the speed of the sound in water the depth of the sea bottom can be calculated.

A multibeam sonar allows to map more than one location of the sea floor with one single ping. The bottom locations are arranged to map a contiguous strip perpendicular to the path of the survey vessel. The dimension of this stripe is the swath width. The advantage of a multibeam system in comparison to a singlebeam system is a higher survey speed.

In order to determine the exact position of the echoes occurring along the ship, the projector and hydrophone array are installed perpendicular to each other (Mills cross arrangement). Using this arrangement, the area of the ocean floor ensonified by the projectors intersects with the area observed by the hydrophones only in a small area. The dimensions of this area correspond approximately to the projector and hydrophone array beam widths. The range of the instrument is limited by the amount of attenuation and by the noise level. Errors that would occur due to yaw and pitch motion of the vessel are fully compensated by a transmit technique of the *Seabeam 3050* by splitting the transmitted fan in several sections which can be steered individually.

The *Multibeam SB 3050* system on *Poseidon* is designed to operate in depths from 3 m to approximately 3000 m. The operating frequency is in the 50 kHz band. Maximum ping rate is 50 swaths per second and the maximum number of beams is 315. The maximum across-ship swath coverage sector is 140 degrees.

The hardware components of the *Seabeam 3050* system include a motion sensor, a positioning system, a sound velocity profiler and a surface sound velocity sensor. An operating computer receives the preprocessed data stream. Bathymetric data can be visualised in real time using the *Hypack* (2) mapping tool. A schematic diagram of these different components can be seen in Figure 9.

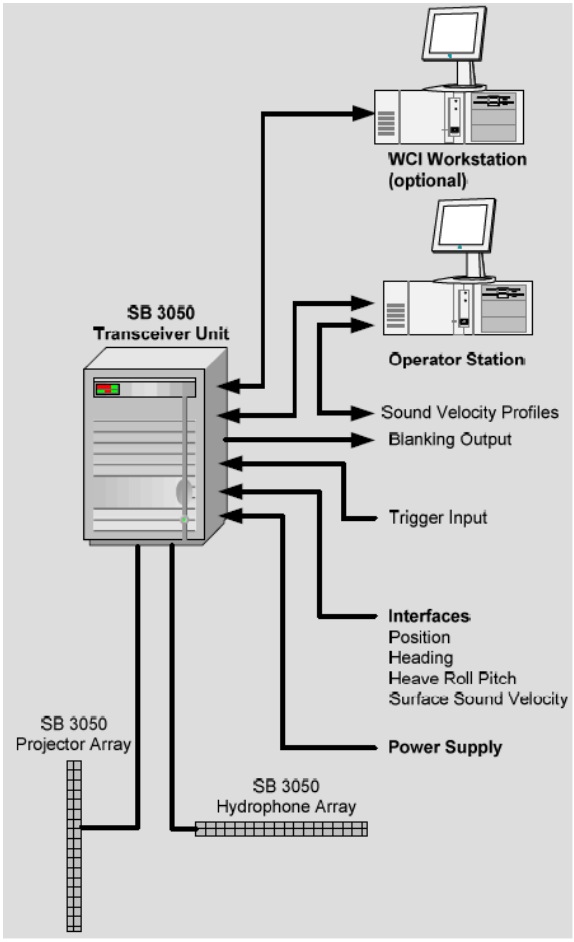

Figure 9: Layout of the Multibeam system recently installed on RV *Poseidon*. See text.

5.2. *In situ* temperature measurements

(M. Tryon, T. Fleischmann)

On cruise P429 the *in situ* temperature gradients were measured with miniaturised autonomous Miniature Temperature Loggers (MTLs, Fig. 10a). For technical specifications and detailed information, refer to Pfender & Villinger (2002).

Parameters of autonomous temperature data loggers:

Instruments serial no.:	sediment and water temp. logger: 18543-65C, -67C, -68C, -70C, -75C, -77C, -78C, -79C
Sample rate:	1 sec
Spacing:	usually 1 m, 2 m, 3m, etc. below the weight set; sometimes variable spacing depending on length of gravity corer; one water temperature sensor at weight set with sensor tip looking up.

Measurements (seafloor penetration) were realised by mounting the MTLs to gravity core barrel using fins and receptacles and get gradient at the chosen spacing as well as reference temperature in the

water column. The probe remains in the seafloor sediment for several minutes to allow for some dissipation of artificial frictional heat from inserting the gravity corer.

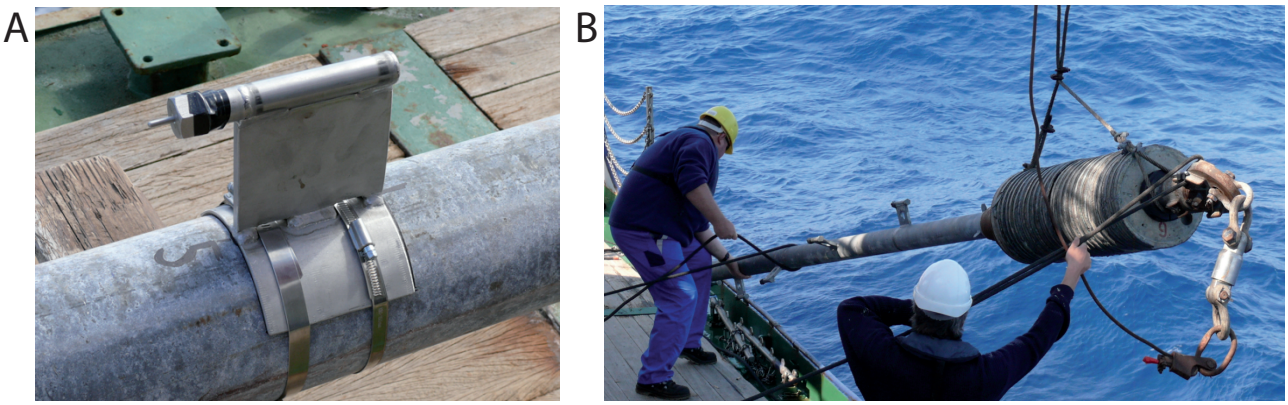

Figure 10: a) MTL prior to deployment of the gravity corer on cruise P429. The pointy end with the thermistor is facing downward. b) MARUM T-probe with outriggers for placing MTLs. See text.

Using the exact same principle, a 5-m long rod with a sharp pointy tip (opening angle appx 40°) was developed at MARUM Bremen recently. The upper end of the rod has the same geometry as a gravity core barrel, so that the weight set can be used to drive the T-probe into the sediment (Fig. 10b). Deployment is pogo-style.

5.3. *In situ* CPT testing

(A. Steiner, G. Wiemer, A. Kopf)

On R/V *Poseidon* cruise P429, we used the MARUM free-fall CPTu probes (see Stegmann et al., 2006, 2007). Cone Penetration Testing (CPT) is an effective method for *in situ* measurements of these geotechnical parameters with one instrument (Lunne et al., 1997), namely sedimentary strength (tip resistance, sleeve friction), pore pressure, tilt and acceleration. For these measurements, the CPT system relies on 15 cm^2 cone and pore pressure (u1, u2 and u3 positions depending on instrument and configuration; see below) and a pressure housing containing a all other sensors and the microprocessor at the top. In addition, deceleration and tilt are monitored for vertical profiling of the penetrated sediment column.

SW CPTU Instrument

The lightweight FF-CPTu instrument for shallow marine use consists of an industrial 15 cm2 piezocone and a pressure-tight housing containing a microprocessor, standard secure digital memory card (SD), battery package and accelerometer (see Fig. 11, top; and Stegmann et al., 2006). Strain gauges inside of the FF-CPTu probe measure the total cone resistance and sleeve friction by subtraction. A single pore pressure port (u2) is equipped with absolute 1 MPa (CPTu-25), 2 MPa (CPTu-100) or 5 MPa pressure sensors. An inclinometer is installed to monitor the penetration angle

at +/-20° relative to vertical. Five different accelerometers with different ranges (+/- 1.7g, +/- 18g, +/- 35g, +/- 50g and +/- 120g) provide information about the descent deceleration behaviour of the FF-CPTu instrument upon penetration. These data allow the researcher to calculate penetration velocity and depth during multiple deployments by 1st and 2nd integration. The aluminium pressuretight housing tolerates a minimum 5 MPa confining pressure (approx. 500 m water depth) and hosts the power supply and microprocessor (Fig. 11, bottom). The frequency of data acquisition is variable and depends on the operation purpose of the FF-CPTu instrument (e.g. sub-seafloor profiling or pore pressure dissipation). Binary data are temporarily stored on a standard secure digital memory card (SD) and then downloaded to a personal computer (PC). The three non-volatile battery packs available provide performance times of about twelve and twenty-four hours, respectively.

The length of the FF-CPTu instrument is variable from 0.5 m to a maximum length of 6.5 m depending on what type of sediment is anticipated. The extension is accomplished by adding 1.0 m long metal rods and internal extension data/power cables within them. Hence, the weight of the FFCPTu instrument ranges from approx. 40 kg to max. 110 kg. If deep penetration is desired, modular weight pieces (15 kg each) can be mounted to the pressure-tight housing at the top, then reaching a max. 170 kg. The FF-CPTu instrument is deployed as individual measurement or pogo-style and remains in the sub-seafloor for appx. 15 minutes.

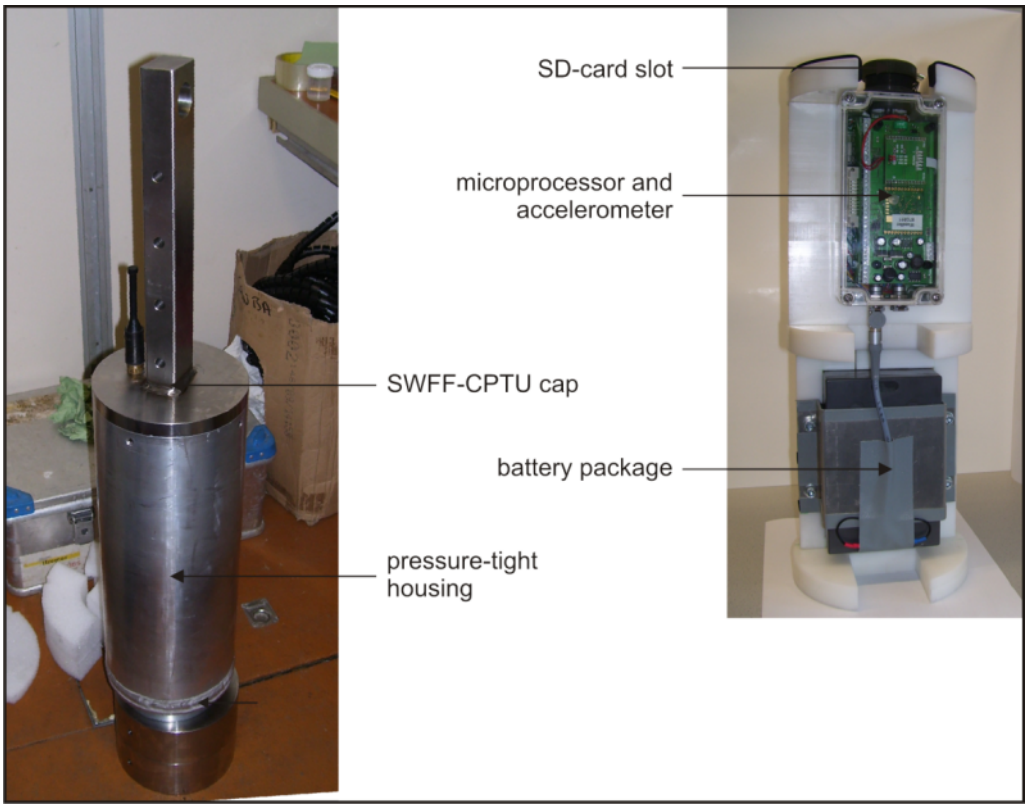

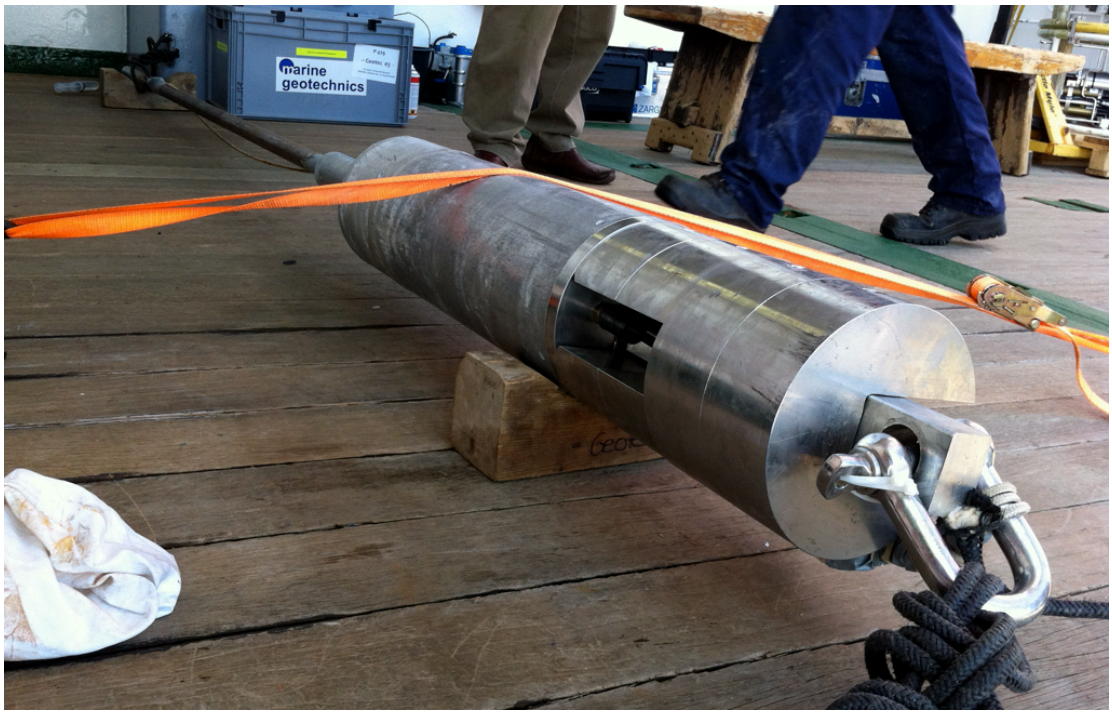

Figure 11: (a) Pressure-tight housing with cap and SWFF-CPTU electronic module; (b) SW-CPTu instrument on deck of RV Poseidon prior to deployment on cruise P429.

DW CPTU Instrument

The free-fall CPT (FF-CPT) instrument for deep (up to 4000 m water depth) marine use consists of a 15 cm^2 piezocone and a water-proof housing containing a microprocessor, volatile memory, battery, and accelerometer (see Fig. 12a; and Stegmann and Kopf, 2007 for details). Two pore pressure port (u_1 and u_3) are equipped with differential pressure transducers. The stainless steel pressure-tight housing containing a microprocessor, standard secure digital memory card (SD), tiltmeter, accelerometer, power supply (battery packages), absolute and differential pore-water sensors as well as power and data interface module (PDIM). The tiltmeter (dual-axis tilt sensor) monitors the penetration angle at +/- 45° relative to vertical. Five different accelerometers with different ranges (+/- 1.7g, +/- 18g, +/- 35g, +/- 70g and +/- 120g) provide information about the descent de/acceleration behaviour of the DWFF-CPTU instrument upon penetration. These data allow the researcher to calculate penetration velocity and depth during multiple deployments by 1st and 2nd integration.

The reference pore-water pressure port at the pressure-tight housing is equipped with an absolute 40.0 MPa (400 bar) pressure sensors (WIKA ECO-1). The pore-water pressure ports at the tip (u_1) and 0.75 m behind the tip (u_3) are connected to the differential pore-water pressure transducers (VALIDYNE P55D) via stainless steel tubing. Pore-water pressure changes can be monitored over a range of 85 kPa (12.5 PSI) to 100-140 kPa (15 - 20 PSI) with a resolution between 8 and 15 Pa (Fig. 12b). The sensors are protected with valves if high excess pore-water pressures are met (e.g. owing to blocked hydraulic tubes). They are further used to bleed the tubing in case of gas is trapped inside,

especially during the initial phase of deployment when the instrument is lowered through the water column.

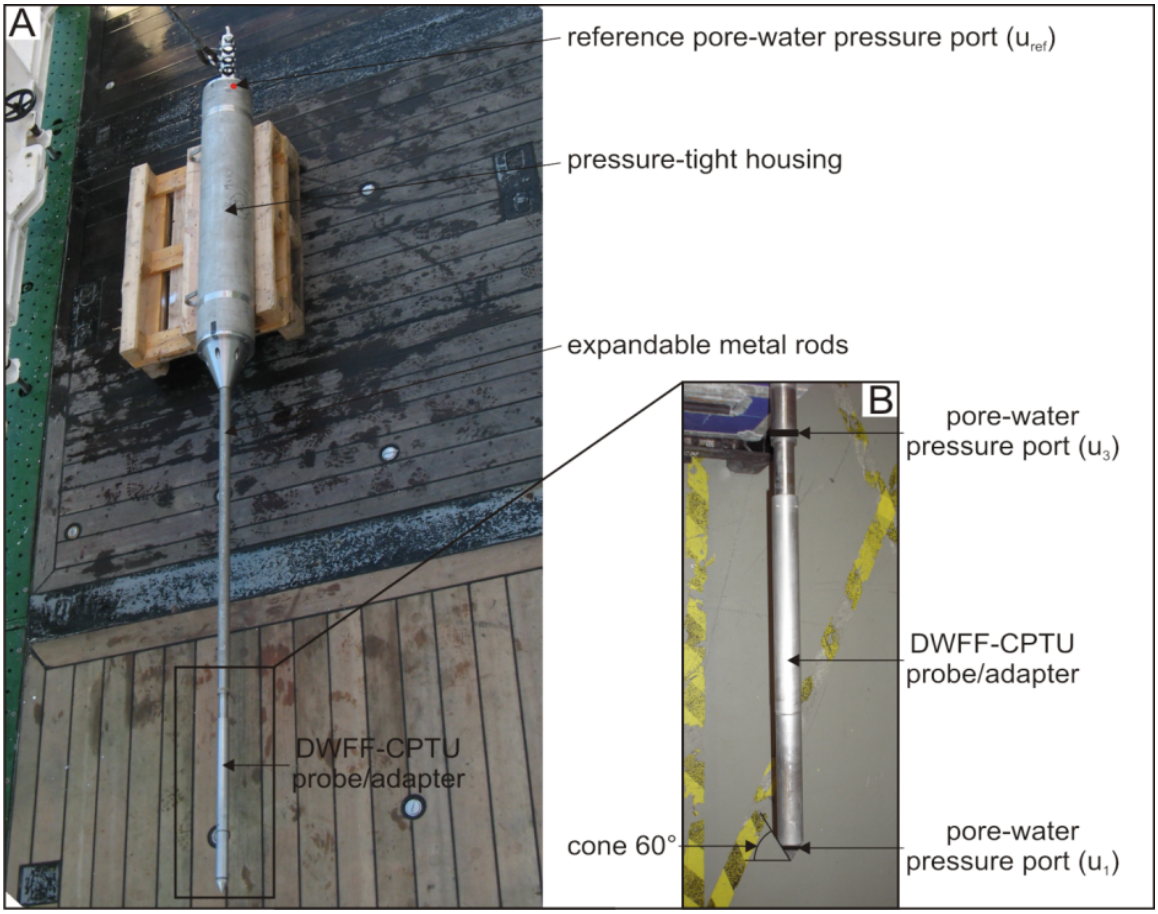

Figure 12: Deep-water FF-CPTu instrument (a). Panel (b) shows blow up of the frontal portion with the pore pressure ports.

The DWFF-CPTu instrument is used in an autonomous mode, at which all sensor and transducer information will be stored on a standard secure digital memory card (SD) with a very high sampling frequency (1 kHz). In addition, a data transmission telemetry system (Seabird Electronics SBE36 CTD) is used to monitor all sensor and transducer parameter on board the research vessel in real-time (lower sampling frequency 1 Hz). The telemetry system consists of a deck unit (SBE36 CTD) and a PDIM. A schematically sketch of the telemetry system is shown in Figure 13. It provides real-time data acquisition and control of the instrument (e.g. operation of the valves) via an attached personal computer (PC) using a self-developed LABVIEW control software.

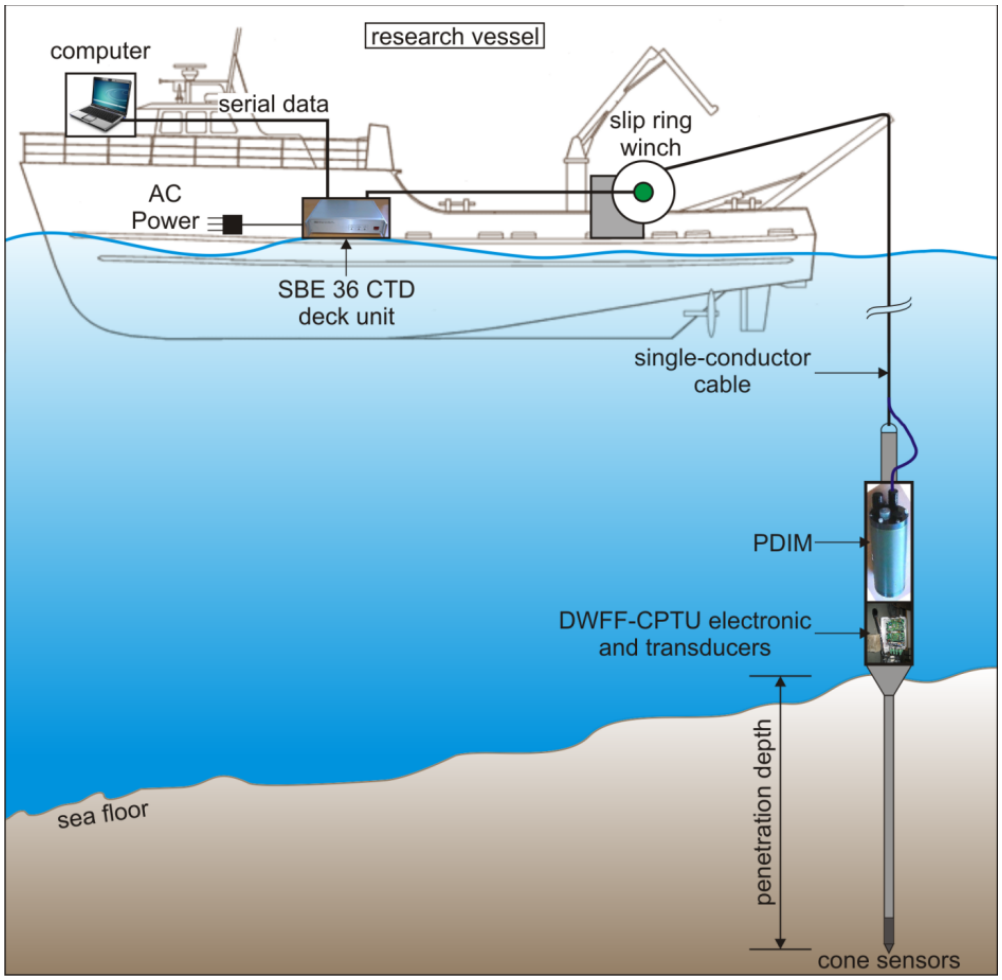

Figure 13: Schematic of SBE36 CTD and PDIM telemetry system.

The frequency of data acquisition is variable and depends on the operation purpose of the DWFF-CPTU instrument (e.g. sub-seafloor profiling or pore-water pressure dissipation). Binary data are temporarily stored on a standard secure digital memory card (SD) and then downloaded via W-LAN to a PC. The two non-volatile battery packs available provide performance times of about eight to twelve hours, respectively. A self-developed deck interface box is used to download the recorded data and to charge the battery packs.

The length of the DWFF-CPTU instrument is variable from 4.1 m to a maximum length of 6.8 m depending on what type of sediment is anticipated. The extension is accomplished by adding 1.4 m long metal rods and internal extension data/power cables as well as steel tubing within them. Hence, the weight of the DWFF-CPTU instrument ranges from approx. 500 kg to max. 550 kg. The DWFF-CPTU instrument is deployed as individual measurement or pogo-style and remains in the sub-seafloor for about 15 minutes.

The DWFF-CPTU instrument was used with a self-developed piezocone probe/adapter (Fig. 12b) equipped with pore-water pressure ports at two locations (at the tip - Δu_1 and 0.75 m behind the tip - Δu_3). During RV *Poseidon* cruise P429, the DWFF-CPTU instrument was generally deployed in 4.1 m long mode (CPTU probe/adapter + 1 rod + pressure-tight housing).

A 1 kHz microprocessor data recording unit (AVISARO microcontroller) was utilised during deployments, focusing at the shape of the pore-water pressure dissipation curve (> 20 min deployment time according telemetry real-time data) and aiming at the sub-seafloor profiling of the sedimentary succession. The sub-seafloor profiling takes less than 7.0 sec and at the high sampling rate, provides the user with data of a vertical resolution < 5.0 x10^{-3} m thickness.

The deployment mode aims (i) at a high-resolution vertical record (1 kHz logging frequency) of crucial in-situ sediment physical properties and (ii) at the recording of the excess pore-water pressure evolution once the DWFF-CPTU instrument is stuck in the sediment (dissipation test). Pore-water pressure dissipation is usually recorded for 20 to 30 min. The DWFF-CPTU instrument was veered at 1.2 m/s winch speed to a level 30 – 50 m above the seafloor, then the winch speed was varied between 0.5 - 1.2 m/s until the DWFF-CPTU probe hits the seafloor and dynamically decelerated until its penetration depth of several meters sub-seafloor (a fix winch speed for each location). The instrument is recovered after the dissipation test.

5.4. CAT-meters, Osmo-lance

(M. Tryon)

CAT meters

The Chemical and Aqueous Transport (CAT) meter (Fig. 14) (Tryon et al., 2001) is designed to quantify both inflow and outflow rates on the order of 0.05 cm/yr to 100 m/yr. At high outflow rates, a time series record of the outflow fluid chemistry may also be obtained. These instruments have been in use since 1998 and have been successful in monitoring long term fluid flow in both seep and non-seep environments (e.g. Tryon et al., 2004, Tryon, 2010).

The CAT meter uses the dilution of a chemical tracer to measure flow through the outlet tubing exiting the top of a collection chamber (Fig. 14). The pump contains two osmotic membranes that separate the chambers containing pure water from the saline side that is held at saturation levels by an excess of NaCl. Due to the constant gradient, distilled water is drawn from the fresh water chamber through the osmotic membrane into the saline chamber at a rate that is constant for a given temperature. The saline output side of the pump system is rigged to inject the tracer while the distilled input side of the two pumps are connected to separate sample coils into which they draw fluid from either side of the tracer injection point (Fig. 14). Each sample coil is initially filled with deionized water. Having two sample coils allows both inflow and outflow to be measured. A unique pattern of chemical tracer distribution is recorded in the sample coils allowing a serial record of the flow rates to be determined. Upon recovery of the instruments the sample coils are subsampled at appropriate intervals and analyzed using a Perkin-Elmer Optima 3000XL ICP-OES. Both tracer concentration and major ion concentration (Na, Ca, Mg, S, K, Sr, B, Li) are determined simultaneously.

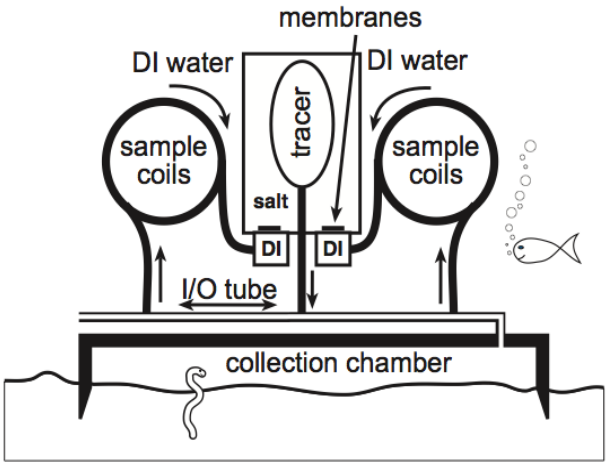

Figure 14: CAT flowmeter schem,atic (from Tryon et al. 2001).

As explained in Tryon et al. (2001), diffusion in the sample coils is negligible. Typical sample sizes are 25-75 cm of tubing, many times the characteristic diffusion length for typical seawater ions at ocean bottom temperatures. Our data has shown that we typically achieve resolutions of ~0.5% of the deployment time in the latest portions of the record and ~2% in the oldest portion for deployments of a year.

Figure 15: CAT flowmeter systems on deck of RV *Poseidon* prior to deployment (cruise P410; Kopf et al., 2012).

During Poseidon cruise P410, four CAT meters each were deployed on mud volcanoes Milano and Napoli, and another one was deployed in a valley south of a large detached block between the inner and outer Mediterranean Ridge close to the Cretan Margin. These sites were determined to be our best strategy for detecting and sampling fluid flow and fluid chemistry, based on the cores retrieved at each site and the temperature gradients measured. A picture of the instruments is given in Figure 15. Main objective of cruise P429 was to successfully recover the 5 CAT meters.

Osmo-lance

Offshore Nice airport, a 5m-long lance resembling the geometry of an IFREMER piezometer was deployed in September 2011 on cruise STEP with RV *L'Europe*. The instrument contains fluid ports at 5 levels, which are connected to osmo-samplers at the head of the instrument.

Details can be found in Figure 16 and Stegmann et al. (2012).

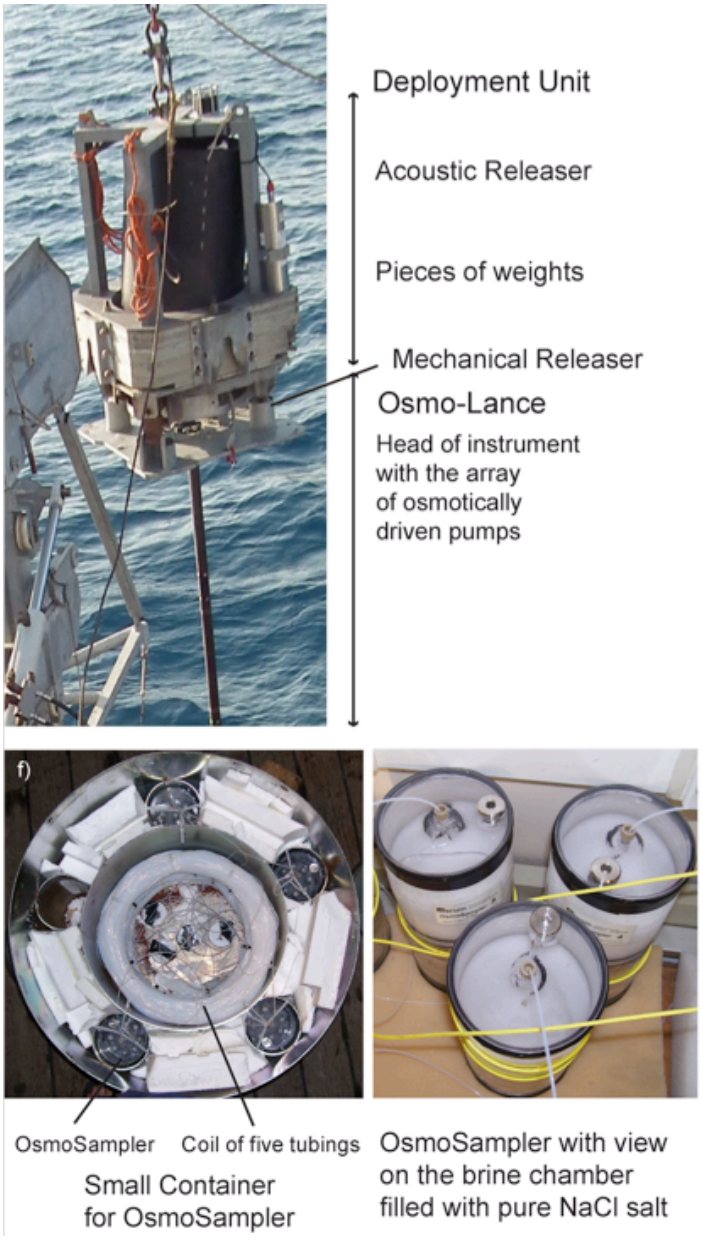

Figure 16: Osmo-lance during deployment in September 2011. Blow up photos show the tubing and osmotoc pumps driving the system. See Stegmann et al. (2012).

5.5. Gravity coring and sediment description

(M. Belke-Brea, M. Geraga, G. Ferentinos, A. Kopf)

In order to recover sediment cores, a gravity corer with tube lengths of 2 and 6 m and a weight of approximately 1.5 tons was used during cruise P429 (Fig. 17). Before using the coring tool, the plastic liners were marked lengthwise with a straight line in order to retain the orientation of the core for potential paleomagnetic analyses and then placed inside the steel tube of the gravity corer.

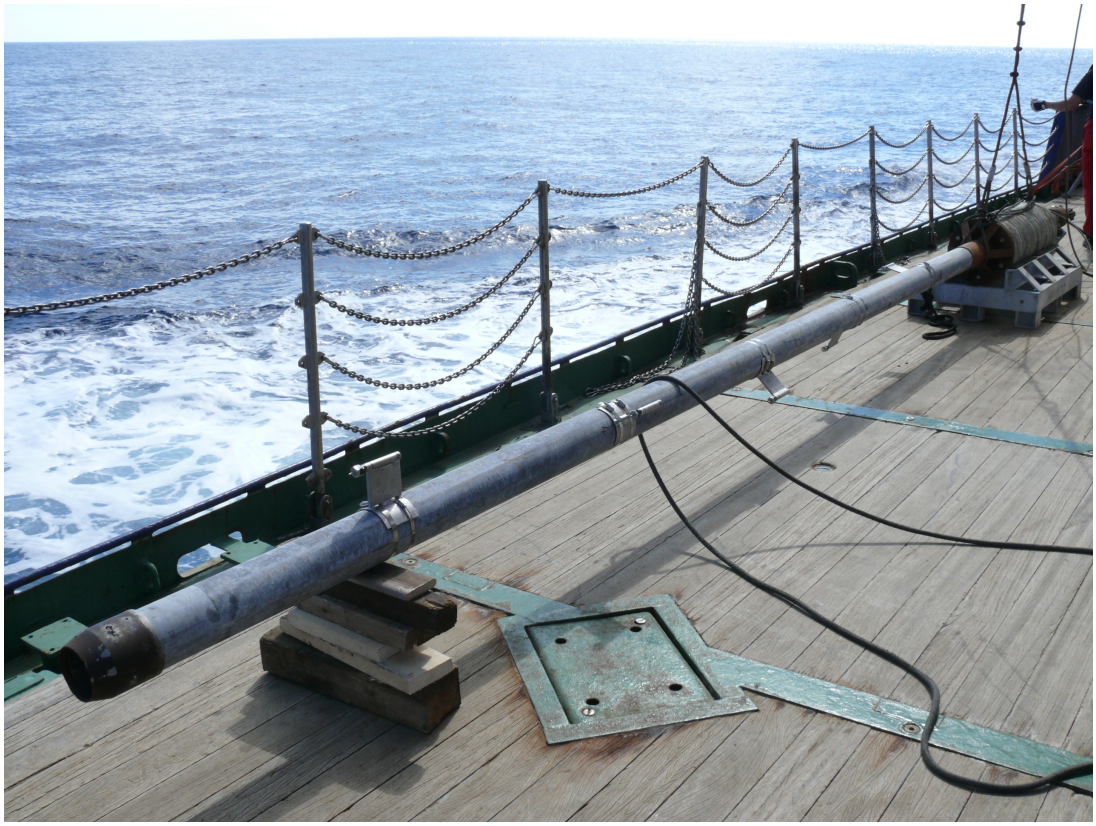

Figure 17: Gravity corer on board RV *Poseidon*.

Once back on deck, the sediment cores were cut into sections of 1 m length, closed with caps on both ends and labelled according to a standard scheme (Fig. 18). By definition, the half core with the marked line was stored as archive half, while description, sampling, etc. were carried out on the remaining half. For the detailed procedures each working half core underwent, see below.

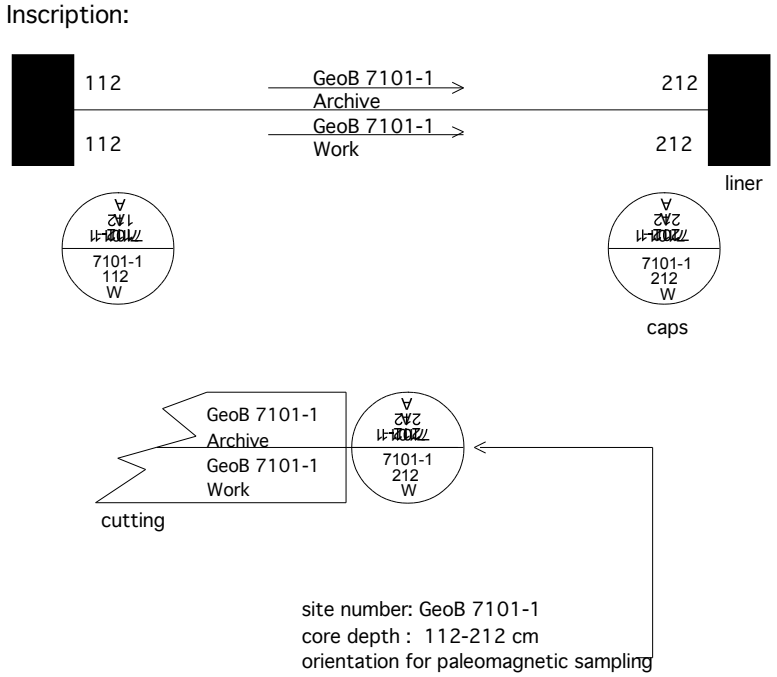

Figure 18: Scheme of the inscription of gravity core segments used during P410.

Sediment description

Split gravity cores were photographed and described from a largely sedimentological standpoint. Grain size and composition of sediments were determined mainly visually using a simple hand-lens, HCl-testing and analyzing smear slides of dominant lithologies under a cross-polarizing microscope in accordance with Rothwell (1989). The size of grains was assessed based on Wenthworth's (1922) classification. The colour of the material was determined visually on board using Munsell's colour chart nomenclature. For each core, a composite one-page core log sheet was compiled. It shows core photographs next to a graphical core log and gives information on redeposition-/event layers (i.e., sand layers, volcanic ash layers or clear evidence for mass movement deposits, such as mud clasts in muddy or sandy matrix, tilted beds and repetition of strata), bioturbation and the assigned lithological units in three different columns. The core log is combined with results from the fall cone penetration test (see below). A wide variety of features, such as sediment lithology, primary sedimentary structures, bioturbation, soft-sediment deformation, and coring disturbance is indicated by patterns and symbols in the graphic logs. A key to the full set of patterns and symbols used on the barrel sheets is shown in Figure 19. The symbols are schematic, but they are placed as close as possible to their proper stratigraphic position. All core photographs are provided in Appendix 9.2 (see below).

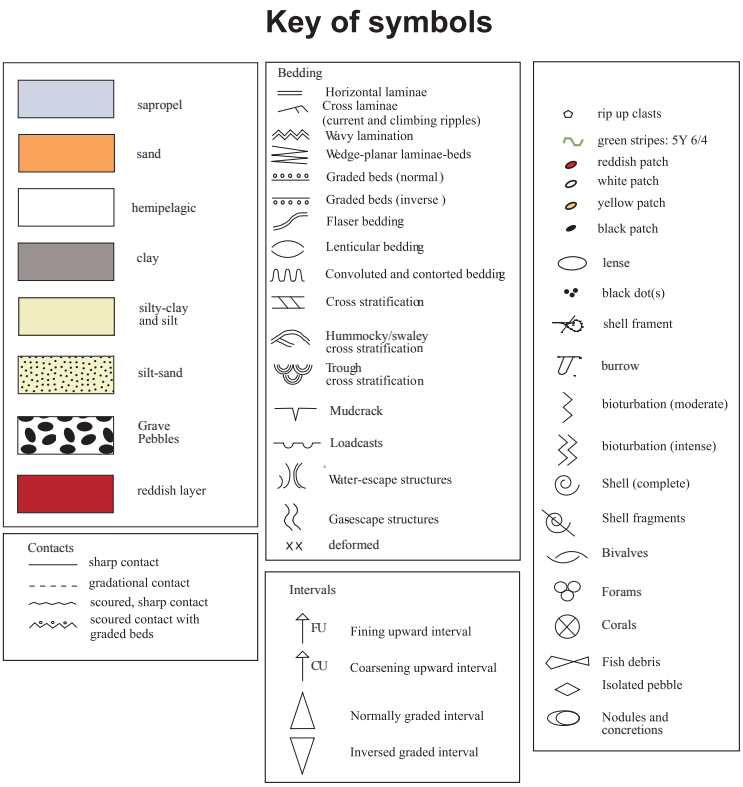

Figure 19: Key of symbols for barrel sheets of gravity core description.

5.6. Physical properties

(G. Wiemer, S. Schlenzek)

During cruise P429, shipboard physical properties measurements were restricted to falling cone penetration tests and vane shear tests on the working half of the core. This procedure was only carried out on cores taken in Area 1 (Cretan Sea) and Area 2 (MedRidge), because all core recovered in Area 3 (Nice slope) remained unsplit for geotechnical post-cruise experiments.

5.7.1. Cone penetrometer

The geotechnical properties along the sediment cores were determined according to British Standards Institutions (BS1377, 1975). A Wykeham-Farrance cone penetrometer WF 21600 (Fig. 20a) was used for a first-order estimate of the sediment's stiffness. For the measurement, the metal cone was brought to a point exactly on the split core face (Wood 1985). A manual displacement transducer was then used to measure the distance prior to and after release of the cone (i.e. penetration after free fall of the cone). Precision is 0.1 mm of displacement. The distances measured can then be translated into sediment strength (see Hansbo, 1957).

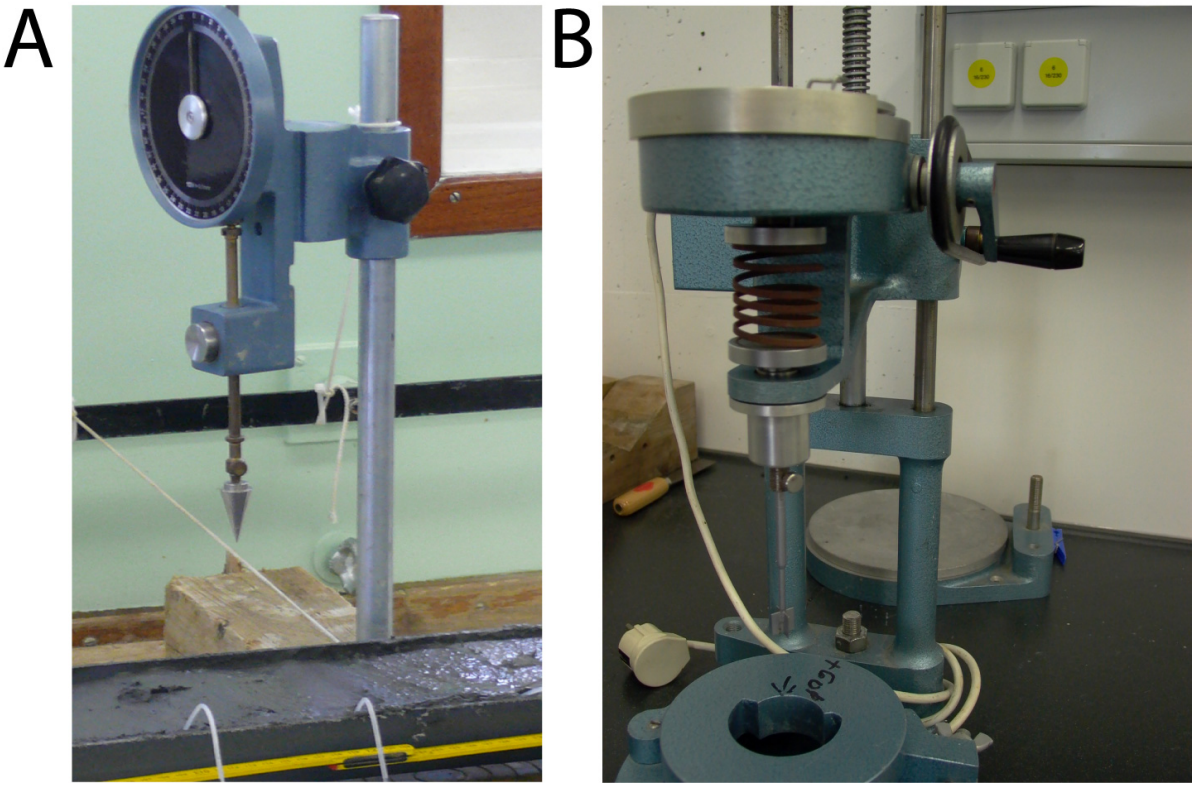

Figure 20: (a) Falling cone penetrometer and (b) vane shear device used on the split core surface.

A falling cone penetrometer with a defined weight (80.51 g) and geometry (30° cone) was used by Hansbo (1957) during a detailed study of the relationship between the cone penetration and soil strength. The undrained shear strength s_u can be calculated from the variables mass and tip angle of the falling cone, gravity *g*, penetration depth *d* and the cone factor *k* via the "cone factor". Wood (1985) calculated from fall-cone and miniature vane tests average values of cone factors (in our case k=0,85 for a 30° cone). The undrained shear strength can then be calculated using the equation $s_u = (k*m*g)/d^2$.

Shore-based laboratory testing will include ring shear experiments as well as dynamic triaxial shear tests to obtain residual strength and rate-dependent frictional properties as well as the liquefaction potential of the materials recovered.

5.7.2 Vane shear testing

In addition to the Cone Penetrometer a double vane shear apparatus by GSC ATLANTIC was used for more information about sediment stiffness and residual shear strength (Fig. 20b). The distance between the two vanes is 15 cm. For the measurements, four-bladed vanes (L = 12.5 mm, h = 6.25 mm, d = 12.5 mm) were inserted into the split undisturbed core faces and rotated at a constant rate of 90°/min. Data are logged via an interface module (GSC ATLANTIC) using the Testpoint software package.

A spring transmits the rotation at the vane. The torque required shearing the sediment along the vertical and horizontal edges of the vane. The undrained shear strength, s_U depends on the torque T,

the vane constant K, the maximum torque angle at failure σ and the spring constant B that relates the deflection angle to the torque (Blum, 1997). The vane constant, K is a function of the vane size and geometry and was used during the measurements with $K=\pi*d^2*(h/2)+\pi*(d^2/6)$ for full dipping vanes. The undrained shear strength can then be calculated using the equation $s_U= T/K$. Shore-based laboratory testing will include ring shear tests to obtain residual strength and rate-dependent frictional properties of the materials recovered.

5.7. Pore water geochemistry

(A. Kopf)

The composition of pore water in marine sediments is one of the most suitable indicators to characterize the benthic system. Thus, vertical, horizontal and temporal changes in concentrations of dissolved constituents can be used for identification and quantification of specific transfer processes, regardless of whether these are mircobially mediated or caused by abiotic reactions. Furthermore, pore water signatures and profiles can reveal the importance fluid transport mechanisms. In the majority of deep sea-sediments molecular diffusion is by far the dominate process, which controls the transport of dissolved components. When advection becomes important at a specific location (e.g. seep sites), the modeling of pore water profiles allows the calculation of the corresponding flow rates. Last but not least, pore water compositions can also indicate to the history of the waters of even to their primary source.

During this cruise, pore water geochemistry sampling was conducted mainly to find indications for the upward transport of fluids from deeply buried formations, caused by the deformation and subduction of the African plate moving northward below the European plate. In this context salinity, mainly expressed by the concentrations of chloride, sodium, sulfate, magnesium, calcium and potassium, is of particular interest. Inorganic geochemical work, however, was restricted to the extraction of pore water using rhizon samplers (~0.4 µm; Seeberg-Elverfeldt et al., 2005) on the split core (Fig. 21). The vacuum necessary to operate the rhizon samplers was created by pulling up 10 ml plastic syringes. The amounts of pore water retrieved by this method were between 5 and 10 ml. In general, the depth resolution varies approximately between 20 and 30 cm.

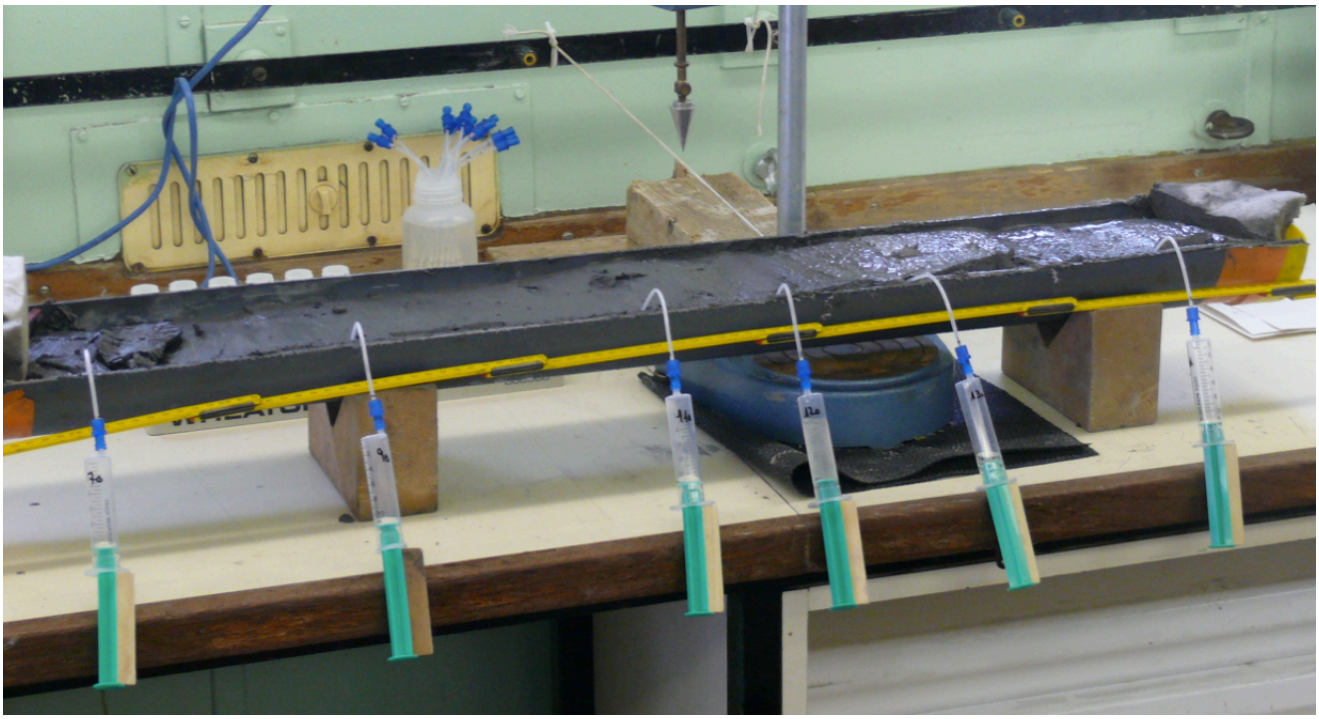

Figure 21: Rhizon pore water extraction in split working half of the gravity core.

6. Preliminary Results

6.1. Seafloor surveys

(S. Kufner)

Swath mapping was carried out in two survey areas (Spatha Ridge and Mediterranean Ridge).

During the Spatha Ridge survey a total of 24 hours of data were recorded in tree nights of survey. The total track length is 295 km, survey speed was between 3 and 5 knotes. The water depth in the survey area ranges between 60 and 850 m.

Data processing was carried out using the software Caris and MBsystem. The final grid has a grid spacing of 7 m. The area between 023.65°E-023.95°E and 35.63°N-35.85°N was covered (Fig. 22).

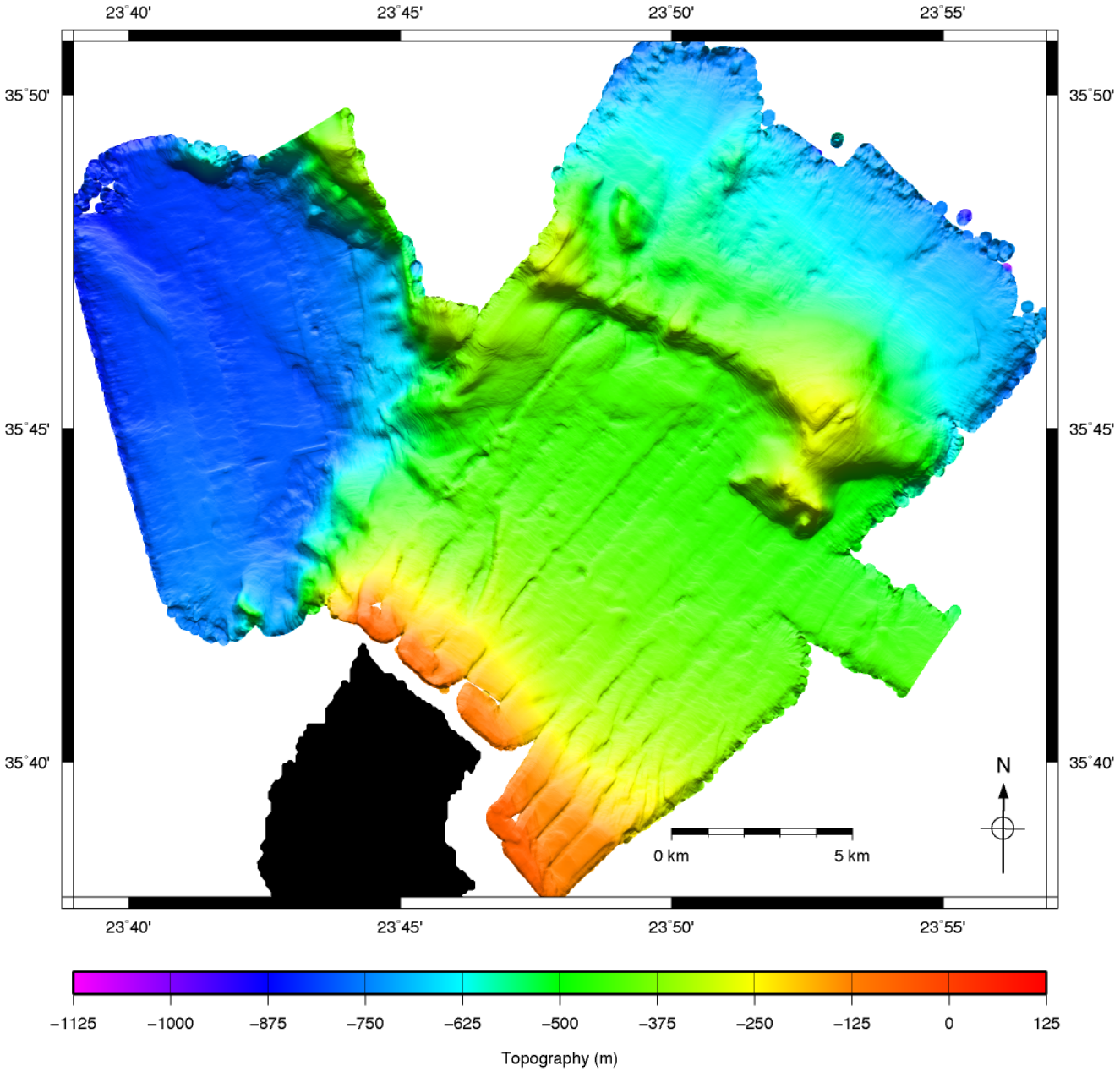

Figure 22: Swath bathymetry map recorded in Area 1 (NW Cretan Sea).

6.2. *In situ* temperature measurements

(M. Tryon, T. Fleischmann)

In order to obtain thermal gradients that may be helpful in identifying sites of active fluid flow or mud volcanism, and to place the sediment and pore fluid samples in the appropriate thermal regime, 3 or 5 Antares miniture temperature loggers (MTLs) were installed on outriggers on the core barrels or onto the HF probe (Fig. 10b), respectively. These sensors have a resolution of approximately 0.001°C and accuracy of ±0.1°C and are programmed to record at 1 Hz (see section 5.2 above). On insertion a temperature spike is caused by friction that rapidly dissipates. The loggers were allowed to equilibrate after core penetration for 7 minutes before retrieval. This was adequate for equilibration for all but the highest temperature changes at Milano MV. In this latter case a qualitative extrapolation was made that indicated only minor changes in temperatures and gradients (<5%) from that at the end of the record before extraction. The results are shown below in Figure 23.

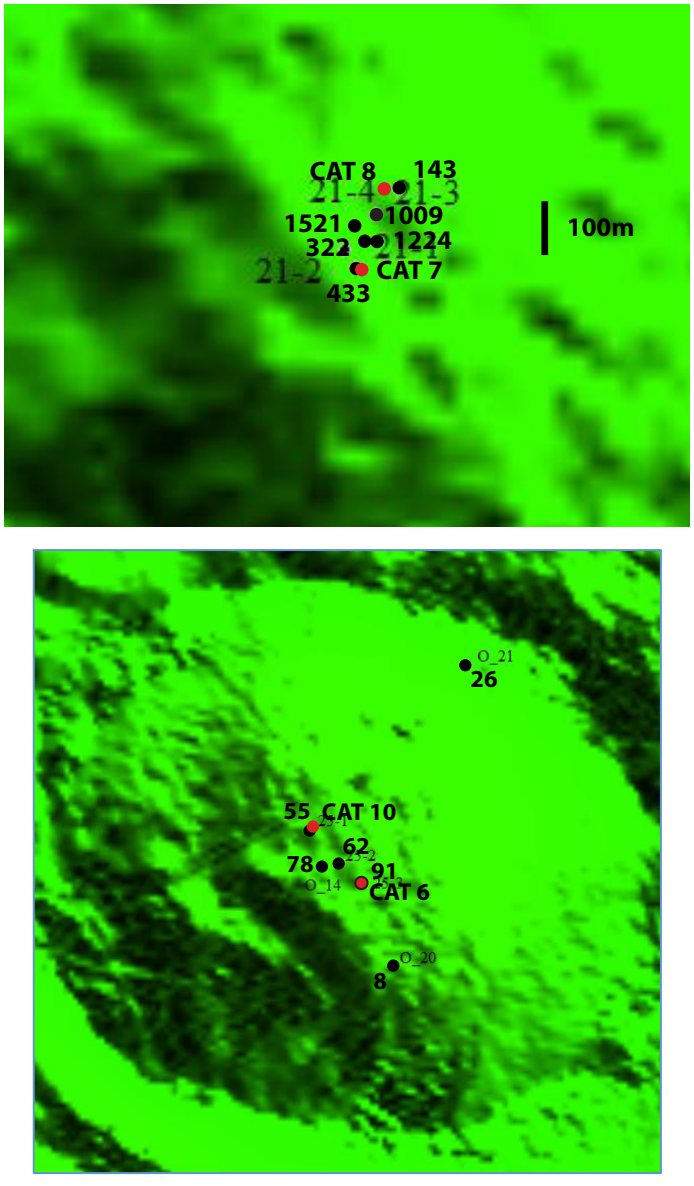

Figure 23: Calculated T gradients (black bold numbers in °C/km) using the linear best fit function. Examples show multiple deployments (pogo-style) on Milano MV (top) and Napoli MV (bottom). Black dots are T-probe deployments, the red dots flowmeter stations; the light numbers are GeoB153xx from cruise P 410. See text.

It can be seen from the thermal gradients that the data from P429 mirror those from P410 (Kopf et al. 2012). Gradients exceed 1000 °C/km in the most active portion of Milano MV on the crest, and drop to values between 100 and 500 °C/km towards the rim. Napoli MV is less active, but still has somewhat elevated gradients in the central part (78 – 91 °C/km), and normal to low gradients at the flanks (8 – 26 °C/km).

6.3. *In situ* CPT testing

(A. Steiner, G. Wiemer, A. Kopf)

During Poseidon cruise P429, a total of 41 shallow-water CPT deployments (Cretan Sea: 26; Nice airport: 15) and only 2 deep-water CPT measurements (one each on Milano and Napoli MVs) were conducted. Results are given in Tables 1, 2 and 3 (see following regional sections).

Cretan Sea landslide east of Spatha Ridge

A total of 26 SWFF-CPTU drops were carried out over the complete study area (Fig. 23) in water depths between 150 m and 440 m (Table 1).

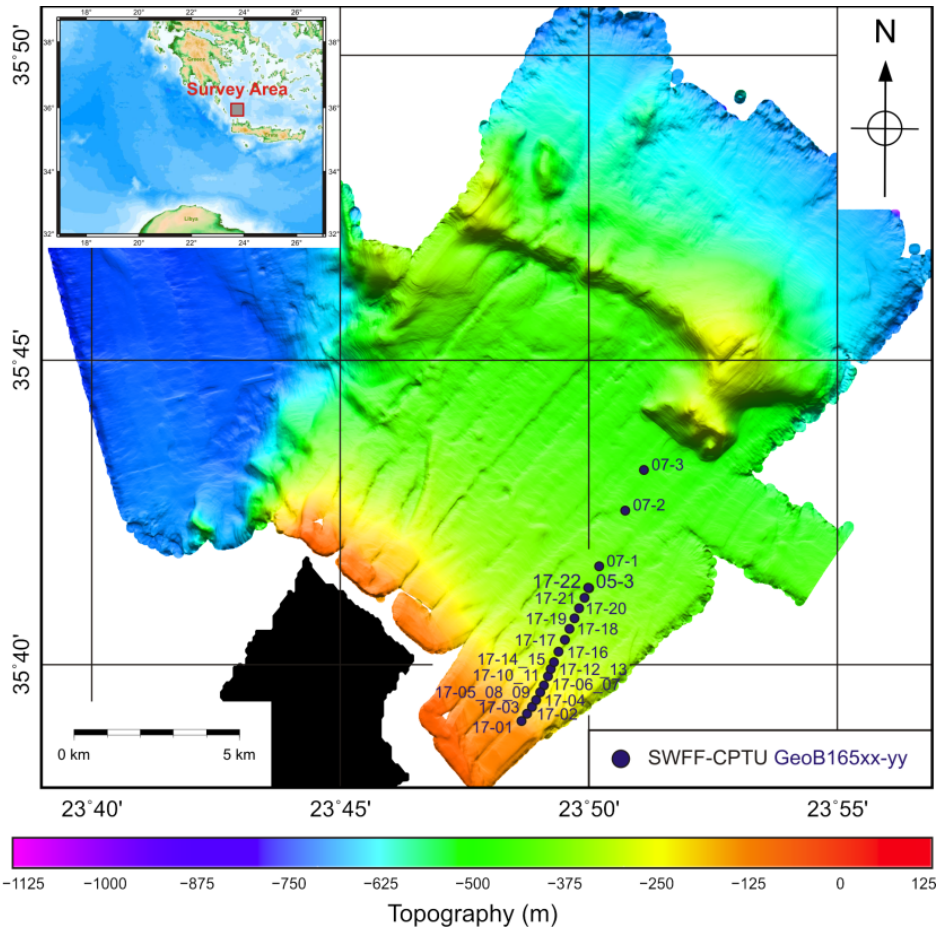

Figure 23: Map showing all SWFF-CPTU deployments during the Poseidon cruise P429. The deployments are represented with the last two/four digits of the GeoB nomenclature.

GeoB165xx	PositionLat	PositionLon	date	WD [m]	equipment	probe
05-3	35° 41,25' N	23° 49,99' E	23.03.2012	366.8	SWFF-CPTU	rods 2m; tip 25,500m; u1
07-1	35° 41,61' N	23° 50,20' E	23.03.2012	381.9	SWFF-CPTU	rods 2m; tip 25,500m; u1
07-2	35° 42,53' N	23° 50,72' E	23.03.2012	422.2	SWFF-CPTU	rods 2m; tip 25,500m; u1
07-3	35° 43,19' N	23° 51,09' E	23.03.2012	439.1	SWFF-CPTU	rods 2m; tip 25,500m; u1
17-1	35° 39,07' N	23° 48,62' E	25.03.2012	146.7	SWFF-CPTU	rods 2m; tip 25,500m; u1
17-2	35° 39,18' N	23° 48,75' E	25.03.2012	175.3	SWFF-CPTU	rods 2m; tip 25,500m; u1
17-3	35° 39,30' N	23° 48,84' E	25.03.2012	196.9	SWFF-CPTU	rods 2m; tip 25,500m; u1
17-4	35° 39,42' N	23° 48,93' E	25.03.2012	223.7	SWFF-CPTU	rods 2m; tip 25,500m; u1
17-5	0° 0,00' N	0° 0,00' E	25.03.2012	0	SWFF-CPTU	rods 2m; tip 25,500m; u1
17-6	35° 39,65' N	23° 49,08' E	25.03.2012	259.2	SWFF-CPTU	rods 2m; tip 25,500m; u1
17-7	35° 39,65' N	23° 49,09' E	25.03.2012	259.4	SWFF-CPTU	rods 2m; tip 25,500m; u1
17-8	35° 39,54' N	23° 49,01' E	25.03.2012	222.6	SWFF-CPTU	rods 2m; tip 25,500m; u1
17-9	35° 39,53' N	23° 49,02' E	25.03.2012	223.6	SWFF-CPTU	rods 2m; tip 25,500m; u1
17-10	35° 39,80' N	23° 49,16' E	25.03.2012	253.4	SWFF-CPTU	rods 2m; tip 25,500m; u1
17-11	35° 39,81' N	23° 49,17' E	25.03.2012	254.9	SWFF-CPTU	rods 2m; tip 25,500m; u1
17-12	35° 39,93' N	23° 49,22' E	25.03.2012	268	SWFF-CPTU	rods 2m; tip 25,500m; u1
17-13	35° 39,93' N	23° 49,22' E	25.03.2012	268.1	SWFF-CPTU	rods 2m; tip 25,500m; u1
17-14	35° 40,04' N	23° 49,28' E	25.03.2012	280.4	SWFF-CPTU	rods 2m; tip 25,500m; u1
17-15	35° 40,04' N	23° 49,29' E	25.03.2012	281.2	SWFF-CPTU	rods 2m; tip 25,500m; u1
17-16	0° 0,00' N	0° 0,00' E	25.03.2012	0	SWFF-CPTU	rods 2m; tip 25,500m; u1
17-17	35° 40,40' N	23° 49,50' E	25.03.2012	314.1	SWFF-CPTU	rods 2m; tip 25,500m; u1
17-18	35° 40,58' N	23° 49,60' E	25.03.2012	330.1	SWFF-CPTU	rods 2m; tip 25,500m; u1
17-19	35° 40,76' N	23° 49,70' E	25.03.2012	340.8	SWFF-CPTU	rods 2m; tip 25,500m; u1
17-20	35° 40,92' N	23° 49,80' E	25.03.2012	351.9	SWFF-CPTU	rods 2m; tip 25,500m; u1
17-21	35° 41,09' N	23° 49,91' E	25.03.2012	360.8	SWFF-CPTU	rods 2m; tip 25,500m; u1
17-22	35° 41,26' N	23° 49,98' E	25.03.2012	367.8	SWFF-CPTU	rods 2m; tip 25,500m; u1

Table 1: Selected protocols from SWFF-CPTU deployments.

The FF-CPTU measurements are addressed to the following scientific goals:

- in-situ characterization of the shallow sub-seafloor sediments (sediment physical- and hydrological properties)
- comparison with seismic data and ground truthing (Ferentinos and Papatheodorou 1989; Fig. 24)
- identification and characterization of shallow-located sliding plans (Fig. 24)
- comparison of the SWFF-CPTU tests with gravity core data (vane-shear and fall-cone tests) in respect of the strain-rate correction of the in-situ data (Fig. 25)

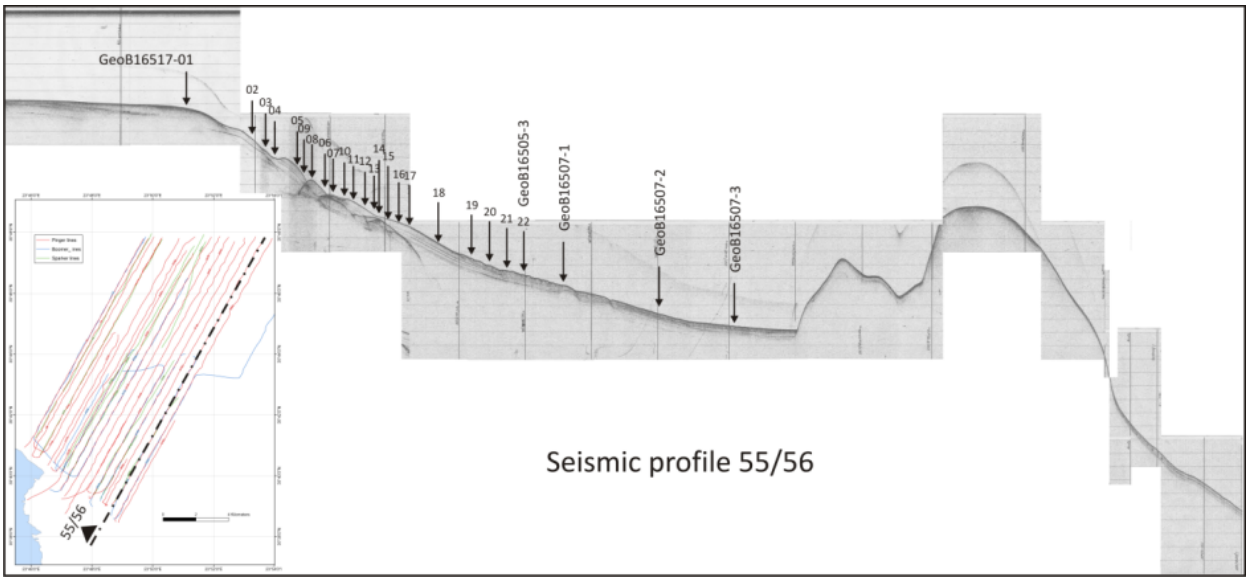

Figure 24: Seismic profile 55/56 along which the SW-CPTu probe was used (see Station numbers).

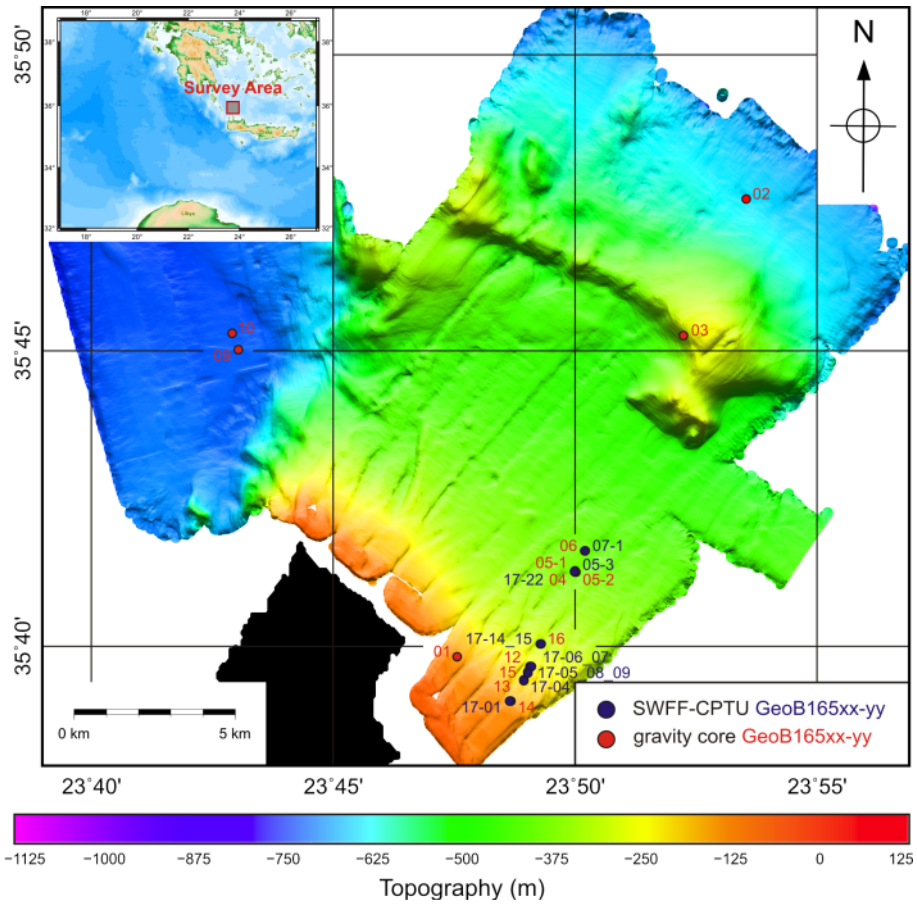

Figure 25: Selected protocols from SW-CPTu deploments.

Most of the tests are deployed at the area where the slumped and slid material are located (western slope). In this area, only penetration depths of 0.5 to 1.5 m were achieved due to very high compaction/consolidation of the sediments. The cause is not clearly understood, right now. One reason is probably the high-rate of seismicity in the northern part of Crete (Papazachos & Papazachou, 1977).

In this cruise report, we present three characteristic results along the seismic profile (Figs. 26-28). The first test is above the slumping/sliding area, the second one is inside of the slumping area and the tired test is below the slumping area (runout region).

When running down the western slope (Fig. 24) an increase of the penetration depth was detected. This is direct correlated with the decrease of the undrained shear-strength of the sediments (Figs. 26-28).The undrained shear-strength varies between 20 and 45 kPa in the upper slope area and between 10 and 30 KPa in the lower slope region. All tests show a very high consolidation state with an undrained shear-strength ratio (su/σ0') higher than 2.0-3.0 (highly over-consolidated).

The comparison of the in-situ measurements with the gravity core data illustrates similar trends in the sediment physical properties. But, the comparison is very difficult due to disturbance of the upper portion of the gravity core sediments (coring process) and heterogeneity of the material (i.e. Fig. 28).

More data will be acquired during post-cruise geological/geotechnical laboratory measurements (standard- and advanced tests). The comparison with the seismic data will also be carried out in this phase (ground truthing).

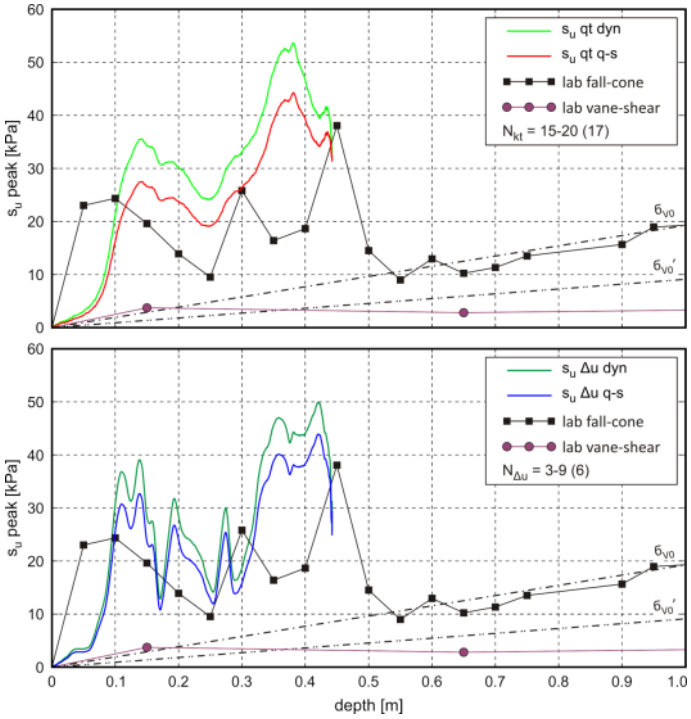

Figure 26: Derived in-situ undrained-shear strenght (s_u) calculated from the corrected cone resistance (upper plot) and calculated from the excess pore-water pressure (lower plot) for the test GeoB16517-04. Additionally, the laboratory tests (fall-cone and vane-shear) are also illustrated (GeoB16513). Note: empirical cone factor (N_{kt}) and empirical excess pore-water factor ($N_{\Delta u}$). Both were used to calculate the in-situ undrained shear-strength.

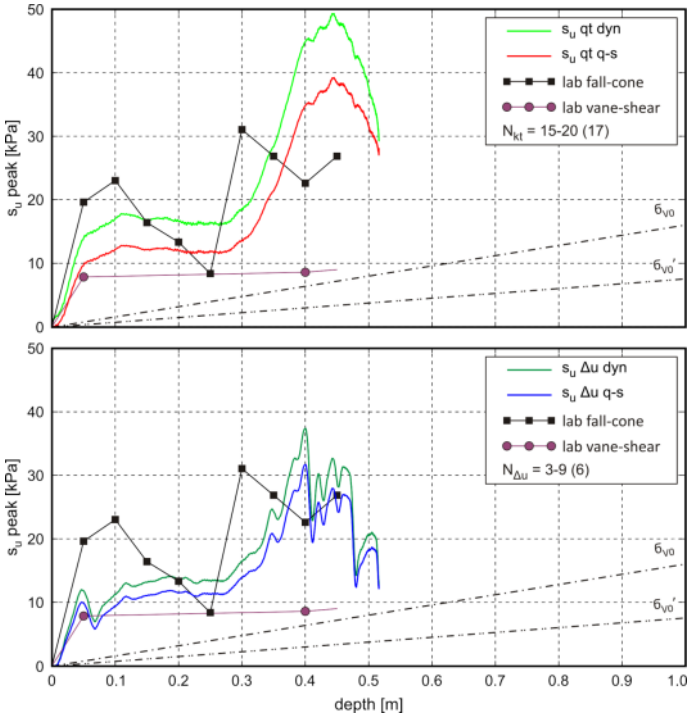

Figure 27: Derived in-situ undrained-shear strenght (s_u) calculated from the corrected cone resistance (upper plot) and calculated from the excess pore-water pressure (lower plot) for the test GeoB16517-15. Additionally, the laboratory tests (fall-cone and vane-shear) are also illustrated (GeoB16516). Note: empirical cone factor (N_{kt}) and empirical excess pore-water factor ($N_{\Delta u}$). Both were used to calculate the in-situ undrained shear-strength.

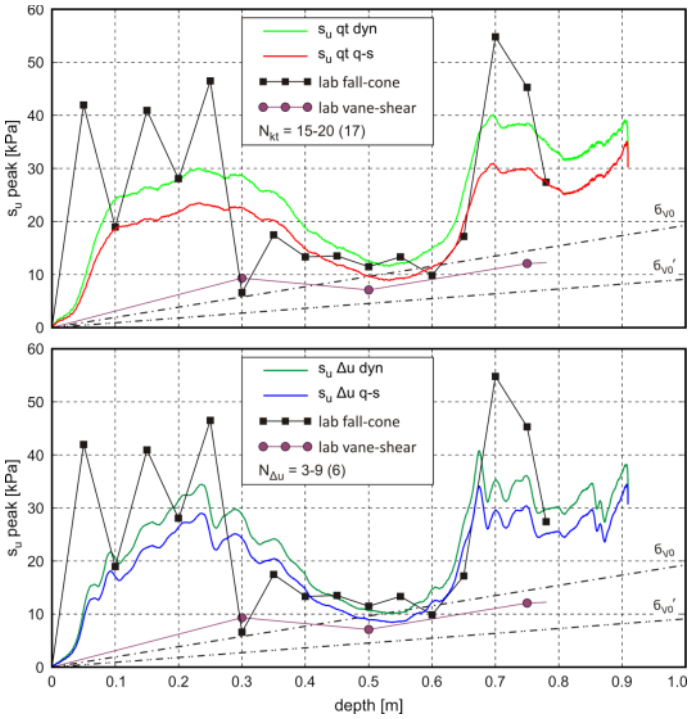

Figure 28: Derived in-situ undrained-shear strenght (s_u) calculated from the corrected cone resistance (upper plot) and calculated from the excess pore-water pressure (lower plot) for the test GeoB16517-22. Additionally, the laboratory tests (fall-cone and vane shear) are also illustrated (GeoB16505-2). Note: empirical cone factor (N_{kt}) and empirical excess pore-water factor ($N_{\Delta u}$). Both were used to calculate the in-situ undrained shear-strength.

Mediterranean Ridge mud volcanoes

The first DWFF-CPTU deployment was undertaken on the MV Milano and the second one was carried out at MV Napoli (Fig. 29). The water depth varies between 1900 and 1950 mbsl (meter below sea-level) (Table 2). The penetration depth ranges between 2.0 and 2.5 m.

The DWFF-CPTU tests address following strategies:

- Comparison between DWFF-CPTU measurements and gravity core data (vane-shear and fall-cone tests) with respect to the strain-rate correction of the *in-situ* data.

In-situ characterization of the MV shallow sediment succession in order to evaluate the fluid/gas conditions, consolidation settings (active or not active MV) and strength properties.

GeoB165xx	PositionLat	PositionLon	date	WD [m]	equipment	probe
22	33° 44,02' N	24° 46,57' E	29.03.2012	1923.3	DWFF-CPTU	rods 4.1m; tip pp; u1 and u3
24	33° 43,64' N	24° 40,86' E	29.03.2012	1909.2	DWFF-CPTU	rods 4.1m; tip pp; u1 and u3

Table 2: Protocols from DWFF-CPTU deployments from Milano and Napoli MV.

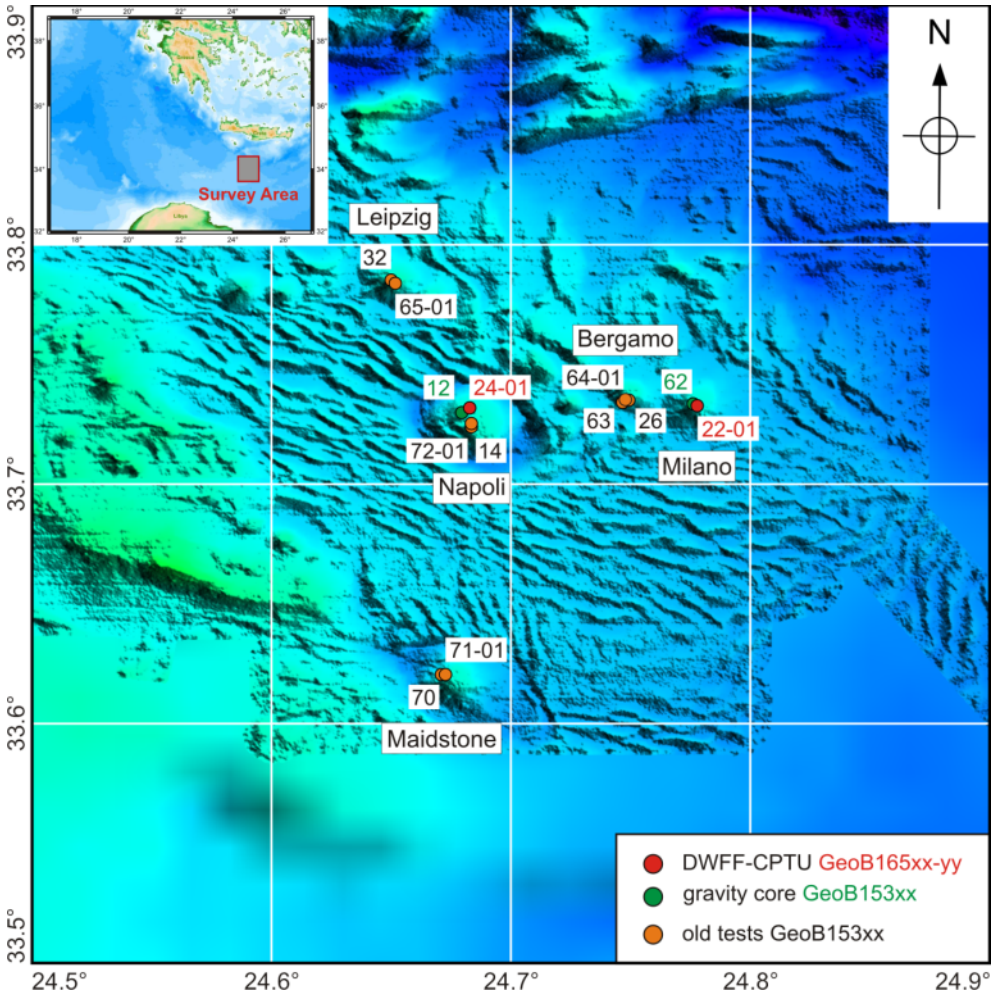

Figure 29: Map showing all DWFF-CPTU deployments during the Poseidon cruise P429. The deployments are represented with the last two digits of the GeoB nomenclature.

The excess pore-water pressure of the sediments for MV Milano varies between 20 and 40 kPa and the derived undrained shear-strength is between 5.0 and 10 kPa (Fig. 30). Hence, this sediment is characterized as normally- to slightly over-consolidated with an undrained shear-strength ratio (su/σ0') of 0.2 to 0.7. The results indicate that this MV is probably active.

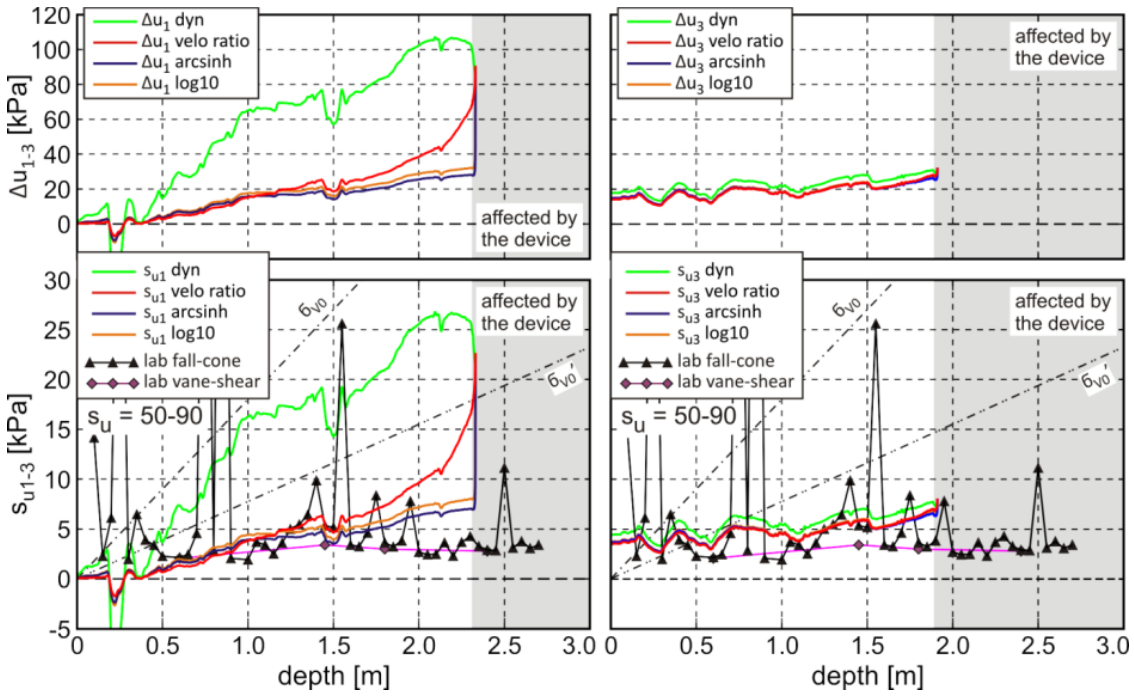

Figure 30: Protocols from DW-CPTu deploments from Milano MV: Measured and corrected excess pore-water pressure at the tip (Δu1) and 0.35 m behind the tip (Δu3) for the Milano MV. Additionally, the derived undrained shear-strength (su) of the DWFF-CPTU measurements (GeoB16522-01) compared with the laboratory tests (P410 GeoB15362) are illustrated. The green line represents the measured (dynamic) parameters. The red, blue and orange lines show corrected (quasi-static) parameters taking into account the empirical strain-rate solutions (Dayal & Allen 1975, Mitchell 1976, A. Steiner, unpublished data).

The measurements for the MV Napoli show excess pore-water pressures between 20 and 60 kPa and an undrained shear-strength of 5.0 to 15.0 kPa (Fig. 31). Characteristic for these sediments is the slightly- to highly over-consolidated behavior with an undrained shear-strength ratio (su/σ0') of 0.5 to 1.0. Consequently, this deployment is outside of the active region.

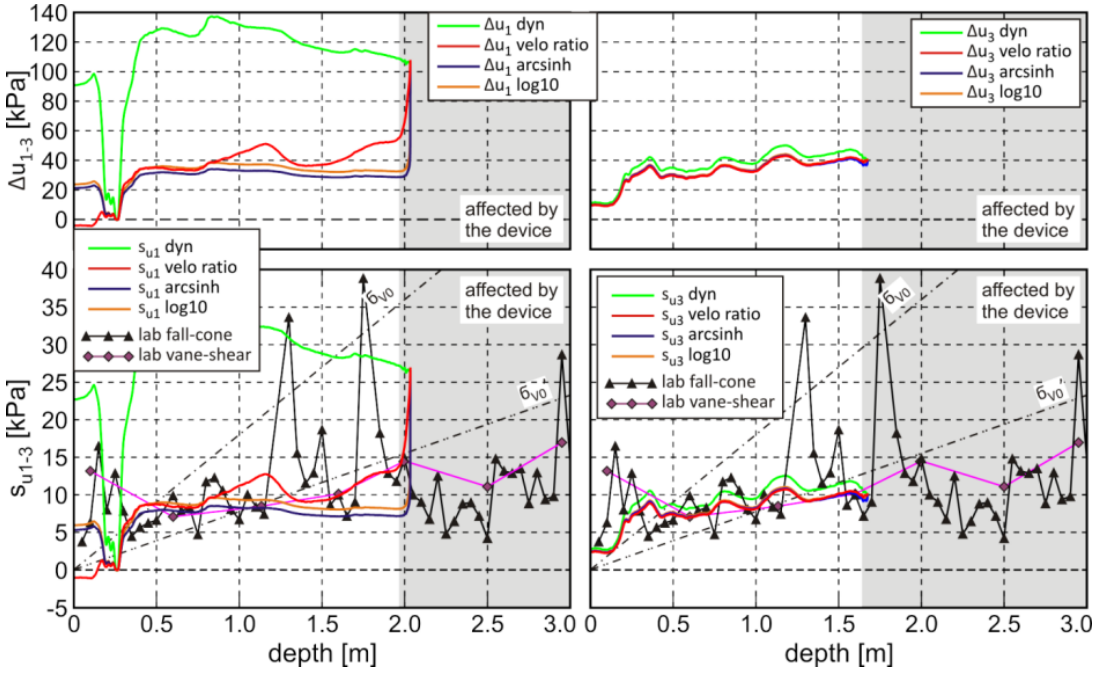

Figure 31: Measured and corrected excess pore-water pressure at the tip (Δu1) and 0.35 m behind the tip (Δu3) for the Napoli MV. Additionally, the derived undrained shear-strength (su) of the DWFF-CPTU measurements (GeoB16524-01) compared with the laboratory tests (P410 GeoB15312) are illustrated. The green line represents the measured (dynamic) parameters. The red, blue and orange lines show corrected (quasi-static) parameters taking into account the empirical strain-rate solutions (Dayal & Allen 1975, Mitchell 1976, A. Steiner, unpublished data).

In all tests, fluid/gas structures, coarser sediments and angular to well rounded clasts are scattered along the sediment succession. More data will be acquired during post-cruise geological/geotechnical laboratory measurements (standard- and advanced tests).

Nice airport landslide

During P429 cruise, a total of 15 shallow-water in-situ measurements were conducted in this research area to complete the existing SWFF-CPTU data sets of the M73 and P386 cruises (Kopf et al., 2008 and Kopf et al., 2009). The locations are given in Fig. 32.

Main objective was to collect SWFF-CPTU data with the pore-water pressure port u1 (location at the tip). These CPTU results are used to detect hydrogeological- and slope stability relevant layers in the associated gravity cores (see Ch. 6.5). The sediments of these layers are utilized for post-cruise geological/geotechnical laboratory experiments.

All collected data sets are utilized for comparisons with available pushed CPTU tests (Sultan et al., 2008) and laboratory data in order to improve available and new empirical or geotechnical solutions (i.e. strain-rate effect, soil classification).

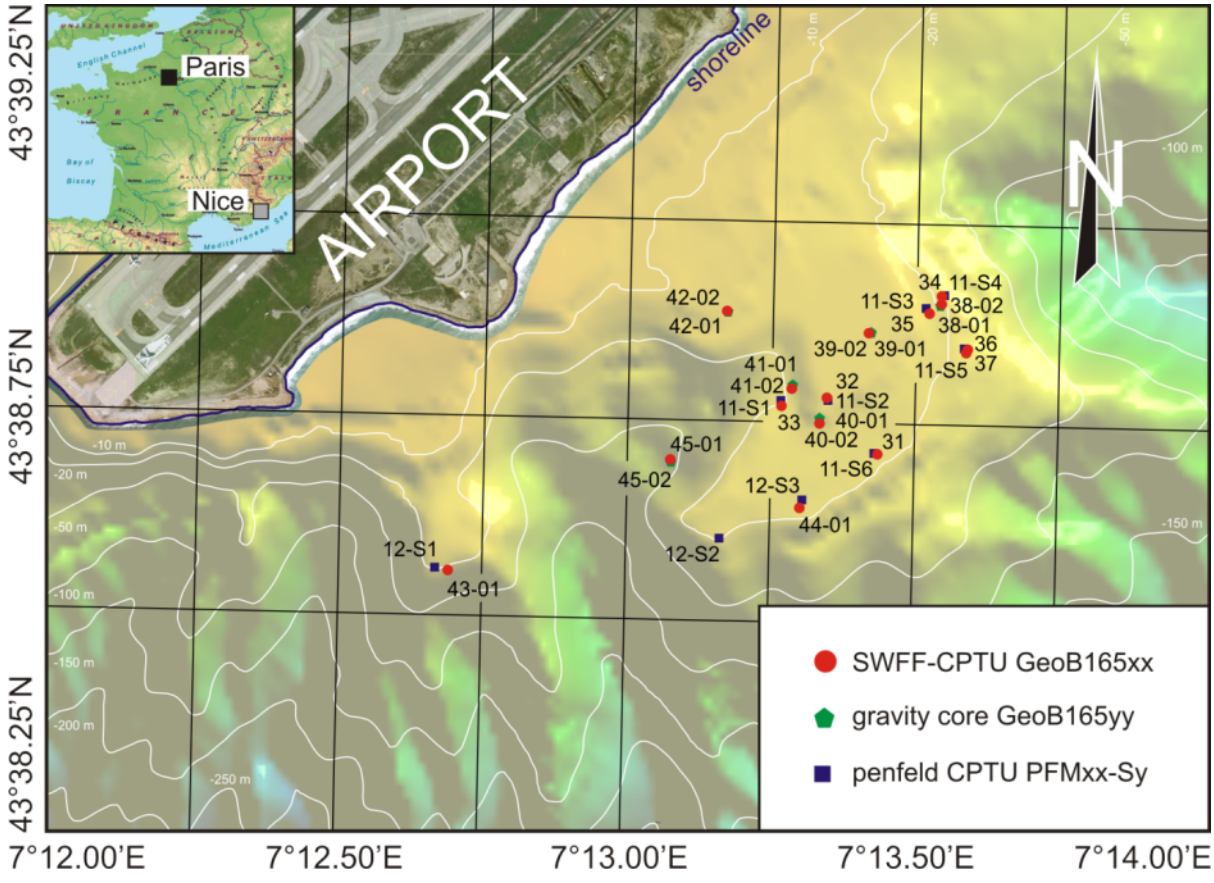

Figure 32: Map showing all SWFF-CPTU deployments offshore Nice during the Poiseidon cruise P429. Additionally, the available pushed CPTU tests (IFREMER Penfeld penetrometer) are illustrated in this map. The deployments are represented with the last two/four digits of the GeoB nomenclature.

The water depth varies between 12 and 45 mbsl (Table). The penetration depth ranges between 2.0 and 3.5 m according to the sediment physical properties.

GeoB165xx	PositionLat	PositionLon	date	WD [m]	equipment	probe
31	43° 38,70' N	7° 13,43' E	04.04.2012	21.8	SWFF-CPTU	rods 3m; tip 25,200m; u1
32	43° 38,71' N	7° 13,35' E	04.04.2012	16.2	SWFF-CPTU	rods 3m; tip 25,200m; u1
33	43° 38,77' N	7° 13,26' E	04.04.2012	12.4	SWFF-CPTU	rods 3m; tip 25,200m; u1
34	43° 38,91' N	7° 13,54' E	04.04.2012	18.8	SWFF-CPTU	rods 3m; tip 25,200m; u1
35	43° 38,89' N	7° 13,53' E	04.04.2012	17.7	SWFF-CPTU	rods 3m; tip 25,200m; u1
36	43° 38,84' N	7° 13,59' E	04.04.2012	22.4	SWFF-CPTU	rods 3m; tip 25,200m; u1
37	43° 38,84' N	7° 13,59' E	04.04.2012	22.8	SWFF-CPTU	rods 3m; tip 25,200m; u2
38-2	43° 38,90' N	7° 13,54' E	05.04.2012	18.3	SWFF-CPTU	rods 3m; tip 25,200m; u1
39-2	43° 38,87' N	7° 13,42' E	05.04.2012	12.4	SWFF-CPTU	rods 3m; tip 25,200m; u1
40-2	43° 38,75' N	7° 13,33' E	05.04.2012	14.8	SWFF-CPTU	rods 3m; tip 25,200m; u1
41-2	43° 38,79' N	7° 13,29' E	05.04.2012	12	SWFF-CPTU	rods 3m; tip 25,200m; u1
42-2	43° 38,88' N	7° 13,17' E	05.04.2012	12.7	SWFF-CPTU	rods 3m; tip 25,200m; u1
43	43° 38,56' N	7° 12,69' E	05.04.2012	39.2	SWFF-CPTU	rods 3m; tip 25,200m; u1
44	43° 38,65' N	7° 13,30' E	05.04.2012	19.9	SWFF-CPTU	rods 3m; tip 25,200m; u1
45-1	43° 38,69' N	7° 13,07' E	05.04.2012	45	SWFF-CPTU	rods 3m; tip 25,200m; u1

Table 3: Protocols from SWFF-CPTU deployments for the Nice airport landslide area.

In this cruise report, we present two SWFF-CPTU data sets, collected at the same position (Fig. 32), but the tests were carried out with different pore-water pressure ports (GeoB16536-01 and GeoB16537-01). The first test was undertaken with pore-water pressure port u1 and the second one was conducted with pore-water pressure port u2 (Figs. 33-36).

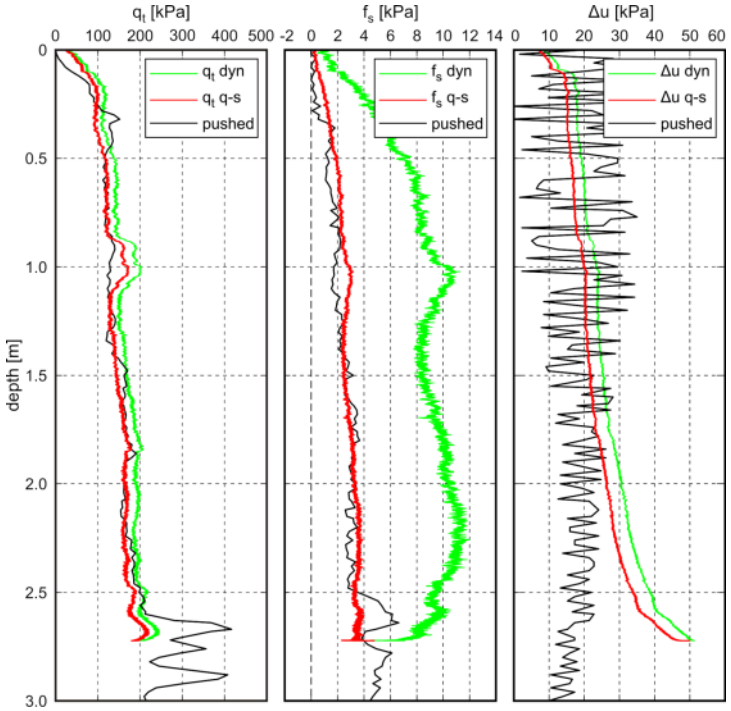

Figure 33: Measured and corrected SWFF-CPTU records for station GeoB16536-01. The green lines represent the measured (dynamic) parameters. The red lines show corrected (quasi-static) parameters taking into account the empirical strain-rate solutions (Dayal & Allen 1975, Mitchell 1976, A. Steiner, unpublished data). The black lines illustrate the pushed CPTU records (Sultan et al. 2008). Note: corrected cone resistance (qt), sleeve friction (fs), excess pore-water pressure at failure (Δu).

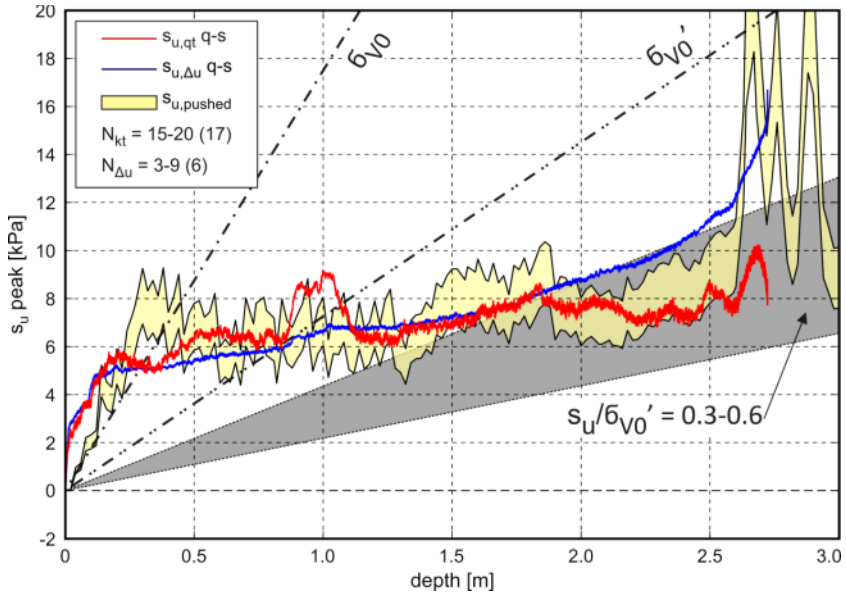

Figure 34: In-situ undrained shear-strength (su) derived from the corrected cone resistance (red line) and from the excess pore-water pressure at failure (blue line) at station GeoB16536-01. These results were compared with pushed CPTU data (yellow area, PFM11-S5, Sultan et al. 2008). Note: total vertical stress (σv0), effective vertical stress (σv0').

The quasi-static SWFF-CPTU parameters fit very good with the pushed CPTU data (i.e. Figs. 34 and Figure). The minor variations are depended on the different type of equipments (i.e. heavy pushed CPTU rig vs. lightweight FF-CPTU instrument) and that the tests are not deployed at the exact same position.

The corrected cone resistance for both tests varies between 100 and 200 kPa considering a strain-rate correction of 10-20 %. The sleeve friction for both deployments ranges from 2.0-4.0 kPa taking into account a strain-rate correction of 50-70 %. The pore-water pressure at failure for both tests are not higher than 35 kPa, using a strain-rate correction of ~15 % (Figs. 33 and 35).

The derived in-situ undrained shear strength varies from 5.0 to 10 kPa with an increase to approx. 25 kPa at >2.7 mbsf (Figs. 34 and 36). This increase is based on interbedded layers of stiff clays or probably coarse sediments. The dominated sediments are normally-consolidated to slightly over-consolidated due to a undrained shear-strength ratio (su/σv0') of 0.3-06. More data will be acquired during post-cruise geological/geotechnical laboratory measurements (standard- and advanced tests).

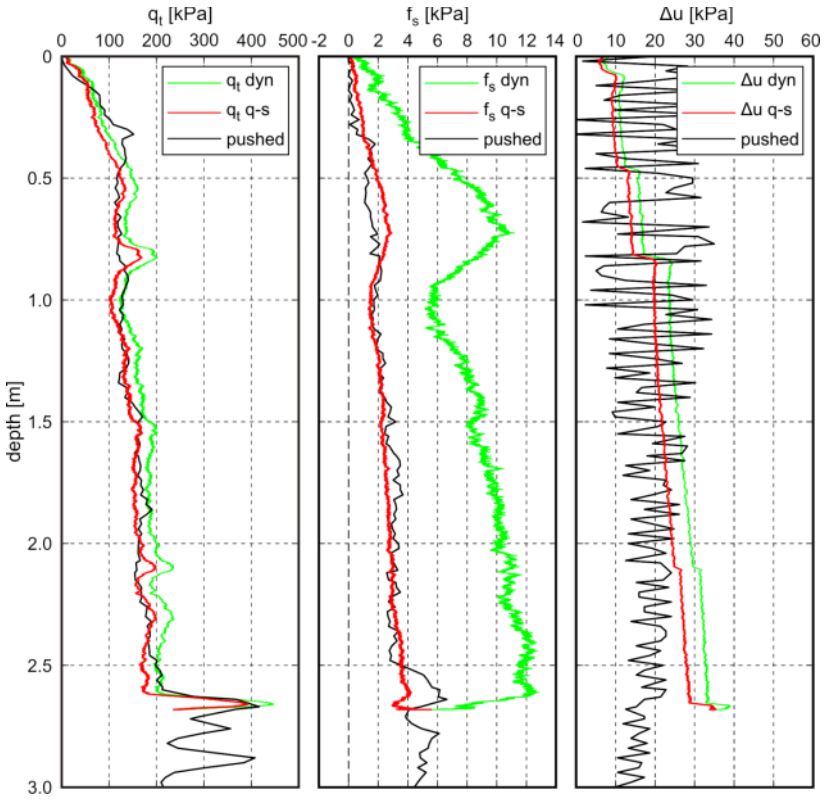

Figure 35: Measured and corrected SWFF-CPTU records for station GeoB16537-01. The green lines represent the measured (dynamic) parameters. The red lines show corrected (quasi-static) parameters taking into account the empirical strain-rate solutions (Dayal & Allen 1975, Mitchell 1976, A. Steiner, unpublished data). The black lines illustrate the pushed CPTU records (Sultan et al. 2008). Note: corrected cone resistance (qt), sleeve friction (fs), excess pore-water pressure at failure (Δu).

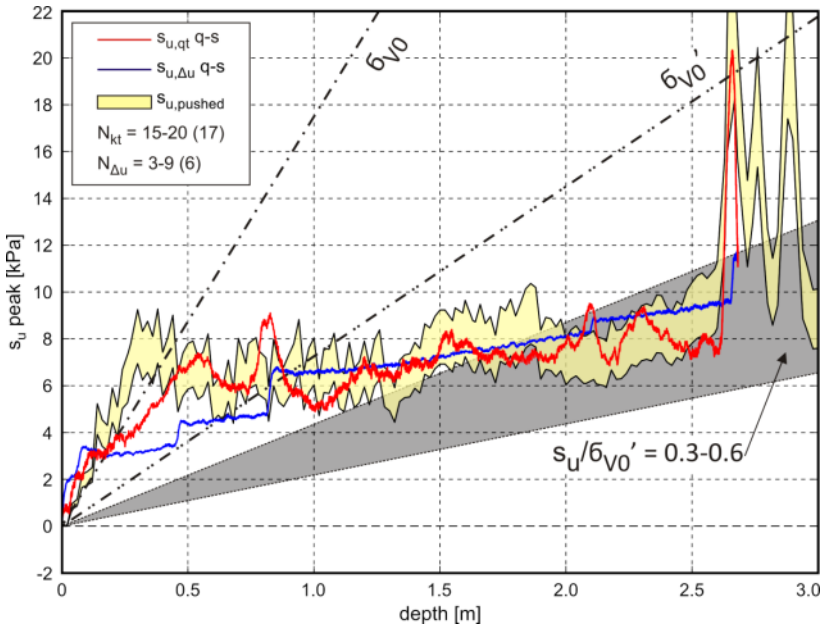

Figure 36: In-situ undrained shear-strength (su) derived from the corrected cone resistance (red line) and from the excess pore-water pressure at failure (blue line) at station GeoB16537-01. These results were compared with pushed CPTU data (yellow area, PFM11-S5, Sultan et al. 2008). Note: total vertical stress (σv0), effective vertical stress (σv0').

6.4. CAT-meters
(M. Tryon)

The five CAT meters deployed during cruise P410 were successfully recovered from the potential outcrop of the backthrust fault separating the "modern" MedRidge from the Inner Ridge (see Fig. 37). For positions, see also Table 4.

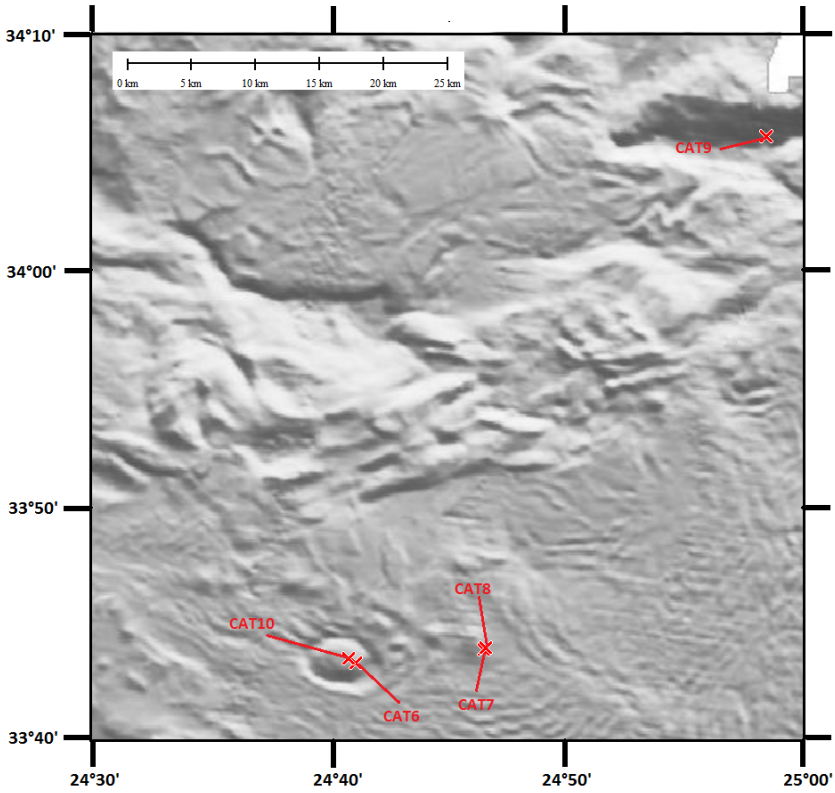

Figure 37: Map showing the locations of the CAT meter deployments. Background bathymetry courtesy of J. Mascle, Geosciences Azur, Villefranche-sur-Mer, France.

meter	release serial #	deploy date	recovery date	Latitude	Longitude	location
CAT 6	34152	28-03-11	29-03-12	33°43.45	24°41.15	center of Napoli mud volcano
CAT 7	34149	28-03-11	29-03-12	33°44.02	24°46.56	center of Milano mud volcano
CAT 8	34151	15-03-11	29-03-12	33°44.10	24°46.61	center of Milano mud volcano
CAT 9	34150	26-03-11	30-03-12	34°05.65	24°58.44	valley S of large ridge on inner-outer ridge border
CAT 10	34147	17-03-11	29-03-12	33°43.64	24°40.86	center of Napoli mud volcano

Table 4: Positions of CAT meters recovered during cruise P429.

6.5. Gravity coring and sediment description

(M. Belke-Brea, M. Geraga, G. Ferentinos, A. Kopf)

A total of 17 gravity cores were taken during cruise P429. Usually, either the 2m or 6m long version was used, sometimes equipped with outriggers containing MTLs (see sections 5.2 and 6.2 above). The cores can be divided into three subgroups on a regional basis:

- Sediment near the Spatha Ridge, NW Cretan Sea
- Inner Ridge-Cretan Margin transition, Mediterranean Ridge accretionary complex
- Nice Slope, Ligurian Margin.

The subdivision of the cores into these three categories is listed in Table 5. Note that cores from the Nice Slope were not opened on the vessel, but kept intact as WRs for post-cruise geotechnical experiments. They are hence not described in this section.

Region	Core GeoB165-	Length (cm)	Comments
Cretan Sea	02	0-425	yellowish-brown silt, brown and dark layers at top, patches of organic material, sand, etc.
	05	0-100	beige clayey silt
	06	0-80	light greyish brown silt, contains dark laminae
	09	0-40	reddish brown (top) to beige (bottom) soft silt
	12	0-137	greyish-beige sandy silt, coarser intervals
	13	0-186	greyish-beige sandy silt, water-rich
	14	0-15	silty sand with coral fragments
	15	0-78	greyish-beige sandy silt
	16	0-55	greyish-beige sandy silt
Inner Ridge – Cretan Margin	28	CC	firm dark grey mud, also indurated background silt (brown/beige), some mud breccia
	29	0-183	intensely layered clayey silt, some sapropel patches, dark grey mud shear zones, dip all 20°
	30	0-200	soft clayey silt on top, shill layer, carbonate crust, stiffer mud with and w/out clasts below
Nice airport			
	2	0-139	not opened
	3	0-485	not opened
	29	0-280	not opened
	30	0-150	not opened
	31	0-291	not opened

Table 5: List of gravity core stations during cruise P429.

Sediments from a landslide prone slope, Spatha Ridge

Gravity coring NW of Crete focused on two existing seismic profiles, line S6 from an unpublished report by Ferentinos & Papatheodorou (1989) and line 55/56 from a more recent survey (Ferentinos et al., unpublished). Only two stations were tried along line S6, with only a single core of 40 cm length

being recovered in an area of assumed mass wasting deposits (GeoB16509). For details, refer to Appendix 9.2.

All other coring investigated the well-imaged succession of sliding blocks, deformed sediment cover with cobblestone topography and intact sediment cover between the Spathan shelf and the Spatha Ridge further east. The reference core (i.e. unaffected by mass wasting) was taken eastward of the rise of presumed evaporitic origin. There, 4.25 m of undisturbed clayey silt with occasional layering, shell fragments and dark patches were recovered (GeoB16502). In contrast, much harder material was encountered along the shelf edge and slope further west (Fig. 38). At the shelf edge, very little material containing sand-sized and larger coral fragments were found (GeoB16514). Further downslope, cores were rather similar and showed indurated silt of beige, light grey, yellowish-brown or reddish colour. The only core with higher water content and low shear strength was GeoB16512, which appears to be located between two sliding blocks and may have provided access to the clayey silt underlying the coherent sliding blocks. The top of this unit can be followed as a coherent reflector in deep-towed Boomer profiles along the track of line 55/56 and may represent the sliding surface (Ferentinos et al., unpubl. data).

For details and complete core photographs, see Appendix 9.2.

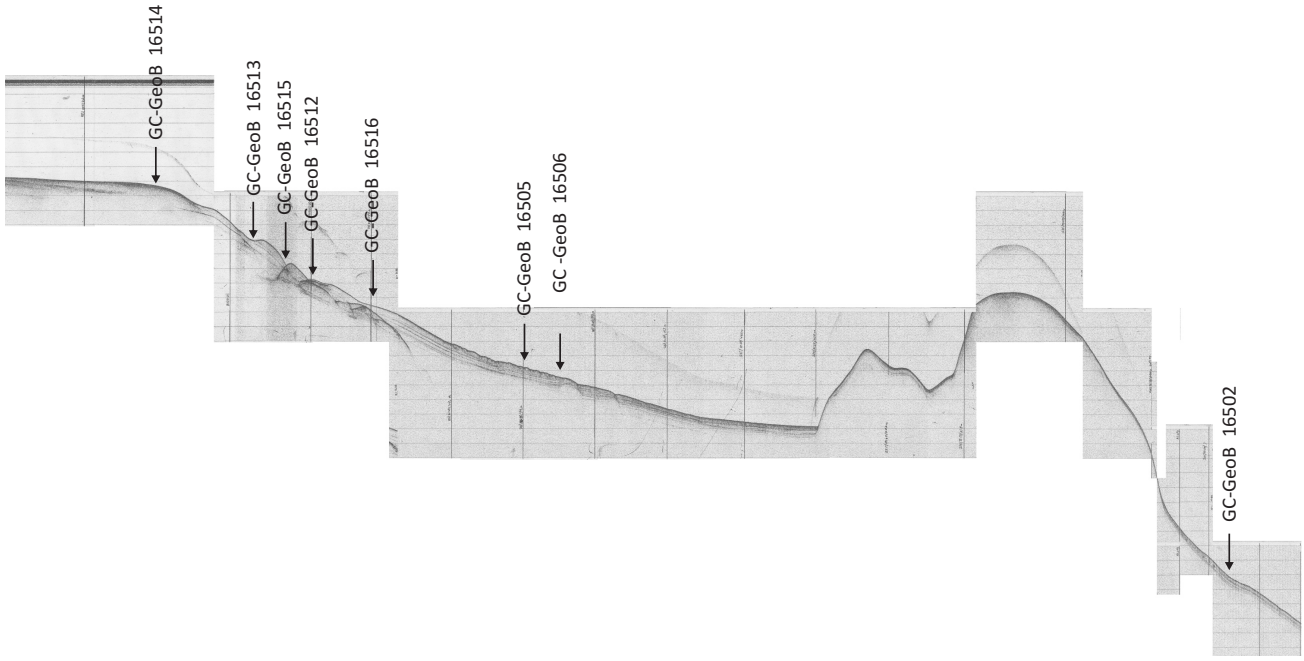

Figure 38: Seismic profile 55/56 along which the gravity cores were taken (see Station numbers).

Inner Ridge – Cretan Margin, Hellenic subduction zone

Three cores were taken along the contact between the Inner Ridge ancient accretionary complex and the Cretan Margin (see Table 5 and Fig. 39). In general, these cores are not so dissimilar from the ones recovered at the Inner deformation front, Inner ridge and Cretan margin a year earlier (P410; Kopf et al. 2012).

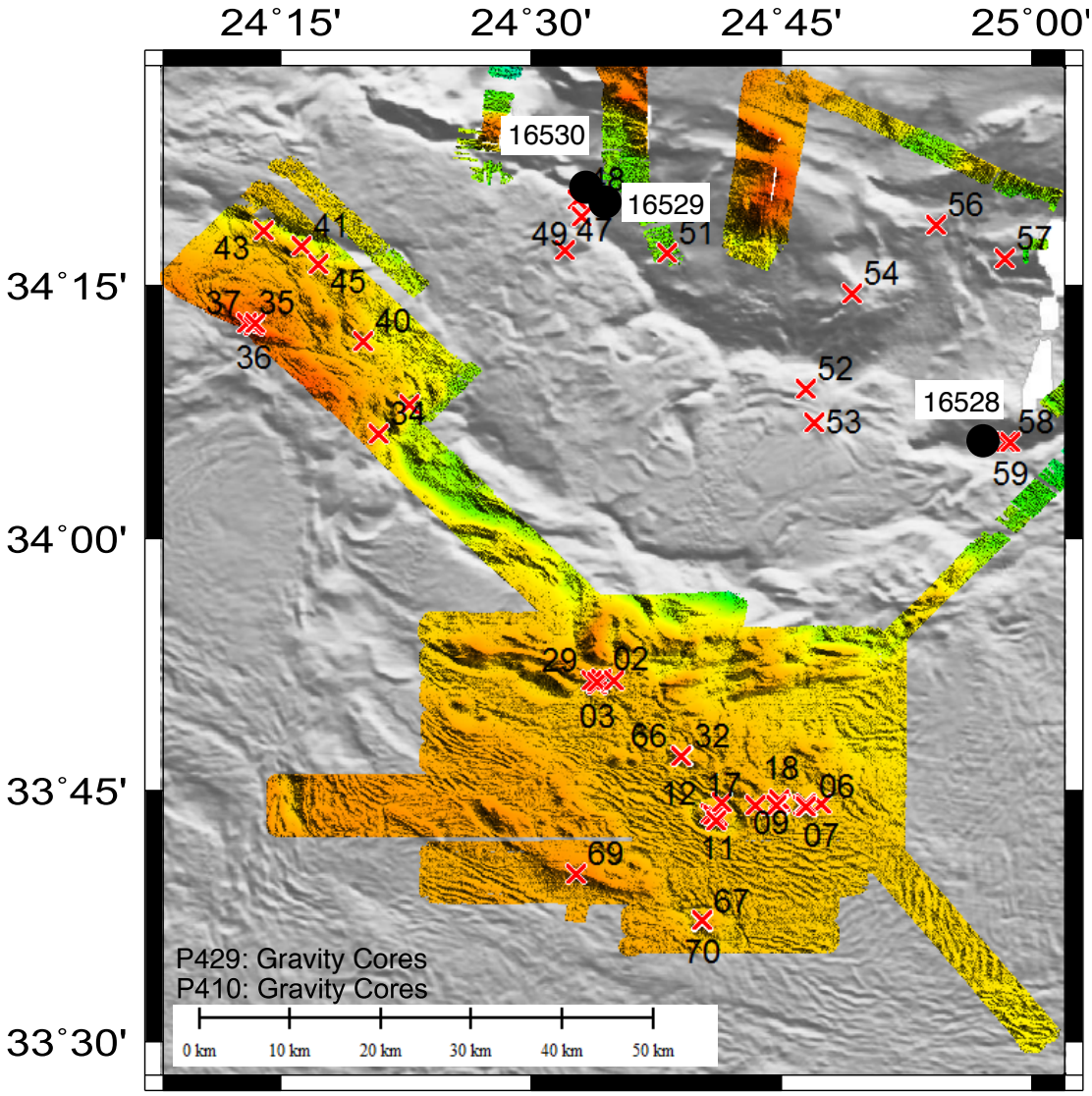

Figure 39: Map showing the gravity core locations visited during cruise P429 (white background on labels) and P410 (Kopf et al. 2012). Background bathymetry courtesy of J. Mascle, Geosciences Azur, Villefranche-sur-Mer, France.

Core GeoB16528 was taken in close proximity to former stations GeoB15358-1 and -3. No soft sediment was recovered, because the gravity corer apparently hit something rather hard and then toppled over. Along the 2m-long core barrel and stack of weights, however, soft sediment was found on one side. In the lower portion (appx. 100-200 cm), grey mud breccia with a muddy matrix and up to 8mm diameter claystone clasts was found. Above (0-100 cm and part of the weight set) greyish to brownish background hemipelagics were attached to the core barrel. In the core catcher, some 10-15 cm of hard dark grey clay as well as well-indurated clasts of various lithologies were found (Fig. 40). They were mainly lithified mud breccia (light and dark grey materials, some time in the same pebble) and well indurated brown, beige and light grey sediment. The latter showed fractures with alterations (reddish, dark brown; see Fig. 40), and may represent indurated hemipelagic material.

Figure 40: Clasts recovered in the CC at station GeoB16528, backthrust fault zone (?) onto Cretan Margin.

Some 23 nm further NW along the same tectonic suture, two cores were taken (GeoB16529 and -30; see Table 2). Core -29 recovered intensely sheared material containing breccia layers and rip up clasts. The succession of deformed background sediments of light grey and brownish colours with clasts of organic material (former sapropel layers?) and indurated silt and clay is interbedded with dark grey to greenish mud that behaved in a ductile/plastic manner and probably took up the larger portion of the strain (Fig. 41). This material is macroscopically very similar to the grey indurated muds seen in cores GeoB15358-1, -3 and GeoB15334 during P410 (Kopf et al. 2012). The background sediment was found in many of the GeoB153xx cores, however, was never observed in such a highly deformed state. At the top of core GeoB16529, a 2 cm-thick carbonate crust with abundant layering was found; this fragment may be part of a more continuous cover and is tentatively interpreted as sediment lithified by authigenic precipitation of methane-rich fluids ascending in this location (Fig. 42).

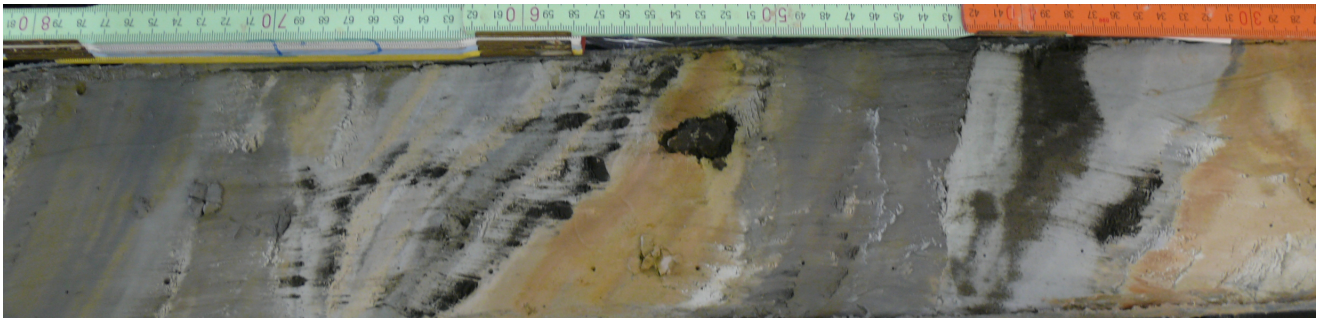

Figure 41: Sheared grey mud separating different packages of highly deformed and tilted hemipelagic sediment. Station GeoB16529 is located along the suture (backthrust FZ) separating the Inner Ridge and Cretan Margin. Shown is a blowup of section 2; for full description and photograph, see Appendix 9.2.

Figure 42: Carbonate crust recovered at the top of the core at station GeoB16529, backthrust fault zone (?) onto Cretan Margin.

Core GeoB16530, only 100 m NNW of -29, recovered 2m of rather different material. In its lower part (appx 150 cmbsf and below), indurated background sediment is seen. On top, a sheared light-grey mud breccia with various types of clasts (all 1 cm or smaller) is observed from ca. 130-150 cmbsf (Fig. 43). The material overlying the shear zone shows half an order of magnitude lower shear strength and is extremely water rich (see Appendix 9.2). Several intervals contain olive grey rounded rip up clasts, which point towards a downslope mass wasting mechanism with moderate transport length, most likely from the Cretan margin. Interestingly, a 10 cm-long piece of carbonate crust is seen beneath a layer of shell fragments (appx. 60 cmbsf), which is similar to the carbonate crust found at the top of core GeoB16529.

Figure 43: Sheared mud breccia with fragments of claystone, silstone and sapropel (130-150 cmbsf) separating indurated background sediment (right) from watery soft deposits (left/top) at station GeoB16530, Cretan Margin.

For full lithological description and core photographs of all split cores of expedition P429, refer to Appendix 9.2.

Nice Slope

A total of six gravity cores were taken south of the airport of Nice. They partly revisited sites of earlier deployment of instruments or gravity coring and were also accompanied by SW-CPTu

deployments in u1 configuration (see Ch. 6.3 above). None of the cores were opened on board so that sedimentological description is lacking. Cores will be transported to MARUM, undergo MSCL runs on the unsplit core, and get then cut into smaller whole round portions for geotechnical laboratory testing.

Core GeoB16538 is located close to core GeoB13941 and should contain gas-rich, undisturbed muds of the shelf break. After cutting in 1m-long segments, end caps were bulging owing to the gas trapped in the pores. Core -39 is located further west towards the retrogressive channel cut as a consequence of the 1979 event. Further west, a transect of three gravity cores (-40 through -42) along CHIRP profile 100 (P. Henry, unpubl. data) from the eastern plateau across the retrogressive channel (see Fig. 44). Finally, core -45 was taken in 47 m water depth at the slope from the 1979 scar towards the SW' edge of the eastern plateau. Some information on the gravity cores is also provided in Table 6.

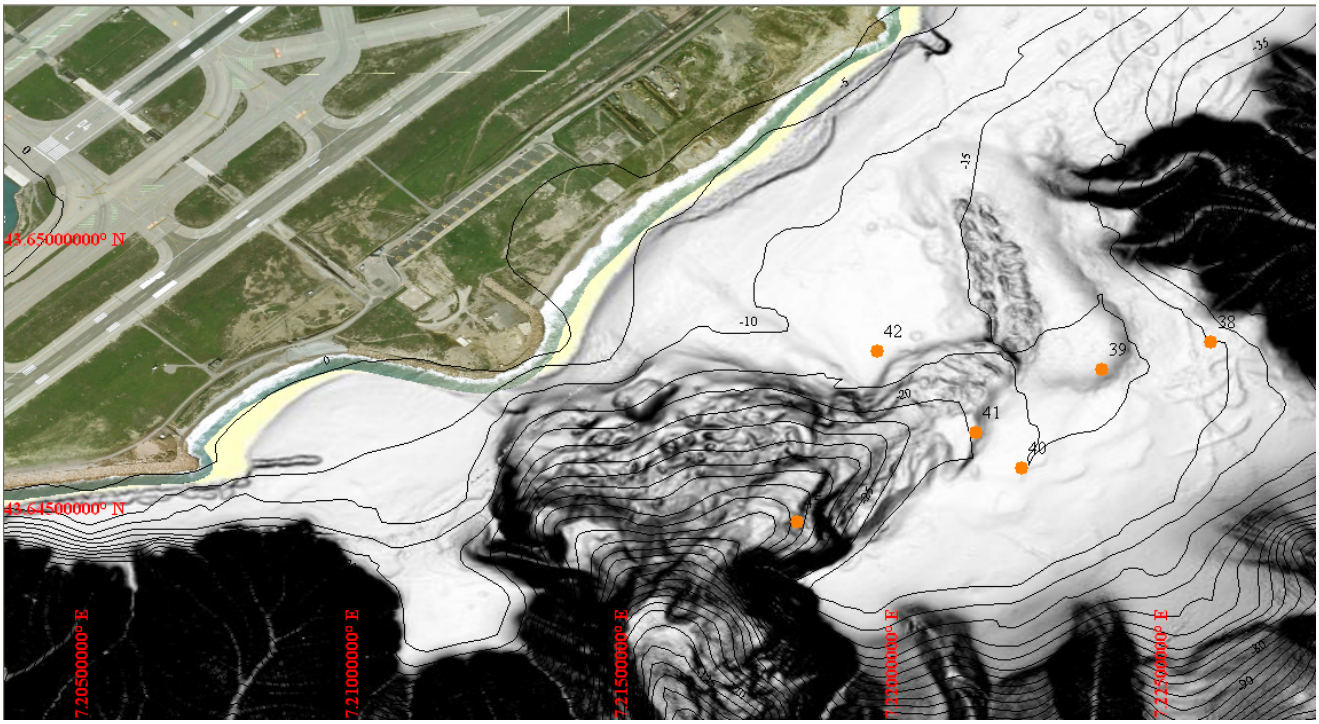

Figure 44: Map and satellite view of the Nice Airport area including the 1979 landslide scar and the 6 gravity cores taken during cruise P429. Numbers represent the GeoB165**XX** nomenclature.

Core	Adjacent Core	Related in situ test
GeoB16538	GeoB13941	Penfeld CPTu PFM11-S3, PFM11-S4
	Prisme KS 63	STEP-FFCPT-15, -16, -22
GeoB16539	-	-
GeoB16540	-	Penfeld CPTu PFM11-S2
		STEP-FFCPT-17
GeoB16541	-	Penfeld CPTu PFM11-S1
		STEP-FFCPT-18
GeoB16542	-	-
GeoB16545	Prisme KS 58	-

Table 6: Position, water depth, length of core recovered as well as comments referring to earlier cruises for the six gravity cores taken during cruise P429.

6.6. Physical properties

(G. Wiemer, S. Schlenzek)

All sediments of on board split cores have been analyzed for their undrained shear strength. Those data are presented next to the lithological core logs in Appendix 9.2. The following chapter will be divided according to the two main study areas where cores have been split on board. As the sediment cores from the third main study area, the Nice slope were brought to Bremen as whole rounds for further geotechnical analysis, no vane shear or penetrometer data is available.

Spatha Ridge, Cretan Sea

The first sediment core (GeoB16502) was taken north of the supposedly salt dome (Fig. 25). The shear strength of this hemipelagic 'reference sediment' increases linearly from ~20kPa to ~40kPa at ~4.25 mbsf. A harder package of sediment (τ ~60 kPa) extends from 2.10 – 2.60 mbsf. Those 40 cm of sediment are most likely overconsolidated. The first meter of sediment seems to be slightly overconsolidated whereas the lower portion of the cored sediment is normally consolidated. GeoB16505 and GeoB16506 are located within the creeping slope (Fig. 25). GeoB16505 has been cored where the sea floor is cobbled and GeoB16506 has been taken ~730 m further north, where an upwelling structure seems to act as a backstop for the creeping sediment. An attempt was set to reach the sediment of the up-doming sediments. Unfortunately low sediment coverage was achieved at both locations, GeoB16505 and GeoB16506. Highly overconsolidated (τ ~30 - 40 kPa) sediments situated close to the sea floor (0-40 cmbsf) are probably responsible for low recovery in that area. However, at 40 cmbsf the shear strength decreases rapidly to a stat of normal consolidation for ~20 cm. At 70 cmbsf a sudden increase in shear strength can be observed in core GeoB16505. Further up slope another package of sediment is highly disturbed and seems to move slowly toward the basin. GeoB16514 has been taken on the shelf edge for reference. The liner contains 16 cm of coarse grained coral sand, wrapped in a muddy matrix. The shear strength of this sediment has not been determined. GeoB16513 shows a similar shear strength pattern than the core GeoB16505. An overconsolidated (τ ~20 - 30 kPa) top layer (0- ~60 cmbsf) overlies a ~60cm package of normally consolidated sediment. This package is again followed by overconsolidated sediment (τ ~25 - 35 kPa). Although core GeoB16512 is about twice as long as core GeoB16516, they both show that pattern, too, but less pronounced. Core GeoB16515 shows ~10 cm thick, alternating packages of normally consolidated sediment though the sediment seems to be homogeneous. Creeping and seismic strengthening might be two effects induced by frequent earthquake shaking of this slope. The exception to this strengthening is core GeoB16512, which appears macroscopically water-rich and showed relatively low shear strength throughout. Given its location between two sliding units (and adjacent to

GeoB16515 with similar shear strength), one possible explanation is that it was covered by stronger (less permeable) sediment for a while and then was subjected to recent unroofing. Alternatively, the sediment's higher water content results from recent redeposition.
GeoB16509 has been taken along the seismic line S6 from Ferentinos & Papatheodou (1989). This sediment equally shows a state of overconsolidation (τ ~20 -30 kPa) at depth of only 20 cmbsf.

Inner ridge to Cretan margin

Three gravity cores (GeoB16528; -29; -30) have been taken in the trench located between the inner Mediterranean ridge and the Cretan margin. This area is characterized by the outcrop of a back thrust fault. The core GeoB16528 containes only gravel constituted of mud clasts, hard carbonate rock and lithified carbonate crust. Shear strength data is therefore not available. The shear strength of the sediment present in GeoB16529 has been determined at a usual spacing of 5 cm only for the lower part (~110 cmbsf - ~200 cmbsf). High matter of shall fragments made penetrometer and vane shear data obsolete. The lower part of the core shows shear strengths varying from ~20 kPa to ~70 kPa and shows thus overconsolidated sediment. The core GeoB16530 shows an alternation of highly overconsolidated and slightly over- to -normally consolidated layers of sediment. From a depth of ~80 cmbsf to ~180 cmbsf the state of overconsolidation stays at a high level. The shear strength ranges from 40 kPa to 120 kPa within this meter of sediment. Distinct peaks high shear strength (τ ~200 kPa) may be related to the presence of mud clasts within the extremely disturbed deposits.

Nice Slope

Cores taken within and around the Nice Airport landslide area have not been split on board. Those whole round samples have been brought to MARUM intact for further geotechnical laboratory tests. Thus, no shear strength data is available in this report.

6.7. Pore water geochemistry

(A. Kopf)

During this cruise, pore waters were sampled regularly in gravity cores recovered from Area 1 (NW Crete) and Area 2 (MedRidge and Inner Ridge). No analyses were carried out onboard RV *Poseidon*, so that results will only be available post-cruise and cannot be included into this report.

7. References

Assier-Rzadkiewicz, S., Heinrich, P., Sabatier, P.C., Savoye, B., and Bourillet, J.F., 2000. Numerical Modelling of a Landslide-generated Tsunami: The 1979 Nice Event. Pure and Applied Geophysics, 157, 1707-1727.

Bebout, G.E., Ryan, J.G., Leeman, W.P., Bebout, A.E., 1999. Fractionation of trace elements by subduction zone metamorphism - effect on convergent margin thermal evolution. Earth Planet. Sci. Letts., 171: 63-81

Bjorlykke, K., Hoeg, K., 1997. Effects of burial diagenesis on stresses, compaction and fluid flow in sedimentary basins. *Mar. Petr. Geol*., 14/3: 267-276

Blum P., 1997. Physical properties handbook: a guide to the shipboard measurement of physical properties of deep-sea cores, Techn Note 26, ODP.

Brenan, J.M., Shaw, H.F., Ryerson, F.J., Phinney, D.L., 1995. Mineral-aqueous fluid partitioning of trace elements at 900°C and 2 GPa: constraints on the trace element geochemistry of mantle and deep crustal fluids. *Geochim. Cosmochim. Acta*, 59: 3331-3350

Burrus, J., Bessis, F. and Doligez, B., 1987. Heat flow, subsidence and crustal structure of the Gulf of Lions (NW Mediterranean): a quantitative discussion of the classical passive margin model. In: Sedimentary Basins and Basin-Forming Mechanisms (C. Beaumont & A.J. Tankard, eds). *Mem. Can. Soc. Petrol. Geol.,* 12, 1–15.

Byerlee, J.D., 1978. Friction of rocks. *Pure and Applied Geophys.* 116, 615-626.

Chaumillon, E., Mascle, J., 1997. From foreland to forearc domains: new multichannel seismic reflection survey of th e Mediterranean Ridge accretionary complex (Eastern Mediterranean). Mar. Geology, 138: 237-259

Chronis, G., Lykousis, V., Anagnostus, C., Karageorgis, A., Stavrakakis, S., Poulus, S., 2000. Sedimentological processes in the southern margin of the Crete Sea (NE Mediterranean). Progress in Oceanography 46, 143-160

Cochonat, P., Dodd, L., Bourillet, J.F., Savoye, B., 1993. Geotechnical characteristics and instability of submarine slope sediments, the Nice slope (NW Mediterranean Sea). Marine Georesources and Geotechnology, 11, 131-151.

Dählmann, A., de Lange, G.J., 2003. Fluid-sediment interactions at Eastern Mediterranean mud volcanoes : a stable isotope study from ODP Leg 160. *Earth Planet. Sci. Letts.,* 212: 377-391.

Dan, G., Sultan, N., Savoye, B., 2007. The 1979 Nice Harbour Catastrophe revisited: Trigger mechanism inferred from geotechnical measurements and numerical modelling, *Marine Geology*, 245 (1-4), 40-64.

Dayal U., Allen J.H. 1975. The effect of penetration rate on the strength of remolded clay and sand samples. *Can. Geotech. J.* 12:336–348

Dewhurst, D.N., Yang, Y., Aplin, A., 1999. Permeability and fluid flow in natural mudstones. *Geol. Soc. London, Spec. Publ.* 158: 23-43

Deyhle, A., Kopf, A., 2001. Deep fluids and ancient pore waters at the backstop: Stable isotope systematics (C, B, O) of mud volcano deposits on the Mediterranean Ridge accretionary wedge. *Geology*, 29/11: 1031-1034.

Deyhle, A., Kopf, A., 2002. Strong B enrichment and anomalous $d^{11}B$ in pore fluids from the Japan Trench forearc. *Marine Geology* 183: 1-15.

Deyhle, A., Kopf, A.J., 2005. The use and usefulness of boron isotopes in natural silicate-water systems. *Physics and Chemistry of the Earth*,30: 1038-1046.

Dia, A.N., Castrec-Rouelle, M., Boulègue, J., and Boudou, J.P., 1995. Major and trace elements and Sr isotope constraints on fluid circulations in the Barbados accretionary complex. Part 1: Fluid origin. *Earth Planet. Sci. Letts.*, 134: 69-85.

Elliot, T., Plank, T., Zindler, A., White, W., Bourdon, B.,1997. Element transport from slab to volcanic front at the Mariana arc. *J Geophys Res* 102: 14,991-15,019.

Emeis, K.-C., Robertson, A.H.F., Richter, C., Shipboard Scientific Party, 1996. Proc. ODP, Init. Repts., 160, College Station, TX (Ocean Drilling Program), 972pp.

Ferentinos, G. 1992 Recent gravitative mass movements in a highly tectonically active arc system: The Hellenic Arc. Marine Geology 104: 93-107

Ferentinos, G., Lykousis, V., Papatheodorou G. and Iatrou, M. (accepted for publication). Hellenic Arc Shelf: Late Quaternary Tectonics, Sea-level changes, Sedimentation and Geo-hazards. Special Publications British Geological Society

Ferentinos, G. and Papatheodorou, G. 1989. Submarine Geological Survey in the Kythera Straits for the laying of submarine power cables between Peloponessos and Crete. Internal Report N^0 5, Laboratory of Marine Geology and Physical Oceanography, University of Patras, Greece.

Gennesseaux, M., Mauffret, A., Pautot, G. 1980. Les glissements sous-marins de la pente continentale niçoise et la rupture des câbles en mer Ligure (Méditerranée occidentale). C.R. Acad. Sc. Paris 290 t.

Gerya , T.V., Stöckhert , B., Perchuk, A.L., 2002. Exhumation of high-pressure metamorphic rocks in a subduction channel—a numerical simulation. Tectonics, 21, 1056, doi:10.1029/2002TC001406

Giresse, P., Buscail, R., Charriere, B., 2003. Late Holocene multisource material input into the Aegean Sea: depositional and post-depositional processes. Oceanologica Acta 26, 657-672

Guangzhi, T., 1996. *Low-Temperature Geochemistry*. Bejing, China (Science Press), 216pp.

Hansbo S., 1957. A new approach to the determination of the shear strength of clay by the fall-cone test. Royal Swedish Geotechnical Institute Proc. No. 14, Stockholm.

Hedberg, H., 1974. Relation of methane generation to undercompacted shales, shale diapirs and mud volcanoes. *AAPG Bull*., 58: 661-673

Henry, P., Le Pichon, X., Lallemant, S., Lance, S., Martin, J. B., Foucher, J.-P., Fiala-Médioni, A., Rostek, F., Guilhaumou, N., Pranal, V., and Castrec, M., 1996. Fluid flow in and around a mud volcano field seaward of the Barbados accretionary wedge: Results from Manon cruise. Journal of Geophysical Research 101(B9), 20297-20323

Higgins, G.E., Saunders, J.B., 1974. Mud volcanoes – Their nature and origin. *Verhandlungen der Naturforschenden Gesellschaft Basel*, 84: 101–152

Hubbert, M., Rubey, W.W., 1959. Role of fluid pressure in mechanisms of overthrust faulting: I. Mechanics of fluid-filled porous solids and its application overthrust faulting. *GSA Bull*., 70: 115-160

Johnson, M.C., Plank, T., 1999. Dehydration and melting experiments constrain the fate of subducted sediments. *Geochemistry, Geophysics, Geosystems - G* ^{3} 1:paper1999GC000014

Kamber, B.S., Collerson, K.D., 2000. Role of "hidden" deeply subducted slabs in mantle depletion. *Chem Geol* 166: 241—254.

Kastens K., 1991. Rate of outward growth of the Mediterranean Ridge accretionary complex.

*Tectonophysics*199: 25-50

Kawamura, K., Ogawa, Y., 2004. Progressive change in pelagic clay microstructureduring burial process: examples from piston cores and ODP cores. *Marine Geol*. 207: 131-144

Kogiso T., Tatsumi Y., Nakano S., 1997. Trace element transport during dehydration processes in the subducted oceanic crust: 1. Experiments and implications for the origin of oceanic island basalts. *Earth Planet Sci Lett* 148: 193-205

Kokkalas, S., Xypolias, P. Koukouvelas, I. & Doutsos, T. 2006. Post-Collisional Contractional and Extensional Deformation in the Aegean region. In: Dilek, Y., Pavlides, S. (eds) Post Collisional Tectonics & Magmatism in the Mediterranean Region and Asia, Geological Society of America Special Paper,409, 97-123

Kopf, A., Robertson, A.H.F., Clennell, M.B., Flecker, R., 1998. Mechanisms of mud extrusion on the Mediterranean Ridge Accretionary Prism. Geo-Marine Letters, 18: 97-114.

Kopf, A., Behrmann, J.H., 2000. Extrusion dynamics of mud volcanoes on the Mediterranean Ridge accretionary complex. In: Vendeville, B., Mart, Y. & Vigneresse, J.-L. (eds.), From the Arctic to the Mediterranean: Salt, shale, and igneous diapirs in and around Europe. Geol. Soc. London, Spec. Publ., 174: 169-204

Kopf, A., Deyhle, A., Zuleger, E., 2000. Evidence for deep fluid circulation and gas hydrate dissociation using boron and boron isotopes in forearc sediments from Costa Rica (ODP Leg 170). Marine Geology, 167: 1-28

Kopf, A., Klaeschen, D., Mascle, J., 2001. Extreme efficiency of mud volcanism in dewatering accretionary prisms. *Earth Planet. Sci. Letters*, 189/3-4: 295-313

Kopf, A., 2002. Significance of mud volcanism. *Reviews of Geophysics*, 40/2, 52pp. [DOI 10.1029/2000RG000093]

Kopf, A.J., Deyhle, A., 2002. Back to the roots: Source depths of mud volcanoes and diapirs using boron and B isotopes. *Chem. Geology*, 192: 195-210.

Kopf, A., P.R. Castillo, A. Deyhle, 2002. Water-Rock Interaction in the Upper Seismogenic Zone in the Nankai Trough Subduction Factory. *EOS, Trans. AGU (Supplement),* 83/47, F1294.

Kopf, A., Mascle, J., Klaeschen, D., 2003a. The Mediterranean Ridge: A mass balance across the fastest growing accretionary complex on Earth. *J. Geophys. Research* 108, 2372-2403, doi:10.1029/2001JB000473.

Kopf, A., Clennell, M.B., Brown, K.M., 2005. Physical properties of extruded muds and their relationship to episodic extrusion and seismogenesis. Martinelli, G., Panahi, B. (Eds.), Mud volcanoes, geodynamics and seismicity. *NATO Sci. Ser. IV*: 263-283

Kopf, A., Alves, T., Heesemann, B., Kaul., N.E., Kock, I., Krastel, S., Reichelt, M., Schäfer, R., Stegmann, S., Strasser, M., Thölen, M., 2006. REPORT & PRELIMINARY RESULTS OF POSEIDON CRUISE P336: CRESTS - Cretan Sea Tectonics and Sedimentation. *Berichte aus dem Fachbereich Geowissenschaften, Univ. Bremen,* No. 253: 140pp.

Kopf, A., and shipboard party, 2008. REPORT AND PRELIMINARY RESULTS OF METEOR CRUISE M73/1: LIMA-LAMO. *Berichte aus dem Fachbereich Geowissenschaften der Univ. Bremen,* No. 264: 169pp.

Kopf, A., R. Apprioual, J. Blandin, J.-P. Brulport, P. Crassous, T. Fleischmann, A. Förster, G. Guyader, S. Hammerschmidt, P. Henry, R. Jacinto Silva, J. Legrand, A. Mayer, S. Pape, P. Pelleau, P. Pichavant, T. Pichler, R. Price, M. Seydel, S. Stegmann, K. Weber, 2009. REPORT AND PRELIMINARY RESULTS OF POSEIDON CRUISE P386: NAIL (Nice Airport

Landslide), *Berichte aus dem Fachbereich Geowissenschaften der Univ. Bremen*, No. 271: 161pp

Kopf, A., Stegmann, S., Delisle, G., Panahi, B., Aliyev, C.S., Guliyev, I., 2009. *In situ* CPTU experiments at active Dashgil mud volcano, Azerbaijan: Evidence for excess fluid pressure, updoming, and possible future violent eruption. *Mar. Petrol. Geology*

Kopf, A., Kasten , S., Blees, J., 2010. Geochemical evidence for groundwater-charging of slope sediments: The Nice Airport 1979 landslide and tsunami revisited. *Proc. IGCP511, Submarine mass movements and their consequences*, Houston (TX), 2009.

Kopf, A., Bartsch, C., Castellino, J., Fleischmann, T., Haas, S., Ioakim, C., Kirsch, K., Kufner, S.K., Steiner, A., Tryon, M.D., Wiemer, G., Zabel., M., 2012. REPORT AND PRELIMINARY RESULTS OF POSEIDON CRUISE P410: MudFlow (Mud volcanoes and fluid flow in the Mediterranean Ridge Accretionary Complex), *Berichte aus dem Fachbereich Geowissenschaften der Univ. Bremen*, No. 284: 128 pp.

Lavrushin, V.U., Polyak, B.G., Prasolov, R.M., Kamenskii, I.L., 1996. Sources of material in mud volcano products (based on isotopic, hydrochemical, and geological data). *Lithology Min. Resources,* 31/6: 557-578

Lunne T., Robertson P.K., Powell J.J.M., 1997. Cone penetration testing in geotechnical practice. Spon Press, London

Mascle, J., Huguen, C., Benkhelil, J., Chamot-Rooke, N. Chaumillon, E., Foucher, J.-P., Griboulard, R., Kopf, A., Lamarche, G., Volkonskaia, A., Woodside, J., and Zitter, T., 1999. Images may show start of European-African Plate collision. *EOS Trans. AGU,* 80/37: 421-428

McKenzie, D. 1972. Active tectonics in the Mediterranean region. Geophysical J. Royal Astronomical Society, 30, 109-185

Meier, T., Becker D., Endrun, B., Rische, M., Bohnhoff, M., Stöckhert, B. & Harjes, H.-P., 2007. A model fort he Hellenic subduction zone in the area of Crete based on seismological investigations. In: Taymaz, T., Yilmaz, Y. & Dilek, Y. (eds.), Geodynamics of the Aegean and Anatolia, *Geol. Soc. London, Spec. Publ*., 291: 183-199.

Mitchell J.K. 1976. Fundamentals of Soil Behavior. Wiley New York

Moore, J.C., Saffer, D., 2001. Updip limit of the seismogenic zone beneath the accretionary prism of southwest Japan: An effect of diagenetic to low-grade metamorphic processes and increasing effective stress. *Geology*, 29: 183-186

Morris J.D., Leeman W.P., Tera F.,1990. The subducted component in island arc lavas: Constraints from Be isotopes and B-Be systematics. Nature 344: 31-36.

Papazachos, B. and Papazachou, E. 1977. Earthquakes in Greece, Zitis Publihers, Greece.

Pfender, M., H.W. Villinger, 2002. Miniaturized data logger for deep sea sediment temperature measurements, Mar. Geol. 186: 557-570

Plank, T., Langmuir, C.H., 1998. The chemical composition of subducting sediment and its consequences for the crust and mantle. *Chem. Geol.* 145: 325-394.

Rehault, J.P., Bethoux, N., 1984. Earthquake relocation in the Ligurian Sea (Western Mediterranean): Geological interpretation. Marine Geology, Vol. 55, pp. 429-445.

Rice, J. R., 1992, Fault stress states, pore pressure distributions, and the weakness of the San Andreas fault, *in* Fault Mechanics and Transport Properties of Rocks, B. Evans, T. F. Wong (eds.), pp. 475-503, Academic, San Diego, CA.

Robertson, A.H.F., Kopf, A., 1998. Origin of clasts and matrix within Milano and Napoli mud

volcanoes, Mediterranean Ridge accretionary complex. In: Robertson, A.H.F., Emeis, K.-C., Richter, C., et al., 1998. Proc. ODP, Sci. Results., 160, College Station, TX (Ocean Drilling Program), 575-596

Rollet, N., Deverchère, J., Beslier, M.O., Guennoc P., Réhault, JP., Sosson M., Truffert, C., 2002. Back arc extension, tectonic inheritance, and volcanism in the Ligurian sea, Western Mediterranean. *Tectonics*, 21/3, 218-243.

Rothwell, R.G., 1989.Minerals and mineraloids in marine sediments: an optical identification guide, Elsevier Appl. Sci., London, 279 pp.

Ryan W.B.F., Hsü K.C., et al. 1973. Hellenic Trench Sites 127 and 128. *Proc. DSDP, Init. Results*, 13 (US Govt. Printing Office, Washington), Pt. 2: 243-322

Seeberg-Elverfeldt, J., Schlüter, M., Feseker, T., Kölling, M. (2005) Rhizon sampling of porewaters near the sediment-water interface of aquatic systems. Limnol. Oceanogr. Methods, 3: 361-371.

Shipboard Scientific Party, 2002. Leg 195 summary. *In* Salisbury, M.H., Shinohara, M., Richter, C., et al., *Proc. ODP, Init. Repts.,* 195: College Station, TX (Ocean Drilling Program), 1–63. doi:10.2973/odp.proc.ir.195.101.2002

Spivack, A. J., Palmer, M.R., Edmond, J. M., 1987. The sedimentary cycle of the boron isotopes. *Geochim. Cosmo. Acta* 51, 1939-1949

Stegmann, S., Moerz, T., Kopf, A., 2006. Initial Results of a new Free Fall-Cone Penetrometer (FF-CPT) for geotechnical *in situ* characterisation of soft marine sediments. *Norwegian Journal of Geology*, 86/3: 199-208.

Stegmann, S., Strasser, M., Anselmetti, F.S., Kopf, A., 2007. Geotechnical *in situ* characterisation of subaquatic slopes: The role of pore pressure transients versus frictional strength in landslide initiation. *Geophysical Research Letts.*, 34/7, doi:10.1029/2006GL029122.

Stegmann, S., Kopf, A., 2007. Marine deep-water Free-fall CPT measurements for landslide characterisation off Crete, Greece (Eastern Mediterranean Sea). Part 1: A new 4000 m cone penetrometer. Lykousis, V., Sakellariou, D., Locat, J. (eds.), Submarine Mass movements and their consequences. Advances in Natural and Technological Hazards Series, Springer, 171-177.

Stegmann, S., Sultan, N., Kopf, A., Apprioual, R., Pelleau, P., 2011. Hydrogeology and its effect on slope stability along the coastal aquifer of Nice, France. Marine Geology, 280: 168-181

Stegmann, S., Sultan, N., Pelleau, P., Apprioual, R., Garziglia, S., Kopf, A., Zabel, M., 2012. A long-term monitoring array for landslide precursors. A case study at the Ligurian Slope. *OTC Proceedings*, Houston April 2012, paper number OTC-23271-PP

Strozyk, F., Huhn, K., Strasser M., Krastel, S., Kock, I., A.J. Kopf 2009. New evidence for massive gravitational mass-transport deposits in the southern Cretan Sea, eastern Mediterranean. *Marine Geology, 263: 97-107*

Strozyk, F., Strasser, M., Foerster, A., Kopf, A., Huhn, K., 2010. Slope failure repetition in active margin environments: Constraints from submarine landslides in the Hellenic forearc, eastern Mediterranean. *J. Geophys. Res., Vol. 115, B08103, 13 PP., doi:10.1029/2009JB006841.*

Sultan, N., and shipboard party, 2008. Prisme Cruise (R/V Atalante Toulon - Toulon; 2007): Reports and Preliminary Results. *IFREMER Internal Report*, Ref: IFR CB/GM/LES/08-11, 180pp.

Tera, F., Brown, L., Morris, J., Sacks, I.S., Klein, J., Middleton, R., 1986. Sediment incorporation in island arc magmas: inferences from ^{10}Be, *Geochim. Cosmochim. Acta*, 50: 636-660

Thomson, S.N., Stöckhert, B., Brix, M.R., 1998. Thermochronology of the high-pressure metamorphic rocks of Crete, Greece: Implications for the speed of tectonic processes. *Geology*, 26/3: 259-262

Tryon, M.D., Brown, K.M., Dorman, L., Sauter, A., 2001. A new benthic aqueous flux meter for very low to moderate discharge rates. *Deep Sea Research* Pt. I, 48: 2121-2146

Tryon, M.D., K.M. Brown, M. Torres (002. Fluid and chemical flux in and out of sediments hosting methane hydrate deposits on Hydrate Ridge, OR, II: Hydrological processes, *Earth Planet. Sci. Lett.,* 201(3-4), 541-557.

Tryon, M.D., Wheat, C.G., Hilton, D.R., 2010. Fluid sources and pathways of the Costa Rica erosional convergent margin. *Geology, Geophysics, and Geosystems (G-Cubed)*, doi:10.1029/2009GC002818

Villinger, H., Gennerich, H.H., Grevemeyer, I., Kaul, N., 2002. INGGAS-Flux: New tools for energy and fluid flux, pore pressure and thermal gradient. *GEOTECHNOLOGIEN Science Rept.,* 1: 139-141

Wentworth, C.K., 1922. A scale of grade and class terms of clastic sediments. *J. Geol.,* 30:377-392.

Wood, D.M., 1985. Some fall-cone tests. Géotechnique*,* 35, 64-68.

You, C.-F., Spivack, A.J., Smith, J.H., Gieskes, J.M., 1993. Mobilization of boron at convergent magins: Implications for boron geochemical cycle. *Geology*, 21: 207-210

You, C.-F., Castillo, P.R., Gieskes, J.M., Chan, L.H., Spivack, A.J., 1996. Trace element behavior in hydrothermal experiments: Implications for fluid processes at shallow depths in subduction zones. *Earth Planet. Sci. Letts*., 140, 41-52

8. Acknowledgements

We thank Master Matthias Günther and his officers on the bridge for his expert manoeuvring in the study area, his cooperation, and outstanding support during complex operations, in particular at night. Special thanks go also to boatswain Frank Schrage and the entire crew of R/V *Poseidon* for their friendly support and efficient technical assistance with the various devices used.

Our colleagues at HCMR, namely Vasilis Lykousis, are acknowledged for their helpful discussion of scientific targets.

Ali Deghani (Univ. Hamburg, Germany) is acknowledged for providing their deck unit for acoustically releasing instruments as back-up for cruise P429.

Partners at MARUM Bremen (Goetz Ruhland, Volker Diekamp) as well as at IfM-GEOMAR (Klas Lackschewitz) have also provided crucial help with expedition planning, logistical decisions, and post-cruise demobilisation. Additionally, Klaus Bohn is thanked for his repeated professional logistical assistance.

Thanks go also to the German Science Foundation (DFG) for providing the funds to realise the *P429* cruise within the frame of MARUM research area SD5 as well as a project termed MUDDY WATERS.

Appendices

9.1. Station list

9.2. Lithologs and shear strength data

Station	GeoB165xx	Date	Time (UTC)	PositionLat	PositionLon	Water Depth [m]	Device
SPATHA RIDGE							
POS429/036-1	01	22.03.12	16:18	35° 39,83' N	23° 47,55' E	139,7	Multibeam
POS429/036-1		22.03.12	18:14	35° 46,90' N	23° 55,64' E	678,8	Multibeam
POS429/036-1		22.03.12	18:34	35° 47,91' N	23° 54,29' E	672,9	Multibeam
POS429/036-1		22.03.12	20:28	35° 40,90' N	23° 46,32' E	106,2	Multibeam
POS429/036-1		22.03.12	20:37	35° 40,44' N	23° 46,83' E	116	Multibeam
POS429/036-1		22.03.12	22:26	35° 47,25' N	23° 54,36' E	654,5	Multibeam
POS429/036-1		22.03.12	22:53	35° 48,21' N	23° 52,32' E	618,5	Multibeam
POS429/036-1		23.03.12	00:38	35° 41,65' N	23° 45,19' E	87,6	Multibeam
POS429/036-1		23.03.12	00:48	35° 41,42' N	23° 45,86' E	130,3	Multibeam
POS429/036-1		23.03.12	02:28	35° 47,55' N	23° 52,60' E	596,1	Multibeam
POS429/036-1		23.03.12	02:43	35° 48,35' N	23° 51,58' E	607,3	Multibeam
POS429/036-1		23.03.12	04:25	35° 41,99' N	23° 44,62' E	74,4	Multibeam
POS429/036-1		23.03.12	04:32	35° 42,37' N	23° 44,10' E	205,4	Multibeam
POS429/036-1		23.03.12	06:12	35° 48,58' N	23° 50,86' E	575,4	Multibeam
POS429/037-1	02-1	23.03.12	06:40	35° 47,56' N	23° 53,52' E	639,1	CTD/rosette water sampler
POS429/037-2	02-2	23.03.12	07:10	35° 47,57' N	23° 53,52' E	637,7	Gravity corer
POS429/038-1	03	23.03.12	08:25	35° 45,25' N	23° 52,23' E	305,3	Gravity corer
POS429/039-1	04	23.03.12	09:14	35° 45,39' N	23° 52,27' E	275,9	Gravity corer
POS429/040-1	05-1	23.03.12	10:48	35° 41,26' N	23° 49,99' E	366,8	Gravity corer
POS429/040-2	05-2	23.03.12	11:36	35° 41,25' N	23° 50,00' E	367,1	Gravity corer
POS429/040-3	05-3	23.03.12	12:15	35° 41,25' N	23° 49,99' E	366,8	Cone penetration testing
POS429/041-1	06-1	23.03.12	13:11	35° 41,61' N	23° 50,19' E	381,8	Gravity corer
POS429/041-2	07-1	23.03.12	13:31	35° 41,61' N	23° 50,19' E	381,5	Cone penetration testing
POS429/042-1	07-2	23.03.12	14:29	35° 42,53' N	23° 50,72' E	422,2	Cone penetration testing
POS429/043-1	07-3	23.03.12	15:25	35° 43,19' N	23° 51,10' E	438,9	Cone penetration testing
POS429/044-1	08	23.03.12	16:30	35° 43,79' N	23° 51,59' E	439,8	Multibeam
POS429/044-1		23.03.12	17:00	35° 45,44' N	23° 53,75' E	395,7	Multibeam
POS429/044-1		23.03.12	17:08	35° 45,01' N	23° 54,34' E	435,2	Multibeam
POS429/044-1		23.03.12	18:57	35° 38,84' N	23° 47,14' E	57,6	Multibeam
POS429/044-1		23.03.12	19:07	35° 38,19' N	23° 47,62' E	86,8	Multibeam
POS429/044-1		23.03.12	20:09	35° 41,50' N	23° 51,83' E	406,3	Multibeam
POS429/044-1		23.03.12	20:14	35° 41,78' N	23° 51,57' E	411,5	Multibeam
POS429/044-1		23.03.12	21:11	35° 38,63' N	23° 47,64' E	100,3	Multibeam
POS429/044-1		23.03.12	21:57	35° 40,77' N	23° 48,63' E	315,1	Multibeam
POS429/045-1	09	24.03.12	11:44	35° 45,01' N	23° 43,03' E	776	Gravity corer
POS429/046-1	10	24.03.12	12:43	35° 45,29' N	23° 42,91' E	777,4	Gravity corer
POS429/047-1	11	24.03.12	13:30	35° 46,54' N	23° 43,28' E	760,7	Multibeam
POS429/047-1		24.03.12	13:51	35° 48,07' N	23° 42,82' E	778,3	Multibeam
POS429/047-1		24.03.12	13:58	35° 48,09' N	23° 42,29' E	791,2	Multibeam
POS429/047-1		24.03.12	15:00	35° 43,41' N	23° 43,64' E	579,4	Multibeam
POS429/047-1		24.03.12	15:06	35° 43,29' N	23° 43,07' E	743	Multibeam
POS429/047-1		24.03.12	16:09	35° 48,40' N	23° 41,38' E	804,9	Multibeam
POS429/047-1		24.03.12	16:24	35° 48,08' N	23° 40,20' E	811,6	Multibeam
POS429/047-1		24.03.12	17:31	35° 42,72' N	23° 41,75' E	736,9	Multibeam
POS429/047-1		24.03.12	17:53	35° 43,02' N	23° 43,66' E	453,1	Multibeam
POS429/047-1		24.03.12	19:48	35° 49,40' N	23° 50,64' E	641,9	Multibeam
POS429/047-1		24.03.12	19:57	35° 49,68' N	23° 50,34' E	643,4	Multibeam
POS429/047-1		24.03.12	21:30	35° 45,87' N	23° 46,45' E	371,6	Multibeam
POS429/047-1		24.03.12	21:41	35° 46,25' N	23° 46,09' E	361,9	Multibeam
POS429/047-1		24.03.12	22:49	35° 49,14' N	23° 43,46' E	460,2	Multibeam
POS429/048-1	12	25.03.12	07:08	35° 39,65' N	23° 49,06' E	247,6	Gravity corer
POS429/049-1	13	25.03.12	07:37	35° 39,43' N	23° 48,93' E	221,1	Gravity corer
POS429/050-1	14	25.03.12	08:04	35° 39,08' N	23° 48,67' E	147,4	Gravity corer
POS429/051-1	15	25.03.12	08:34	35° 39,56' N	23° 49,01' E	235	Gravity corer
POS429/052-1	16	25.03.12	09:03	35° 40,03' N	23° 49,27' E	279,5	Gravity corer
POS429/053-1	17-1	25.03.12	10:08	35° 39,07' N	23° 48,64' E	147,3	Cone penetration testing
POS429/053-2	17-2	25.03.12	10:33	35° 39,19' N	23° 48,74' E	174,7	Cone penetration testing
POS429/053-3	17-3	25.03.12	10:58	35° 39,30' N	23° 48,84' E	194,4	Cone penetration testing
POS429/053-4	17-4	25.03.12	11:20	35° 39,42' N	23° 48,93' E	224,3	Cone penetration testing
POS429/053-5	17-5	25.03.12	11:43	35° 39,53' N	23° 49,01' E	223,3	Cone penetration testing
POS429/053-6	17-6	25.03.12	12:06	35° 39,65' N	23° 49,08' E	259,9	Cone penetration testing
POS429/053-6	17-7	25.03.12	12:18	35° 39,65' N	23° 49,09' E	259,4	Cone penetration testing
POS429/053-6	17-8	25.03.12	12:26	35° 39,65' N	23° 49,09' E	258	Cone penetration testing
POS429/053-6	17-9	25.03.12	12:56	35° 39,54' N	23° 49,01' E	224	Cone penetration testing
POS429/053-6	17-10	25.03.12	13:25	35° 39,81' N	23° 49,17' E	255,5	Cone penetration testing
POS429/053-6	17-11	25.03.12	13:38	35° 39,81' N	23° 49,17' E	254,9	Cone penetration testing
POS429/053-6	17-12	25.03.12	13:52	35° 39,92' N	23° 49,22' E	268	Cone penetration testing
POS429/053-6	17-13	25.03.12	14:05	35° 39,93' N	23° 49,22' E	268,1	Cone penetration testing
POS429/054-1	17-14	25.03.12	14:28	35° 40,03' N	23° 49,28' E	280,3	Cone penetration testing
POS429/054-2	17-15	25.03.12	14:41	35° 40,04' N	23° 49,29' E	281,1	Cone penetration testing
POS429/055-1	17-16	25.03.12	15:20	35° 40,21' N	23° 49,37' E	296,6	Cone penetration testing
POS429/054-3	17-17	25.03.12	15:48	35° 40,40' N	23° 49,51' E	314,3	Cone penetration testing
POS429/056-1	17-18	25.03.12	16:15	35° 40,58' N	23° 49,60' E	329,7	Cone penetration testing

POS429/057-1	17-19	25.03.12	16:47	35° 40,75' N	23° 49,70' E	340,7	Cone penetration testing
POS429/058-1	17-20	25.03.12	17:15	35° 40,92' N	23° 49,79' E	353,6	Cone penetration testing
POS429/059-1	17-21	25.03.12	17:48	35° 41,09' N	23° 49,90' E	360,9	Cone penetration testing
POS429/060-1	17-22	25.03.12	18:18	35° 41,26' N	23° 49,98' E	367,1	Cone penetration testing
POS429/061-1	18	25.03.12	19:59	35° 41,76' N	23° 53,62' E	424,7	Multibeam
POS429/061-1		25.03.12	20:24	35° 40,95' N	23° 52,51' E	390,8	Multibeam
MED RIDGE							
POS429/062-1	19	29.03.12	03:01	33° 57,65' N	24° 59,09' E	2408,4	Multibeam
POS429/062-1		29.03.12	05:46	33° 44,33' N	24° 52,49' E	2134,4	Multibeam
POS429/063-1	20-1	29.03.12	06:30	33° 43,82' N	24° 46,61' E	1928,1	CAT Meter
POS429/063-1	20-2	29.03.12	07:22	33° 44,08' N	24° 46,58' E	0	CAT Meter
POS429/064-1	21-1	29.03.12	07:47	33° 44,00' N	24° 46,57' E	1924,8	Heat Flow
POS429/064-1	21-2	29.03.12	08:06	33° 44,02' N	24° 46,57' E	1918,3	Heat Flow
POS429/064-1	21-3	29.03.12	08:28	33° 44,05' N	24° 46,59' E	1930,3	Heat Flow
POS429/064-1	21-4	29.03.12	09:35	33° 44,10' N	24° 46,64' E	1921,7	Heat Flow
POS429/065-1	22	29.03.12	10:01	33° 44,02' N	24° 46,56' E	1929,5	Cone penetration testing
POS429/066-1	23-1	29.03.12	12:48	33° 43,37' N	24° 41,13' E	0	CAT Meter
POS429/066-1	23-2	29.03.12	12:57	0° 0,00' N	0° 0,00' E	0	CAT Meter
POS429/067-1	24	29.03.12	13:12	33° 43,63' N	24° 40,86' E	0	Cone penetration testing
POS429/067-2	25-1	29.03.12	14:54	33° 43,63' N	24° 40,87' E	1913,5	Heat Flow
POS429/068-1	25-2	29.03.12	15:17	33° 43,54' N	24° 41,00' E	1904,5	Heat Flow
POS429/069-1	25-3	29.03.12	15:44	33° 43,45' N	24° 41,16' E	1902,5	Heat Flow
POS429/070-1	26	29.03.12	17:35	33° 44,41' N	24° 52,55' E	2140,5	Multibeam
POS429/070-1		29.03.12	20:38	33° 30,29' N	24° 45,62' E	2086,9	Multibeam
POS429/070-1		29.03.12	20:50	33° 30,49' N	24° 44,75' E	2081,9	Multibeam
POS429/070-1		30.03.12	02:55	33° 58,10' N	24° 58,21' E	2655,6	Multibeam
POS429/071-1	27	30.03.12	05:02	34° 5,66' N	24° 58,91' E	0	CAT Meter
POS429/072-1	28	30.03.12	06:31	34° 5,61' N	24° 58,42' E	3302	Gravity corer
POS429/073-1	29	30.03.12	11:42	34° 18,69' N	24° 34,38' E	3050,7	Gravity corer
POS429/074-1	30	30.03.12	13:17	34° 18,72' N	24° 34,38' E	3038,8	Gravity corer
NICE SLOPE							
POS429/075-1	31	04.04.12	16:05	43° 38,71' N	7° 13,43' E	20,9	Cone penetration testing
POS429/076-1	32	04.04.12	16:36	43° 38,71' N	7° 13,35' E	16,2	Cone penetration testing
POS429/077-1	33	04.04.12	17:07	43° 38,77' N	7° 13,27' E	12,4	Cone penetration testing
POS429/078-1	34	04.04.12	18:09	43° 38,91' N	7° 13,54' E	19,6	Cone penetration testing
POS429/079-1	35	04.04.12	18:36	43° 38,89' N	7° 13,52' E	17,3	Cone penetration testing
POS429/080-1	36	04.04.12	19:03	43° 38,85' N	7° 13,59' E	23	Cone penetration testing
POS429/080-2	37	04.04.12	19:35	43° 38,84' N	7° 13,59' E	23	Cone penetration testing
POS429/081-1	38-1	05.04.12	07:23	43° 38,90' N	7° 13,54' E	18,9	Gravity corer
POS429/081-2	38-2	05.04.12	07:35	43° 38,90' N	7° 13,54' E	18,2	Cone penetration testing
POS429/082-1	39-1	05.04.12	08:13	43° 38,87' N	7° 13,42' E	12,8	Gravity corer
POS429/082-3	39-2	05.04.12	08:36	43° 38,87' N	7° 13,42' E	12,5	Cone penetration testing
POS429/083-1	40-1	05.04.12	09:11	43° 38,75' N	7° 13,33' E	13,3	Gravity corer
POS429/083-2	40-2	05.04.12	09:20	43° 38,75' N	7° 13,33' E	14,6	Cone penetration testing
POS429/084-1	41-1	05.04.12	10:04	43° 38,80' N	7° 13,28' E	12	Gravity corer
POS429/084-2	41-2	05.04.12	10:10	43° 38,79' N	7° 13,28' E	12	Cone penetration testing
POS429/085-1	42-1	05.04.12	10:56	43° 38,89' N	7° 13,17' E	12,4	Gravity corer
POS429/085-2	42-2	05.04.12	11:00	43° 38,89' N	7° 13,17' E	12,6	Cone penetration testing
POS429/086-1	43	05.04.12	11:49	43° 38,56' N	7° 12,69' E	46,8	Cone penetration testing
POS429/086-1	44	05.04.12	12:42	43° 38,64' N	7° 13,30' E	20,1	Cone penetration testing
POS429/086-1	45-1	05.04.12	14:50	43° 38,70' N	7° 13,08' E	41,4	Cone penetration testing
POS429/086-1	45-2	05.04.12	15:11	43° 38,70' N	7° 13,08' E	44	Gravity corer

9.2 Lithologs and shear strength data

GeoB 16502-2

Study area: Spatha Ridge **Date:** 23.03.2012 **Position:** 35°47.564' N/ 23°53.51' E **Water Depth**: ~675 m **Core Length:** 425 cm

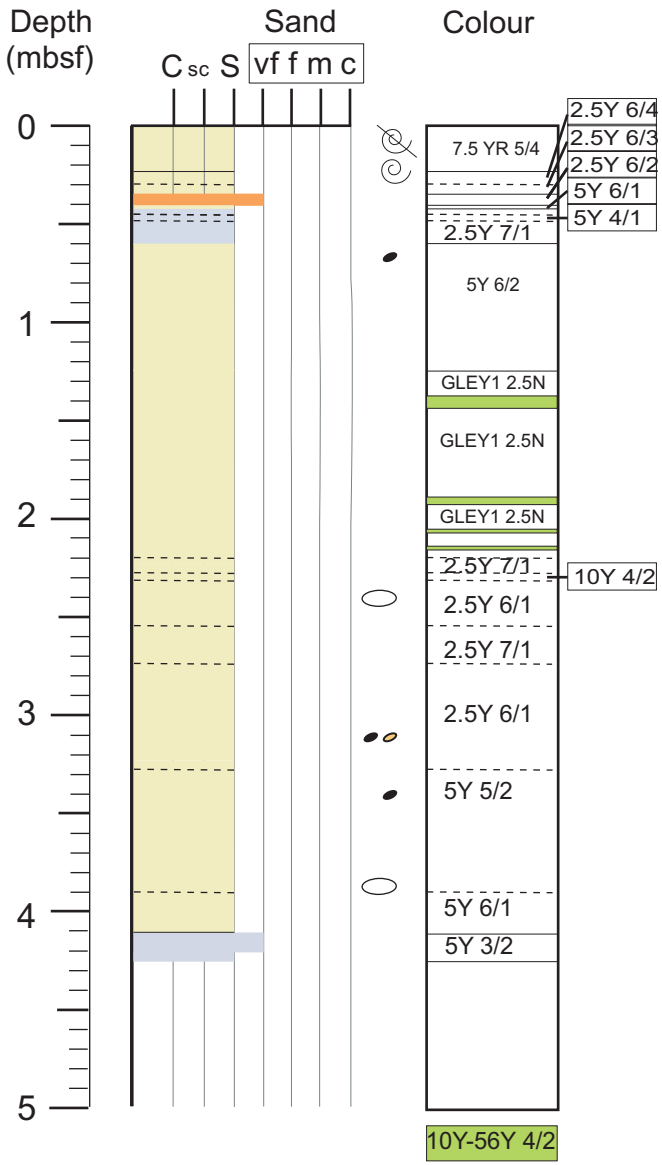

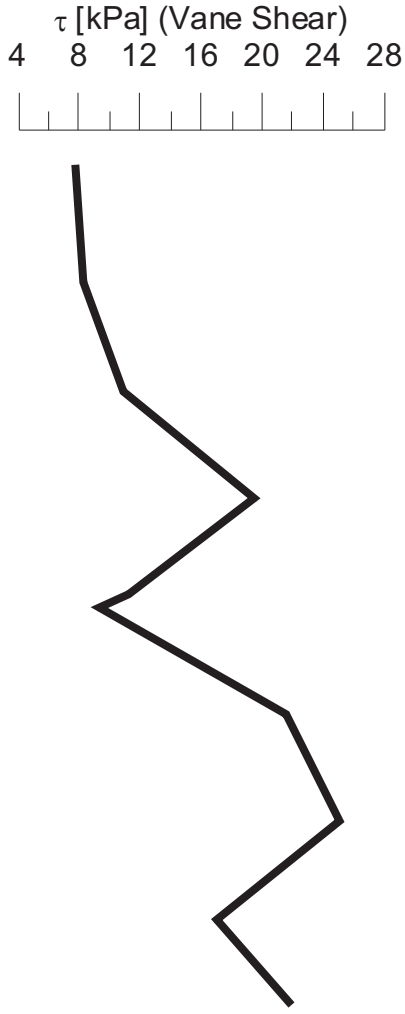

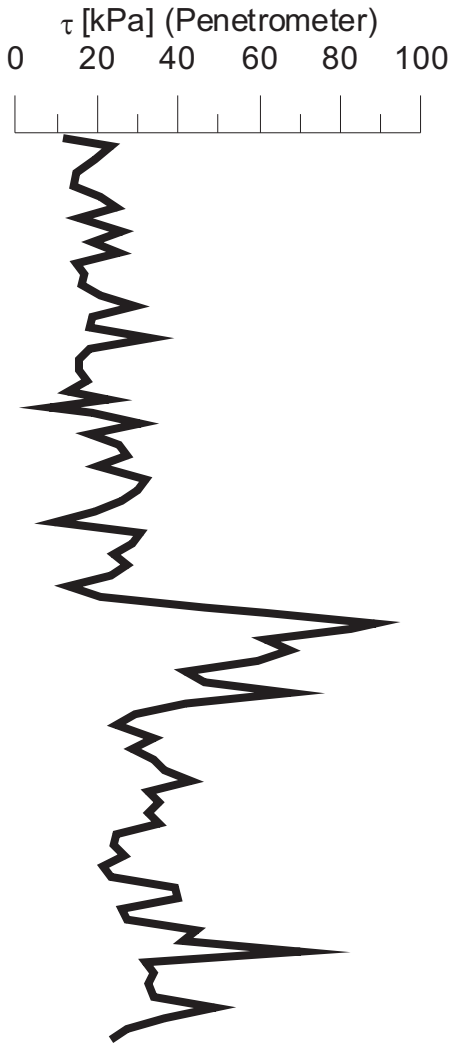

GeoB 16505-1

Study area: Spatha Ridge **Date:** 23.03.2012 **Position:** 35°41.252' N/ 23°50.002' E **Water Depth**: ~390 m **Core Length:** 100 cm

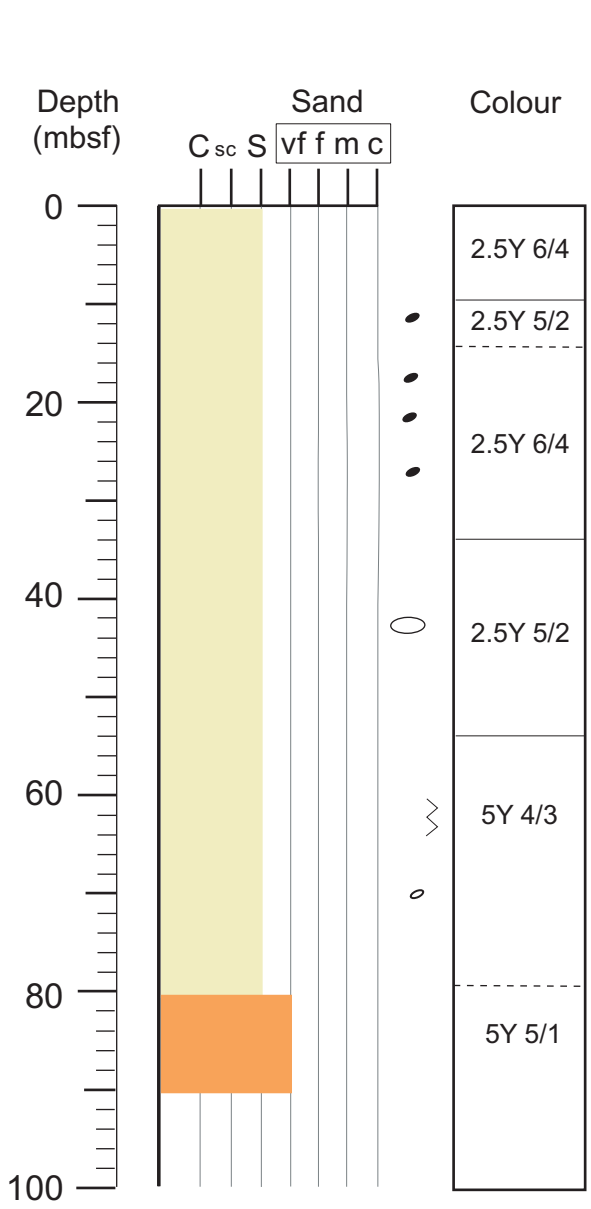

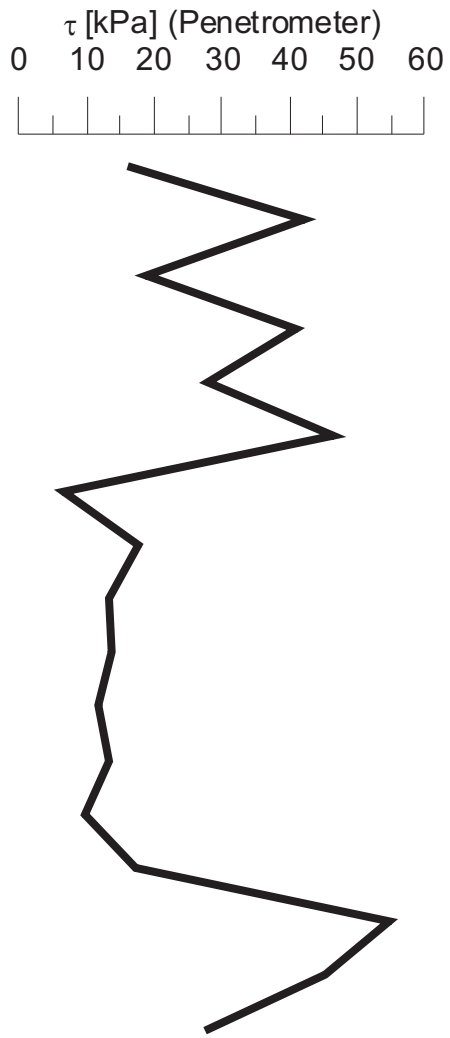

GeoB 16506-1

Study area: Spatha Ridge **Date:** 23.03.2012 **Position:** 35°41.611' N/ 23°50.191' E **Water Depth**: ~300 m **Core Length:** 80 cm

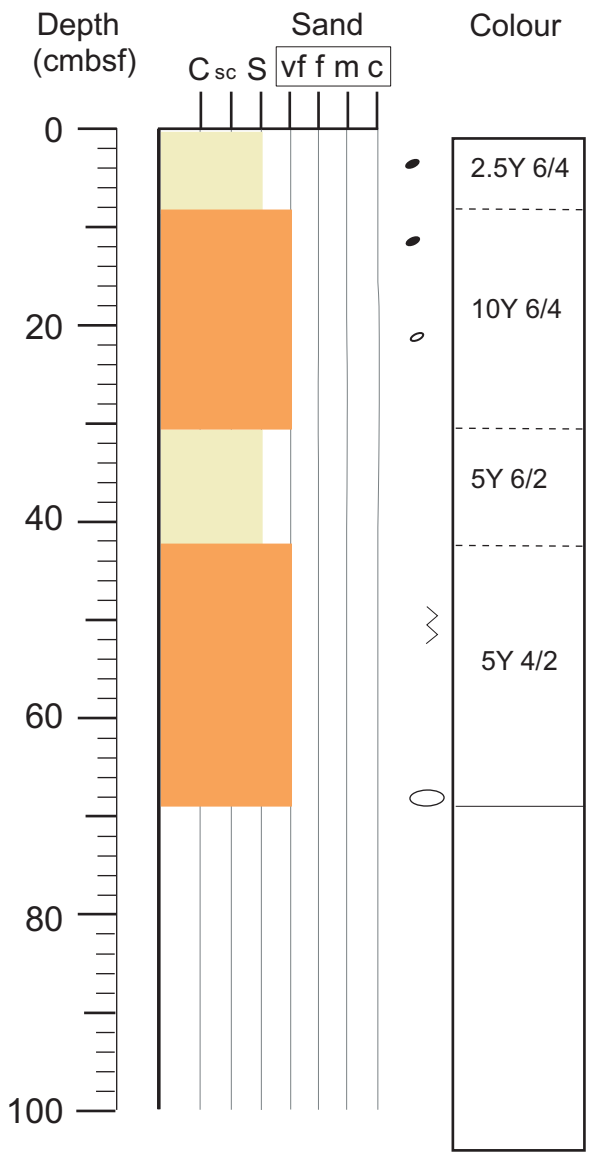

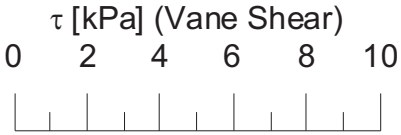

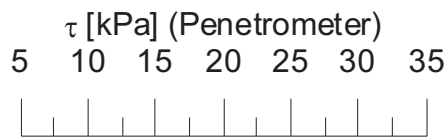

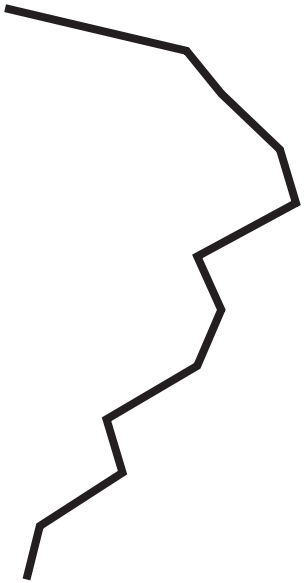

GeoB 16509-1

Study area: Spatha Ridge **Date:** 24.03.2012 **Position:** 35°45.012' N/ 23°43.029' E **Water Depth**: ~820 m **Core Length:** 21 cm

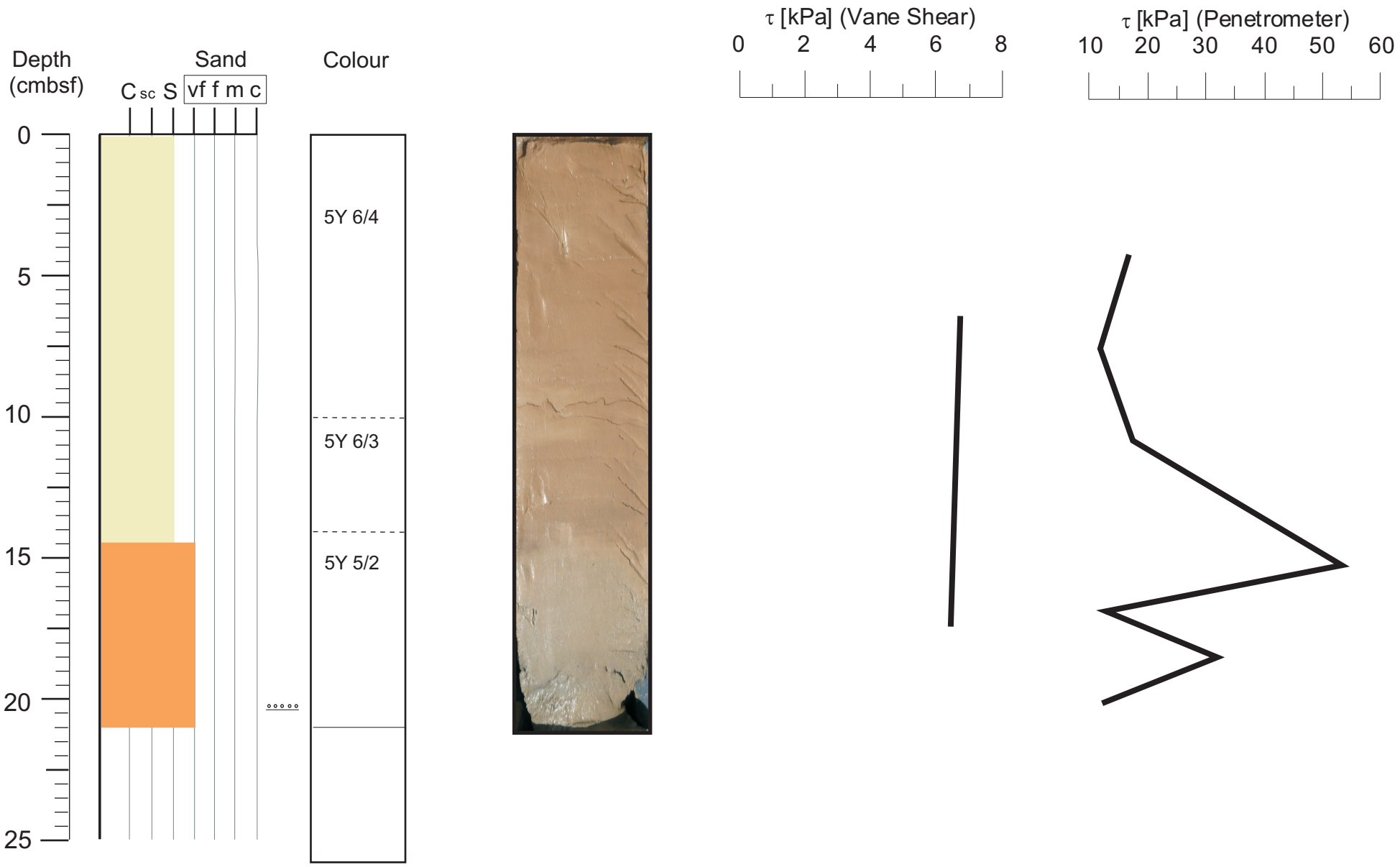

GeoB 16512

Study area: Spatha Ridge **Date:** 25.03.2012 **Position:** 35°39.652' N/ 23°49.059' E **Water Depth**: ~268 m **Core Length:** 150 cm

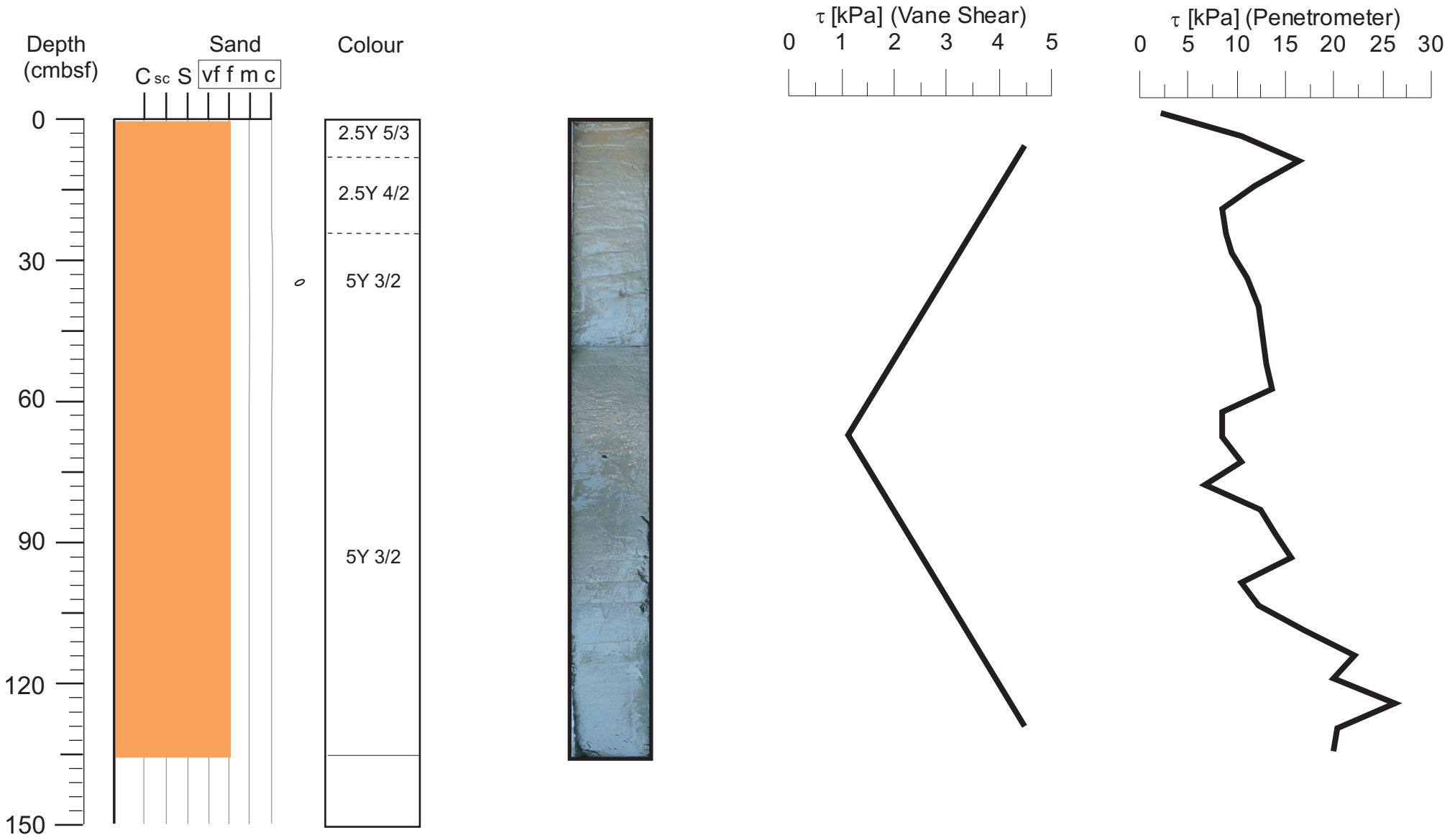

GeoB 16513

Study area: Spatha Ridge **Date:** 25.03.2012 **Position:** 35°39.431' N/ 23°48.929' E **Water Depth**: ~240 m **Core Length:** 186 cm

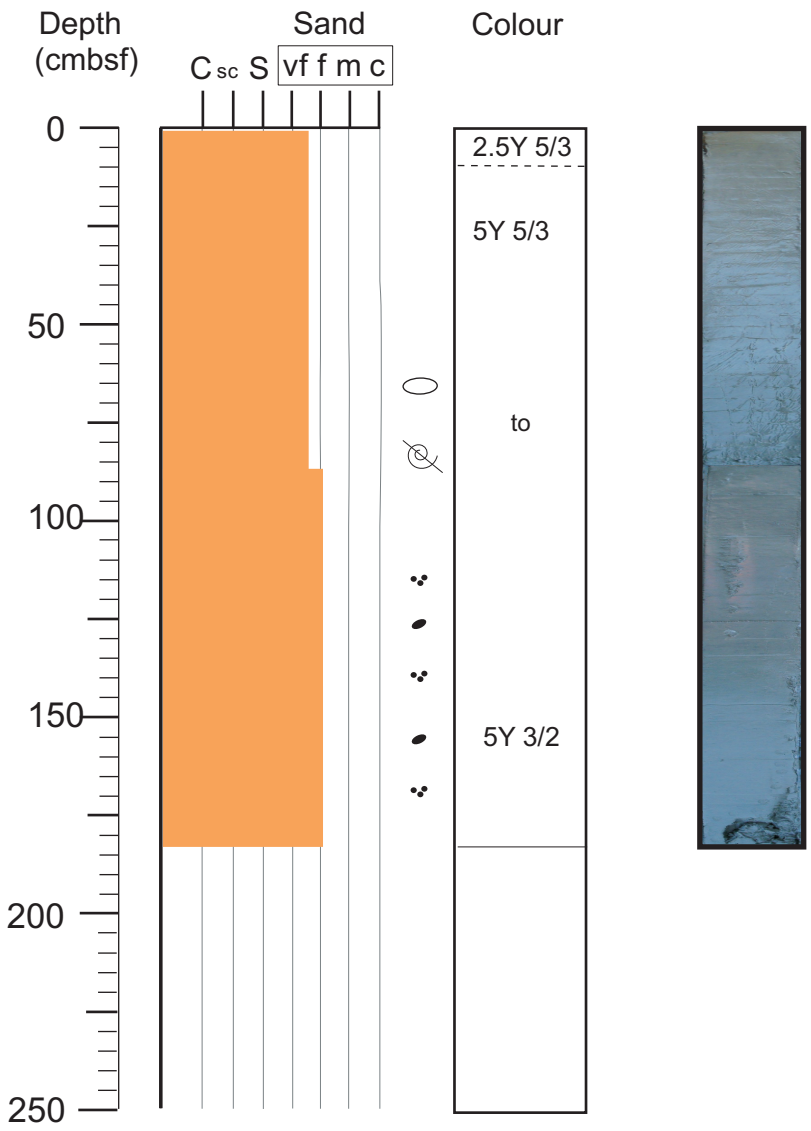

GeoB 16514

Study area:Spatha Ridge **Date**: 25.03.2012 **Position**: 35° 39.073N 23° 48.667' E **Water Depth:** 150 m **Core Length:** 16 cm

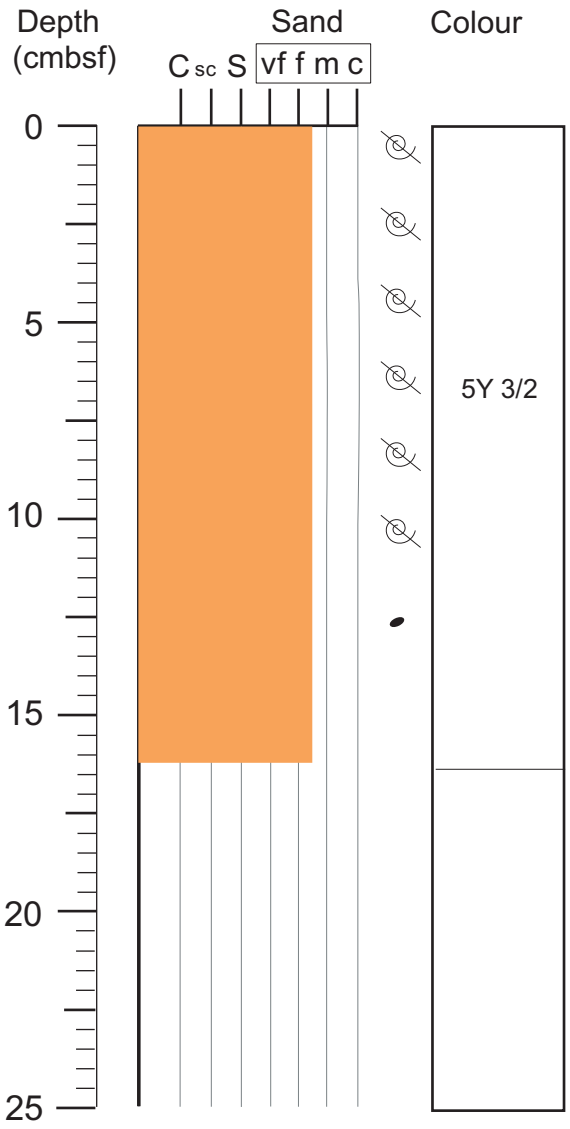

No physical properties

Coral fragments

GeoB 16515

Study area: Spatha Ridge **Date:** 25.03.2012 **Position:** 35°39.563' N/ 23°49.008' E **Water Depth**: ~256 m **Core Length:** 78 cm

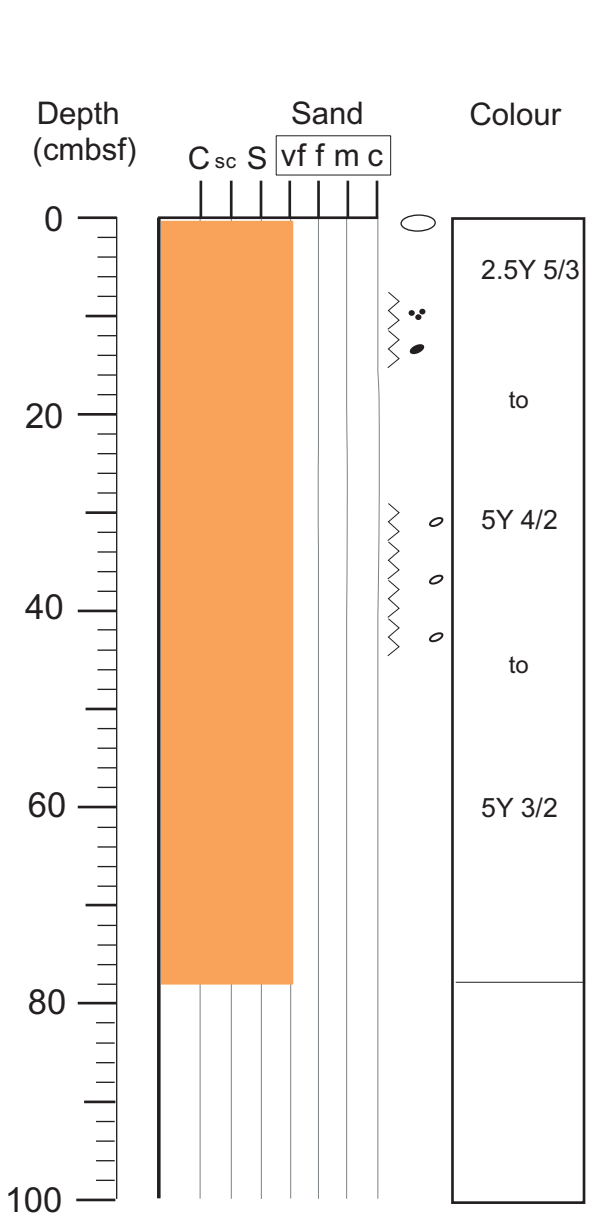

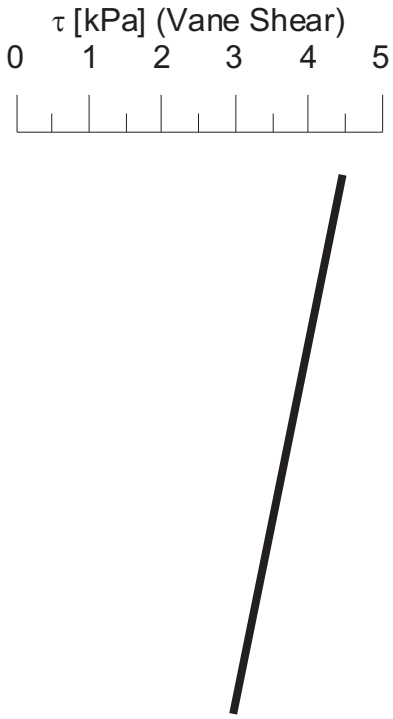

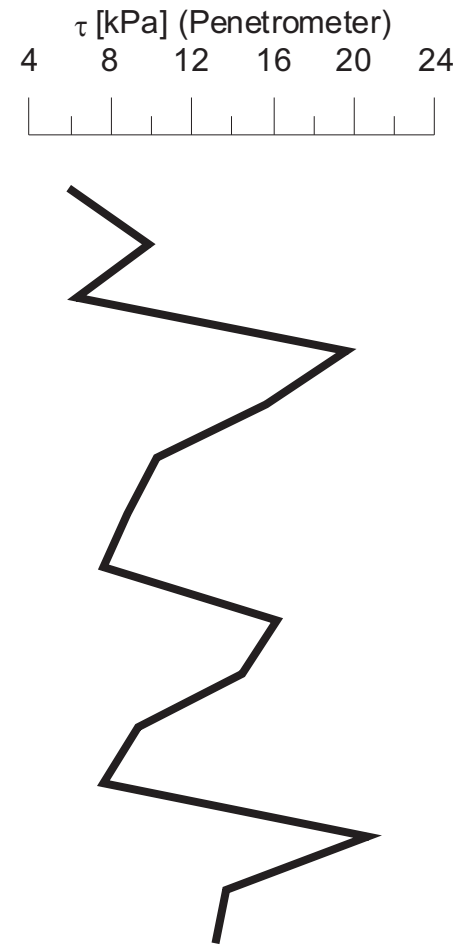

GeoB 16516

Study area: Spatha Ridge **Date:** 25.03.2012 **Position:** 35°40.034' N/ 23°49.267' E **Water Depth**: ~300 m **Core Length:** 55 cm

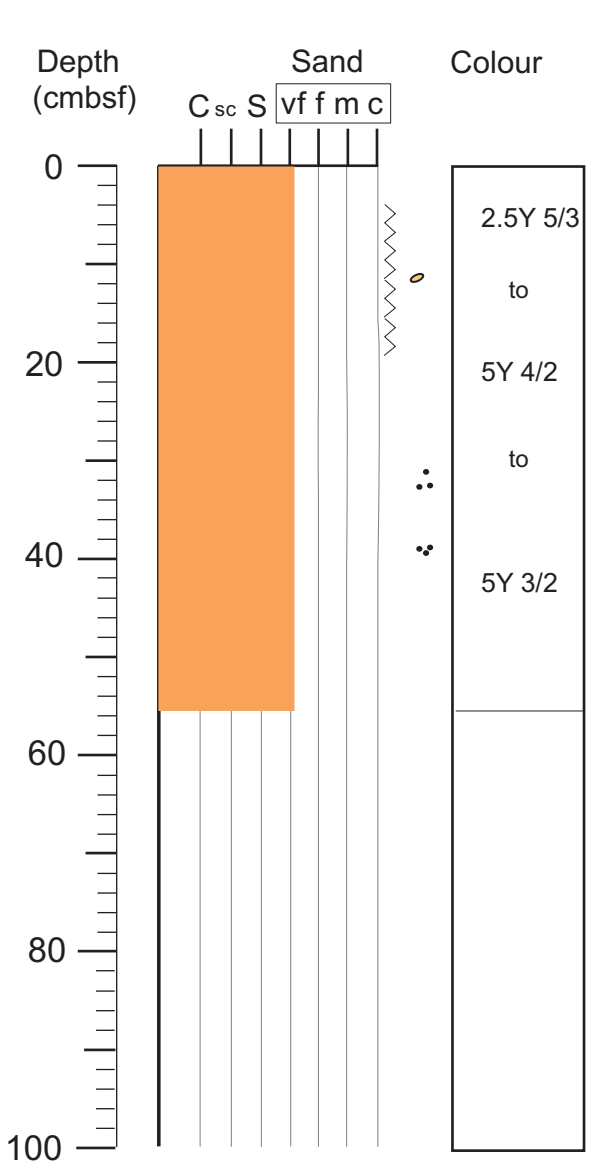

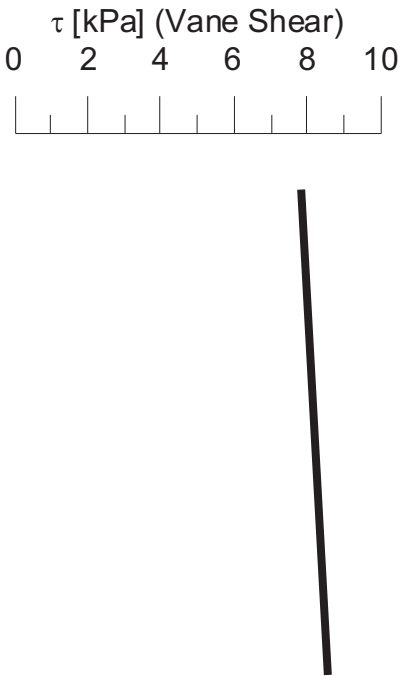

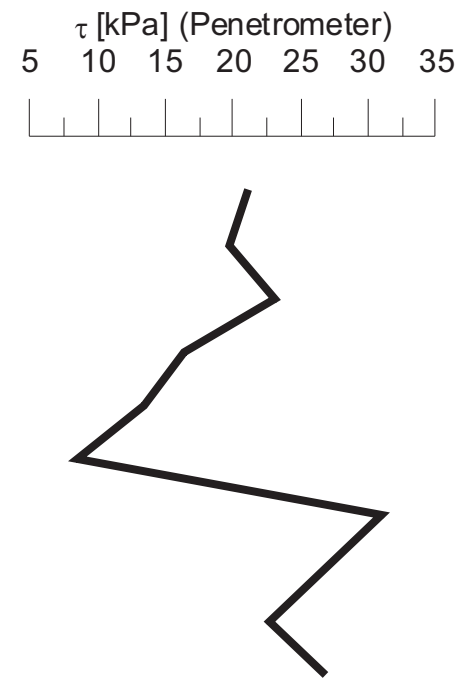

GeoB 16529

Study area: inner ridge back thrust **Date:** 30.03.2012 **Position:** 34°18.694' N/ 24°34.383' E **Water Depth**: 3051 ? m **Core Length:** 183 cm

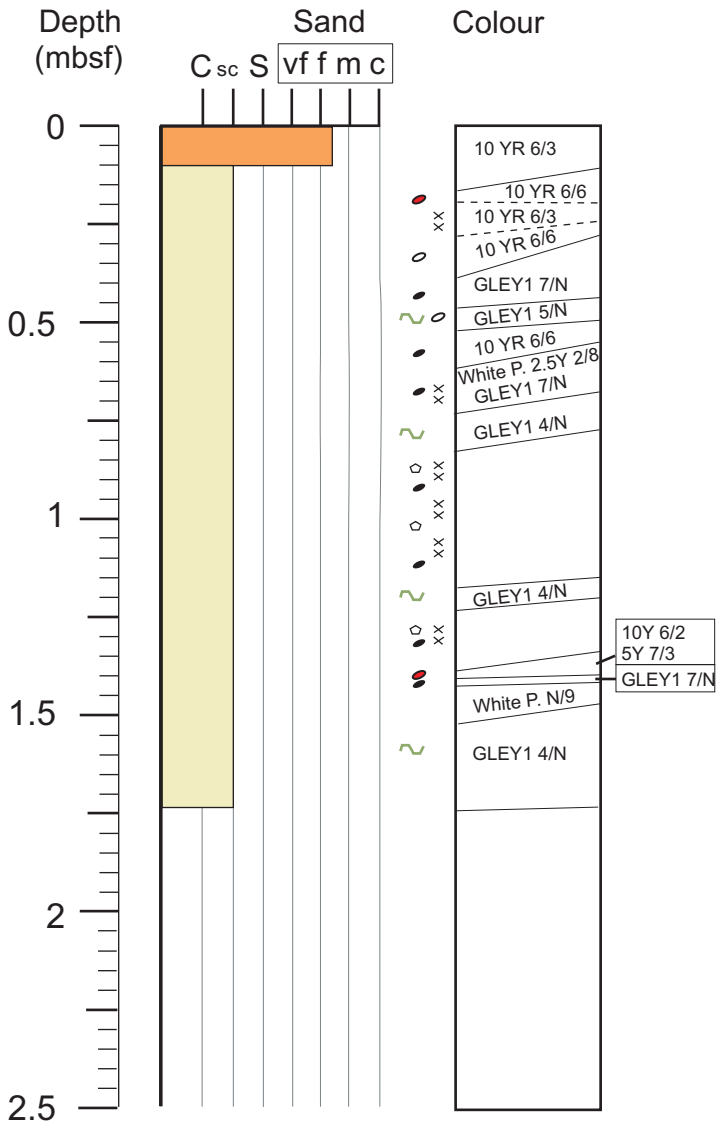

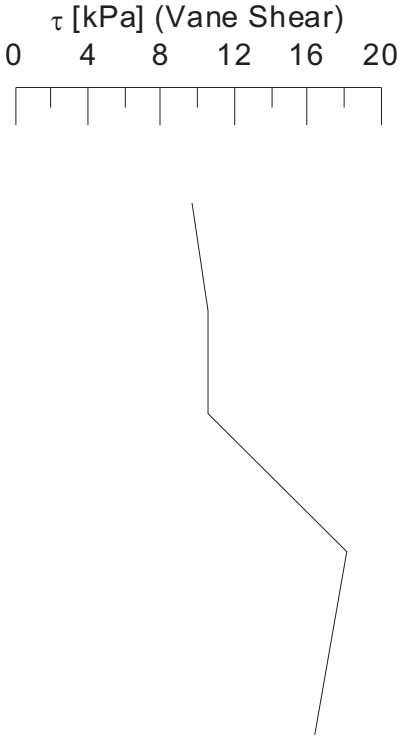

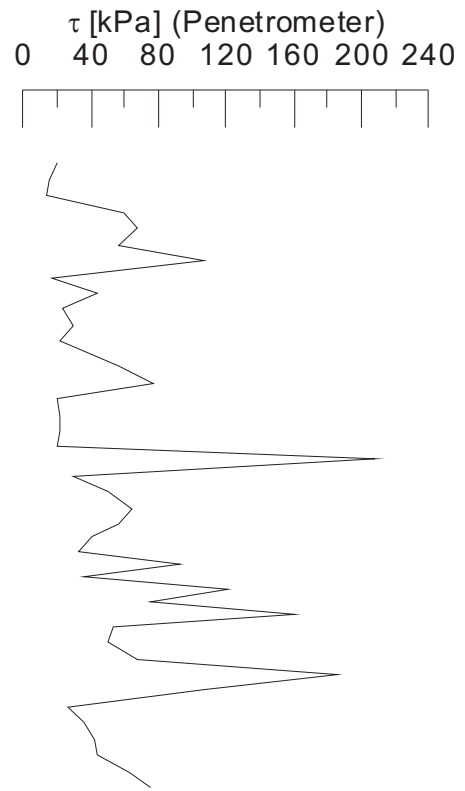

GeoB 16530

Study area: inner ridge to cretan margin (back thrust)

Date: 30.03.2012 **Position:** 34°18.717' N/ 24°34.384' E **Water Depth**: ???? m **Core Length:** 200 cm

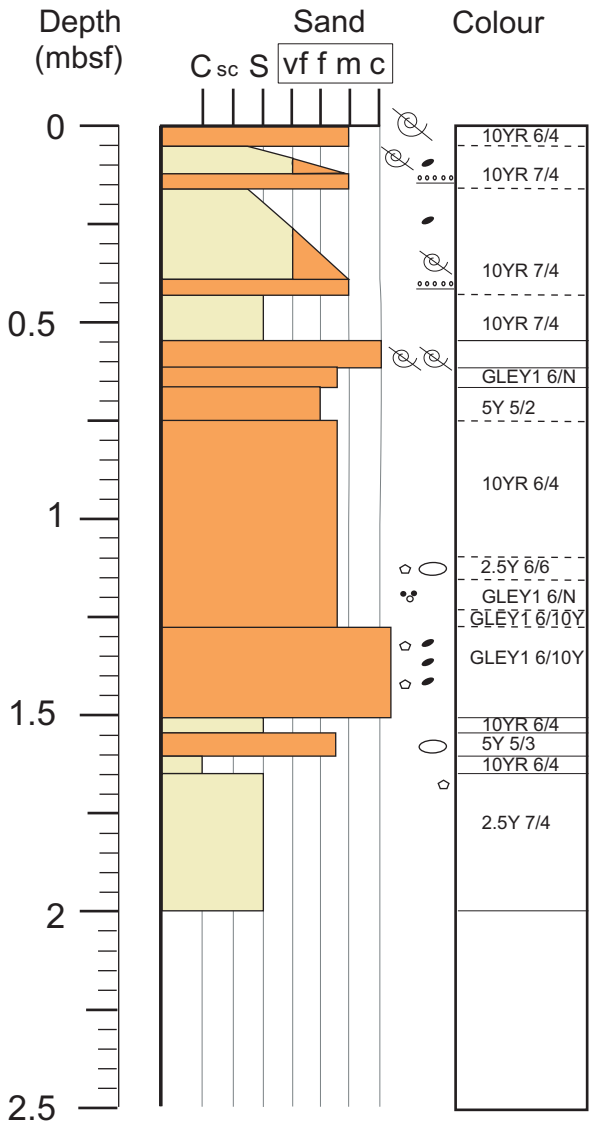

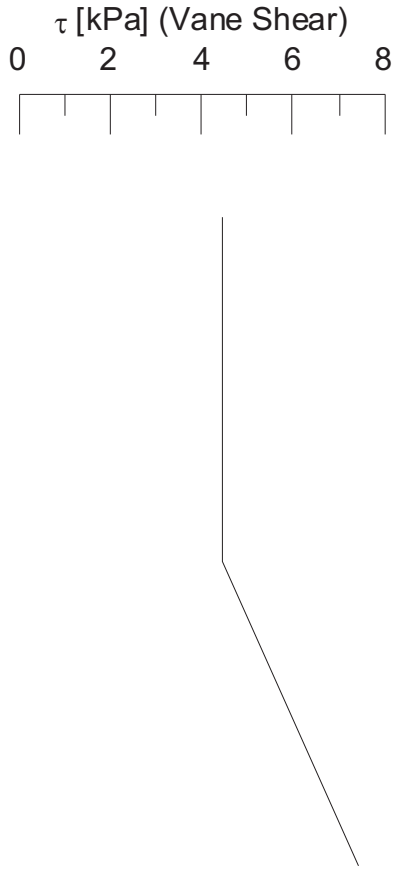

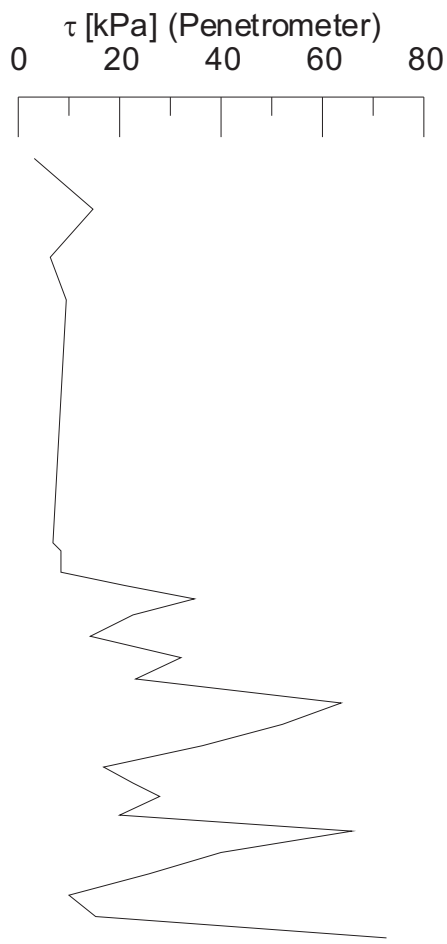

Publications of this series:

No. 1 **Wefer, G., E. Suess and cruise participants**
Bericht über die POLARSTERN-Fahrt ANT IV/2, Rio de Janeiro - Punta Arenas, 6.11. - 1.12.1985.
60 pages, Bremen, 1986.

No. 2 **Hoffmann, G.**
Holozänstratigraphie und Küstenlinienverlagerung an der andalusischen Mittelmeerküste.
173 pages, Bremen, 1988. (out of print)

No. 3 **Wefer, G. and cruise participants**
Bericht über die METEOR-Fahrt M 6/6, Libreville - Las Palmas, 18.2. - 23.3.1988.
97 pages, Bremen, 1988.

No. 4 **Wefer, G., G.F. Lutze, T.J. Müller, O. Pfannkuche, W. Schenke, G. Siedler, W. Zenk**
Kurzbericht über die METEOR-Expedition No. 6, Hamburg - Hamburg, 28.10.1987 - 19.5.1988.
29 pages, Bremen, 1988. (out of print)

No. 5 **Fischer, G.**
Stabile Kohlenstoff-Isotope in partikulärer organischer Substanz aus dem Südpolarmeer (Atlantischer Sektor). 161 pages, Bremen, 1989.

No. 6 **Berger, W.H. and G. Wefer**
Partikelfluß und Kohlenstoffkreislauf im Ozean.
Bericht und Kurzfassungen über den Workshop vom 3.-4. Juli 1989 in Bremen.
57 pages, Bremen, 1989.

No. 7 **Wefer, G. and cruise participants**
Bericht über die METEOR - Fahrt M 9/4, Dakar - Santa Cruz, 19.2. - 16.3.1989.
103 pages, Bremen, 1989.

No. 8 **Kölling, M.**
Modellierung geochemischer Prozesse im Sickerwasser und Grundwasser.
135 pages, Bremen, 1990.

No. 9 **Heinze, P.-M.**
Das Auftriebsgeschehen vor Peru im Spätquartär. 204 pages, Bremen, 1990. (out of print)

No. 10 **Willems, H., G. Wefer, M. Rinski, B. Donner, H.-J. Bellmann, L. Eißmann, A. Müller, B.W. Flemming, H.-C. Höfle, J. Merkt, H. Streif, G. Hertweck, H. Kuntze, J. Schwaar, W. Schäfer, M.-G. Schulz, F. Grube, B. Menke**
Beiträge zur Geologie und Paläontologie Norddeutschlands: Exkursionsführer.
202 pages, Bremen, 1990.

No. 11 **Wefer, G. and cruise participants**
Bericht über die METEOR-Fahrt M 12/1, Kapstadt - Funchal, 13.3.1990 - 14.4.1990.
66 pages, Bremen, 1990.

No. 12 **Dahmke, A., H.D. Schulz, A. Kölling, F. Kracht, A. Lücke**
Schwermetallspuren und geochemische Gleichgewichte zwischen Porenlösung und Sediment im Wesermündungsgebiet. BMFT-Projekt MFU 0562, Abschlußbericht. 121 pages, Bremen, 1991.

No. 13 **Rostek, F.**
Physikalische Strukturen von Tiefseesedimenten des Südatlantiks und ihre Erfassung in Echolotregistrierungen. 209 pages, Bremen, 1991.

No. 14 **Baumann, M.**
Die Ablagerung von Tschernobyl-Radiocäsium in der Norwegischen See und in der Nordsee.
133 pages, Bremen, 1991. (out of print)

No. 15 **Kölling, A.**
Frühdiagenetische Prozesse und Stoff-Flüsse in marinen und ästuarinen Sedimenten.
140 pages, Bremen, 1991.

No. 16 **SFB 261 (ed.)**
1. Kolloquium des Sonderforschungsbereichs 261 der Universität Bremen (14.Juni 1991):
Der Südatlantik im Spätquartär: Rekonstruktion von Stoffhaushalt und Stromsystemen.
Kurzfassungen der Vorträge und Poster. 66 pages, Bremen, 1991.

No. 17 **Pätzold, J. and cruise participants**
Bericht und erste Ergebnisse über die METEOR-Fahrt M 15/2, Rio de Janeiro - Vitoria,
18.1. - 7.2.1991. 46 pages, Bremen, 1993.

No. 18 **Wefer, G. and cruise participants**
Bericht und erste Ergebnisse über die METEOR-Fahrt M 16/1, Pointe Noire - Recife,
27.3. - 25.4.1991. 120 pages, Bremen, 1991.

No. 19 **Schulz, H.D. and cruise participants**
Bericht und erste Ergebnisse über die METEOR-Fahrt M 16/2, Recife - Belem, 28.4. - 20.5.1991.
149 pages, Bremen, 1991.

No. 20 **Berner, H.**
Mechanismen der Sedimentbildung in der Fram-Straße, im Arktischen Ozean und in der Norwegischen See. 167 pages, Bremen, 1991.

No. 21 **Schneider, R.**
Spätquartäre Produktivitätsänderungen im östlichen Angola-Becken: Reaktion auf Variationen im Passat-Monsun-Windsystem und in der Advektion des Benguela-Küstenstroms.
198 pages, Bremen, 1991. (out of print)

No. 22 **Hebbeln, D.**
Spätquartäre Stratigraphie und Paläozeanographie in der Fram-Straße. 174 pages, Bremen, 1991.

No. 23 **Lücke, A.**
Umsetzungsprozesse organischer Substanz während der Frühdiagenese in ästuarinen Sedimenten.
137 pages, Bremen, 1991.

No. 24 **Wefer, G. and cruise participants**
Bericht und erste Ergebnisse der METEOR-Fahrt M 20/1, Bremen - Abidjan, 18.11.- 22.12.1991.
74 pages, Bremen, 1992.

No. 25 **Schulz, H.D. and cruise participants**
Bericht und erste Ergebnisse der METEOR-Fahrt M 20/2, Abidjan - Dakar, 27.12.1991 - 3.2.1992.
173 pages, Bremen, 1992.

No. 26 **Gingele, F.**
Zur klimaabhängigen Bildung biogener und terrigener Sedimente und ihrer Veränderung durch die Frühdiagenese im zentralen und östlichen Südatlantik. 202 pages, Bremen, 1992.

No. 27 **Bickert, T.**
Rekonstruktion der spätquartären Bodenwasserzirkulation im östlichen Südatlantik über stabile Isotope benthischer Foraminiferen. 205 pages, Bremen, 1992. (out of print)

No. 28 **Schmidt, H.**
Der Benguela-Strom im Bereich des Walfisch-Rückens im Spätquartär. 172 pages, Bremen, 1992.

No. 29 **Meinecke, G.**
Spätquartäre Oberflächenwassertemperaturen im östlichen äquatorialen Atlantik.
181 pages, Bremen, 1992.

No. 30 **Bathmann, U., U. Bleil, A. Dahmke, P. Müller, A. Nehrkorn, E.-M. Nöthig, M. Olesch, J. Pätzold, H.D. Schulz, V. Smetacek, V. Spieß, G. Wefer, H. Willems**
Bericht des Graduierten Kollegs. Stoff-Flüsse in marinen Geosystemen.
Berichtszeitraum Oktober 1990 - Dezember 1992. 396 pages, Bremen, 1992.

No. 31 **Damm, E.**
Frühdiagenetische Verteilung von Schwermetallen in Schlicksedimenten der westlichen Ostsee.
115 pages, Bremen, 1992.

No. 32 **Antia, E.E.**
Sedimentology, Morphodynamics and Facies Association of a mesotidal Barrier Island Shoreface (Spiekeroog, Southern North Sea). 370 pages, Bremen, 1993.

No. 33 **Duinker, J. and G. Wefer (ed.)**
Bericht über den 1. JGOFS-Workshop. 1./2. Dezember 1992 in Bremen. 83 pages, Bremen, 1993.

No. 34 **Kasten, S.**
Die Verteilung von Schwermetallen in den Sedimenten eines stadtbremischen Hafenbeckens.
103 pages, Bremen, 1993.

No. 35 **Spieß, V.**
Digitale Sedimentographie. Neue Wege zu einer hochauflösenden Akustostratigraphie.
199 pages, Bremen, 1993.

No. 36 **Schinzel, U.**
Laborversuche zu frühdiagenetischen Reaktionen von Eisen (III) - Oxidhydraten in marinen Sedimenten.189 pages, Bremen, 1993.

No. 37 **Sieger, R.**
CoTAM - ein Modell zur Modellierung des Schwermetalltransports in Grundwasserleitern.
56 pages, Bremen, 1993. (out of print)

No. 38 **Willems, H. (ed.)**
Geoscientific Investigations in the Tethyan Himalayas. 183 pages, Bremen, 1993.

No. 39 **Hamer, K.**
Entwicklung von Laborversuchen als Grundlage für die Modellierung des Transportverhaltens von Arsenat, Blei, Cadmium und Kupfer in wassergesättigten Säulen. 147 pages, Bremen, 1993.

No. 40 **Sieger, R.**
Modellierung des Stofftransports in porösen Medien unter Ankopplung kinetisch gesteuerter Sorptions- und Redoxprozesse sowie thermischer Gleichgewichte. 158 pages, Bremen, 1993.

No. 41 **Thießen, W.**
Magnetische Eigenschaften von Sedimenten des östlichen Südatlantiks und ihre paläozeanographische Relevanz. 170 pages, Bremen, 1993.

No. 42 **Spieß, V. and cruise participants**
Report and preliminary results of METEOR-Cruise M 23/1, Kapstadt - Rio de Janeiro, 4.-25.2.1993. 139 pages, Bremen, 1994.

No. 43 **Bleil, U. and cruise participants**
Report and preliminary results of METEOR-Cruise M 23/2, Rio de Janeiro - Recife, 27.2.-19.3.1993 133 pages, Bremen, 1994.

No. 44 **Wefer, G. and cruise participants**
Report and preliminary results of METEOR-Cruise M 23/3, Recife - Las Palmas, 21.3. - 12.4.1993 71 pages, Bremen, 1994.

No. 45 **Giese, M. and G. Wefer (ed.)**
Bericht über den 2. JGOFS-Workshop. 18../19. November 1993 in Bremen. 93 pages, Bremen, 1994.

No. 46 **Balzer, W. and cruise participants**
Report and preliminary results of METEOR-Cruise M 22/1, Hamburg - Recife, 22.9. - 21.10.1992. 24 pages, Bremen, 1994.

No. 47 **Stax, R.**
Zyklische Sedimentation von organischem Kohlenstoff in der Japan See: Anzeiger für Änderungen von Paläoozeanographie und Paläoklima im Spätkänozoikum. 150 pages, Bremen, 1994.

No. 48 **Skowronek, F.**
Frühdiagenetische Stoff-Flüsse gelöster Schwermetalle an der Oberfläche von Sedimenten des Weser Ästuares. 107 pages, Bremen, 1994.

No. 49 **Dersch-Hansmann, M.**
Zur Klimaentwicklung in Ostasien während der letzten 5 Millionen Jahre: Terrigener Sedimenteintrag in die Japan See (ODP Ausfahrt 128). 149 pages, Bremen, 1994.

No. 50 **Zabel, M.**
Frühdiagenetische Stoff-Flüsse in Oberflächen-Sedimenten des äquatorialen und östlichen Südatlantik. 129 pages, Bremen, 1994.

No. 51 **Bleil, U. and cruise participants**
Report and preliminary results of SONNE-Cruise SO 86, Buenos Aires - Capetown, 22.4. - 31.5.93 116 pages, Bremen, 1994.

No. 52 **Symposium: The South Atlantic: Present and Past Circulation.**
Bremen, Germany, 15 - 19 August 1994. Abstracts. 167 pages, Bremen, 1994.

No. 53 **Kretzmann, U.B.**
57Fe-Mössbauer-Spektroskopie an Sedimenten - Möglichkeiten und Grenzen. 183 pages, Bremen, 1994.

No. 54 **Bachmann, M.**
Die Karbonatrampe von Organyà im oberen Oberapt und unteren Unteralb (NE-Spanien, Prov. Lerida): Fazies, Zyklo- und Sequenzstratigraphie. 147 pages, Bremen, 1994. (out of print)

No. 55 **Kemle-von Mücke, S.**
Oberflächenwasserstruktur und -zirkulation des Südostatlantiks im Spätquartär. 151 pages, Bremen, 1994.

No. 56 **Petermann, H.**
Magnetotaktische Bakterien und ihre Magnetosome in Oberflächensedimenten des Südatlantiks. 134 pages, Bremen, 1994.

No. 57 **Mulitza, S.**
Spätquartäre Variationen der oberflächennahen Hydrographie im westlichen äquatorialen Atlantik. 97 pages, Bremen, 1994.

No. 58 **Segl, M. and cruise participants**
Report and preliminary results of METEOR-Cruise M 29/1, Buenos-Aires - Montevideo, 17.6. - 13.7.1994
94 pages, Bremen, 1994.

No. 59 **Bleil, U. and cruise participants**
Report and preliminary results of METEOR-Cruise M 29/2, Montevideo - Rio de Janiero 15.7. - 8.8.1994. 153 pages, Bremen, 1994.

No. 60 **Henrich, R. and cruise participants**
Report and preliminary results of METEOR-Cruise M 29/3, Rio de Janeiro - Las Palmas 11.8. - 5.9.1994. Bremen, 1994. (out of print)

No. 61 **Sagemann, J.**
Saisonale Variationen von Porenwasserprofilen, Nährstoff-Flüssen und Reaktionen in intertidalen Sedimenten des Weser-Ästuars. 110 pages, Bremen, 1994. (out of print)

No. 62 **Giese, M. and G. Wefer**
Bericht über den 3. JGOFS-Workshop. 5./6. Dezember 1994 in Bremen.
84 pages, Bremen, 1995.

No. 63 **Mann, U.**
Genese kretazischer Schwarzschiefer in Kolumbien: Globale vs. regionale/lokale Prozesse.
153 pages, Bremen, 1995. (out of print)

No. 64 **Willems, H., Wan X., Yin J., Dongdui L., Liu G., S. Dürr, K.-U. Gräfe**
The Mesozoic development of the N-Indian passive margin and of the Xigaze Forearc Basin in southern Tibet, China. – Excursion Guide to IGCP 362 Working-Group Meeting "Integrated Stratigraphy". 113 pages, Bremen, 1995. (out of print)

No. 65 **Hünken, U.**
Liefergebiets - Charakterisierung proterozoischer Goldseifen in Ghana anhand von Fluideinschluß - Untersuchungen. 270 pages, Bremen, 1995.

No. 66 **Nyandwi, N.**
The Nature of the Sediment Distribution Patterns in ther Spiekeroog Backbarrier Area, the East Frisian Islands. 162 pages, Bremen, 1995.

No. 67 **Isenbeck-Schröter, M.**
Transportverhalten von Schwermetallkationen und Oxoanionen in wassergesättigten Sanden. - Laborversuche in Säulen und ihre Modellierung -. 182 pages, Bremen, 1995.

No. 68 **Hebbeln, D. and cruise participants**
Report and preliminary results of SONNE-Cruise SO 102, Valparaiso - Valparaiso, 95.
134 pages, Bremen, 1995.

No. 69 **Willems, H. (Sprecher), U.Bathmann, U. Bleil, T. v. Dobeneck, K. Herterich, B.B. Jorgensen, E.-M. Nöthig, M. Olesch, J. Pätzold, H.D. Schulz, V. Smetacek, V. Speiß. G. Wefer**
Bericht des Graduierten-Kollegs Stoff-Flüsse in marine Geosystemen.
Berichtszeitraum Januar 1993 - Dezember 1995. 45 & 468 pages, Bremen, 1995.

No. 70 **Giese, M. and G. Wefer**
Bericht über den 4. JGOFS-Workshop. 20./21. November 1995 in Bremen. 60 pages, Bremen, 1996. (out of print)

No. 71 **Meggers, H.**
Pliozän-quartäre Karbonatsedimentation und Paläozeanographie des Nordatlantiks und des Europäischen Nordmeeres - Hinweise aus planktischen Foraminiferengemeinschaften.
143 pages, Bremen, 1996. (out of print)

No. 72 **Teske, A.**
Phylogenetische und ökologische Untersuchungen an Bakterien des oxidativen und reduktiven marinen Schwefelkreislaufs mittels ribosomaler RNA. 220 pages, Bremen, 1996. (out of print)

No. 73 **Andersen, N.**
Biogeochemische Charakterisierung von Sinkstoffen und Sedimenten aus ostatlantischen Produktions-Systemen mit Hilfe von Biomarkern. 215 pages, Bremen, 1996.

No. 74 **Treppke, U.**
Saisonalität im Diatomeen- und Silikoflagellatenfluß im östlichen tropischen und subtropischen Atlantik. 200 pages, Bremen, 1996.

No. 75 **Schüring, J.**
Die Verwendung von Steinkohlebergematerialien im Deponiebau im Hinblick auf die Pyritverwitterung und die Eignung als geochemische Barriere. 110 pages, Bremen, 1996.

No. 76 **Pätzold, J. and cruise participants**
Report and preliminary results of VICTOR HENSEN cruise JOPS II, Leg 6, Fortaleza - Recife, 10.3. - 26.3. 1995 and Leg 8, Vítoria - Vítoria, 10.4. - 23.4.1995.
87 pages, Bremen, 1996.

No. 77 **Bleil, U. and cruise participants**
Report and preliminary results of METEOR-Cruise M 34/1, Cape Town - Walvis Bay, 3.-26.1.1996.
129 pages, Bremen, 1996.

No. 78 **Schulz, H.D. and cruise participants**
Report and preliminary results of METEOR-Cruise M 34/2, Walvis Bay - Walvis Bay, 29.1.-18.2.96
133 pages, Bremen, 1996.

No. 79 **Wefer, G. and cruise participants**
Report and preliminary results of METEOR-Cruise M 34/3, Walvis Bay - Recife, 21.2.-17.3.1996.
168 pages, Bremen, 1996.

No. 80 **Fischer, G. and cruise participants**
Report and preliminary results of METEOR-Cruise M 34/4, Recife - Bridgetown, 19.3.-15.4.1996. 105 pages, Bremen, 1996.

No. 81 **Kulbrok, F.**
Biostratigraphie, Fazies und Sequenzstratigraphie einer Karbonatrampe in den Schichten der Oberkreide und des Alttertiärs Nordost-Ägyptens (Eastern Desert, N'Golf von Suez, Sinai). 153 pages, Bremen, 1996.

No. 82 **Kasten, S.**
Early Diagenetic Metal Enrichments in Marine Sediments as Documents of Nonsteady-State Depositional Conditions. Bremen, 1996.

No. 83 **Holmes, M.E.**
Reconstruction of Surface Ocean Nitrate Utilization in the Southeast Atlantic Ocean Based on Stable Nitrogen Isotopes. 113 pages, Bremen, 1996.

No. 84 **Rühlemann, C.**
Akkumulation von Carbonat und organischem Kohlenstoff im tropischen Atlantik: Spätquartäre Produktivitäts-Variationen und ihre Steuerungsmechanismen. 139 pages, Bremen, 1996.

No. 85 **Ratmeyer, V.**
Untersuchungen zum Eintrag und Transport lithogener und organischer partikulärer Substanz im östlichen subtropischen Nordatlantik. 154 pages, Bremen, 1996.

No. 86 **Cepek, M.**
Zeitliche und räumliche Variationen von Coccolithophoriden-Gemeinschaften im subtropischen Ost-Atlantik: Untersuchungen an Plankton, Sinkstoffen und Sedimenten. 156 pages, Bremen, 1996.

No. 87 **Otto, S.**
Die Bedeutung von gelöstem organischen Kohlenstoff (DOC) für den Kohlenstoffffluß im Ozean. 150 pages, Bremen, 1996.

No. 88 **Hensen, C.**
Frühdiagenetische Prozesse und Quantifizierung benthischer Stoff-Flüsse in Oberflächensedimenten des Südatlantiks. 132 pages, Bremen, 1996.

No. 89 **Giese, M. and G. Wefer**
Bericht über den 5. JGOFS-Workshop. 27./28. November 1996 in Bremen. 73 pages, Bremen, 1997.

No. 90 **Wefer, G. and cruise participants**
Report and preliminary results of METEOR-Cruise M 37/1, Lisbon - Las Palmas, 4.-23.12.1996. 79 pages, Bremen, 1997.

No. 91 **Isenbeck-Schröter, M., E. Bedbur, M. Kofod, B. König, T. Schramm & G. Mattheß**
Occurrence of Pesticide Residues in Water - Assessment of the Current Situation in Selected EU Countries. 65 pages, Bremen 1997.

No. 92 **Kühn, M.**
Geochemische Folgereaktionen bei der hydrogeothermalen Energiegewinnung. 129 pages, Bremen 1997.

No. 93 **Determann, S. & K. Herterich**
JGOFS-A6 "Daten und Modelle": Sammlung JGOFS-relevanter Modelle in Deutschland. 26 pages, Bremen, 1997.

No. 94 **Fischer, G. and cruise participants**
Report and preliminary results of METEOR-Cruise M 38/1, Las Palmas - Recife, 25.1.-1.3.1997, with Appendix: Core Descriptions from METEOR Cruise M 37/1. Bremen, 1997.

No. 95 **Bleil, U. and cruise participants**
Report and preliminary results of METEOR-Cruise M 38/2, Recife - Las Palmas, 4.3.-14.4.1997. 126 pages, Bremen, 1997.

No. 96 **Neuer, S. and cruise participants**
Report and preliminary results of VICTOR HENSEN-Cruise 96/1. Bremen, 1997.

No. 97 **Villinger, H. and cruise participants**
Fahrtbericht SO 111, 20.8. - 16.9.1996. 115 pages, Bremen, 1997.

No. 98 **Lüning, S.**
Late Cretaceous - Early Tertiary sequence stratigraphy, paleoecology and geodynamics of Eastern Sinai, Egypt. 218 pages, Bremen, 1997.

No. 99 **Haese, R.R.**
Beschreibung und Quantifizierung frühdiagenetischer Reaktionen des Eisens in Sedimenten des Südatlantiks. 118 pages, Bremen, 1997.

No. 100 **Lührte, R. von**
Verwertung von Bremer Baggergut als Material zur Oberflächenabdichtung von Deponien - Geochemisches Langzeitverhalten und Schwermetall-Mobilität (Cd, Cu, Ni, Pb, Zn). Bremen, 1997.

No. 101 **Ebert, M.**
Der Einfluß des Redoxmilieus auf die Mobilität von Chrom im durchströmten Aquifer. 135 pages, Bremen, 1997.

No. 102 **Krögel, F.**
Einfluß von Viskosität und Dichte des Seewassers auf Transport und Ablagerung von Wattsedimenten (Langeooger Rückseitenwatt, südliche Nordsee). 168 pages, Bremen, 1997.

No. 103 **Kerntopf, B.**
Dinoflagellate Distribution Patterns and Preservation in the Equatorial Atlantic and Offshore North-West Africa. 137 pages, Bremen, 1997.

No. 104 **Breitzke, M.**
Elastische Wellenausbreitung in marinen Sedimenten - Neue Entwicklungen der Ultraschall Sedimentphysik und Sedimentechographie. 298 pages, Bremen, 1997.

No. 105 **Marchant, M.**
Rezente und spätquartäre Sedimentation planktischer Foraminiferen im Peru-Chile Strom. 115 pages, Bremen, 1997.

No. 106 **Habicht, K.S.**
Sulfur isotope fractionation in marine sediments and bacterial cultures. 125 pages, Bremen, 1997.

No. 107 **Hamer, K., R.v. Lührte, G. Becker, T. Felis, S. Keffel, B. Strotmann, C. Waschkowitz, M. Kölling, M. Isenbeck-Schröter, H.D. Schulz**
Endbericht zum Forschungsvorhaben 060 des Landes Bremen: Baggergut der Hafengruppe Bremen-Stadt: Modelluntersuchungen zur Schwermetallmobilität und Möglichkeiten der Verwertung von Hafenschlick aus Bremischen Häfen. 98 pages, Bremen, 1997.

No. 108 **Greeff, O.W.**
Entwicklung und Erprobung eines benthischen Landersystemes zur in situ-Bestimmung von Sulfatreduktionsraten mariner Sedimente. 121 pages, Bremen, 1997.

No. 109 **Pätzold, M. und G. Wefer**
Bericht über den 6. JGOFS-Workshop am 4./5.12.1997 in Bremen. Im Anhang: Publikationen zum deutschen Beitrag zur Joint Global Ocean Flux Study (JGOFS), Stand 1/1998. 122 pages, Bremen, 1998.

No. 110 **Landenberger, H.**
CoTReM, ein Multi-Komponenten Transport- und Reaktions-Modell. 142 pages, Bremen, 1998.

No. 111 **Villinger, H. und Fahrtteilnehmer**
Fahrtbericht SO 124, 4.10. - 16.10.199. 90 pages, Bremen, 1997.

No. 112 **Gietl, R.**
Biostratigraphie und Sedimentationsmuster einer nordostägyptischen Karbonatrampe unter Berücksichtigung der Alveolinen-Faunen. 142 pages, Bremen, 1998.

No. 113 **Ziebis, W.**
The Impact of the Thalassinidean Shrimp Callianassa truncata on the Geochemistry of permeable, coastal Sediments. 158 pages, Bremen 1998.

No. 114 **Schulz, H.D. and cruise participants**
Report and preliminary results of METEOR-Cruise M 41/1, Málaga - Libreville, 13.2.-15.3.1998. Bremen, 1998.

No. 115 **Völker, D.J.**
Untersuchungen an strömungsbeeinflußten Sedimentationsmustern im Südozean. Interpretation sedimentechographischer Daten und numerische Modellierung. 152 pages, Bremen, 1998.

No. 116 **Schlünz, B.**
Riverine Organic Carbon Input into the Ocean in Relation to Late Quaternary Climate Change. 136 pages, Bremen, 1998.

No. 117 **Kuhnert, H.**
Aufzeichnug des Klimas vor Westaustralien in stabilen Isotopen in Korallenskeletten. 109 pages, Bremen, 1998.

No. 118 **Kirst, G.**
Rekonstruktion von Oberflächenwassertemperaturen im östlichen Südatlantik anhand von Alkenonen. 130 pages, Bremen, 1998.

No. 119 **Dürkoop, A.**
Der Brasil-Strom im Spätquartär: Rekonstruktion der oberflächennahen Hydrographie während der letzten 400 000 Jahre. 121 pages, Bremen, 1998.

No. 120 **Lamy, F.**
Spätquartäre Variationen des terrigenen Sedimenteintrags entlang des chilenischen Kontinentalhangs als Abbild von Klimavariabilität im Milanković- und Sub-Milanković-Zeitbereich. 141 pages, Bremen, 1998.

No. 121 **Neuer, S. and cruise participants**
Report and preliminary results of POSEIDON-Cruise Pos 237/2, Vigo – Las Palmas, 18.3.-31.3.1998. 39 pages, Bremen, 1998

No. 122 **Romero, O.E.**
Marine planktonic diatoms from the tropical and equatorial Atlantic: temporal flux patterns and the sediment record. 205 pages, Bremen, 1998.

No. 123 **Spiess, V. und Fahrtteilnehmer**
Report and preliminary results of RV SONNE Cruise 125, Cochin – Chittagong, 17.10.-17.11.1997. 128 pages, Bremen, 1998.

No. 124 **Arz, H.W.**
Dokumentation von kurzfristigen Klimaschwankungen des Spätquartärs in Sedimenten des westlichen äquatorialen Atlantiks. 96 pages, Bremen, 1998.

No. 125 **Wolff, T.**
Mixed layer characteristics in the equatorial Atlantic during the late Quaternary as deduced from planktonic foraminifera. 132 pages, Bremen, 1998.

No. 126 **Dittert, N.**
Late Quaternary Planktic Foraminifera Assemblages in the South Atlantic Ocean: Quantitative Determination and Preservational Aspects. 165 pages, Bremen, 1998.

No. 127 **Höll, C.**
Kalkige und organisch-wandige Dinoflagellaten-Zysten in Spätquartären Sedimenten des tropischen Atlantiks und ihre palökologische Auswertbarkeit. 121 pages, Bremen, 1998.

No. 128 **Hencke, J.**
Redoxreaktionen im Grundwasser: Etablierung und Verlagerung von Reaktionsfronten und ihre Bedeutung für die Spurenelement-Mobilität. 122 pages, Bremen 1998.

No. 129 **Pätzold, J. and cruise participants**
Report and preliminary results of METEOR-Cruise M 41/3, Vítoria, Brasil – Salvador de Bahia, Brasil, 18.4. - 15.5.1998. Bremen, 1999.

No. 130 **Fischer, G. and cruise participants**
Report and preliminary results of METEOR-Cruise M 41/4, Salvador de Bahia, Brasil – Las Palmas, Spain, 18.5. – 13.6.1998. Bremen, 1999.

No. 131 **Schlünz, B. und G. Wefer**
Bericht über den 7. JGOFS-Workshop am 3. und 4.12.1998 in Bremen. Im Anhang: Publikationen zum deutschen Beitrag zur Joint Global Ocean Flux Study (JGOFS), Stand 1/ 1999. 100 pages, Bremen, 1999.

No. 132 **Wefer, G. and cruise participants**
Report and preliminary results of METEOR-Cruise M 42/4, Las Palmas - Las Palmas - Viena do Castelo; 26.09.1998 - 26.10.1998. 104 pages, Bremen, 1999.

No. 133 **Felis, T.**
Climate and ocean variability reconstructed from stable isotope records of modern subtropical corals (Northern Red Sea). 111 pages, Bremen, 1999.

No. 134 **Draschba , S.**
North Atlantic climate variability recorded in reef corals from Bermuda. 108 pages, Bremen, 1999.

No. 135 **Schmieder, F.**
Magnetic Cyclostratigraphy of South Atlantic Sediments. 82 pages, Bremen, 1999.

No. 136 **Rieß, W.**
In situ measurements of respiration and mineralisation processes – Interaction between fauna and geochemical fluxes at active interfaces. 68 pages, Bremen, 1999.

No. 137 **Devey, C.W. and cruise participants**
Report and shipboard results from METEOR-cruise M 41/2, Libreville – Vitoria, 18.3. – 15.4.98. 59 pages, Bremen, 1999.

No. 138 **Wenzhöfer, F.**
Biogeochemical processes at the sediment water interface and quantification of metabolically driven calcite dissolution in deep sea sediments. 103 pages, Bremen, 1999.

No. 139 **Klump, J.**
Biogenic barite as a proxy of paleoproductivity variations in the Southern Peru-Chile Current. 107 pages, Bremen, 1999.

No. 140 **Huber, R.**
Carbonate sedimentation in the northern Northatlantic since the late pliocene. 103 pages, Bremen, 1999.

No. 141 **Schulz, H.**
Nitrate-storing sulfur bacteria in sediments of coastal upwelling. 94 pages, Bremen, 1999.

No. 142 **Mai, S.**
Die Sedimentverteilung im Wattenmeer: ein Simulationsmodell. 114 pages, Bremen, 1999.

No. 143 **Neuer, S. and cruise participants**
Report and preliminary results of Poseidon Cruise 248, Las Palmas - Las Palmas, 15.2.-26.2.1999. 45 pages, Bremen, 1999.

No. 144 **Weber, A.**
Schwefelkreislauf in marinen Sedimenten und Messung von in situ Sulfatreduktionsraten. 122 pages, Bremen, 1999.

No. 145 **Hadeler, A.**
Sorptionsreaktionen im Grundwasser: Unterschiedliche Aspekte bei der Modellierung des Transportverhaltens von Zink. 122 pages, 1999.

No. 146 **Dierßen, H.**
Zum Kreislauf ausgewählter Spurenmetalle im Südatlantik: Vertikaltransport und Wechselwirkung zwischen Partikeln und Lösung. 167 pages, Bremen, 1999.

No. 147 **Zühlsdorff, L.**
High resolution multi-frequency seismic surveys at the Eastern Juan de Fuca Ridge Flank and the Cascadia Margin – Evidence for thermally and tectonically driven fluid upflow in marine sediments. 118 pages, Bremen 1999.

No. 148 **Kinkel, H.**
Living and late Quaternary Coccolithophores in the equatorial Atlantic Ocean: response of distribution and productivity patterns to changing surface water circulation. 183 pages, Bremen, 2000.

No. 149 **Pätzold, J. and cruise participants**
Report and preliminary results of METEOR Cruise M 44/3, Aqaba (Jordan) - Safaga (Egypt) – Dubá (Saudi Arabia) – Suez (Egypt) - Haifa (Israel), 12.3.-26.3.-2.4.-4.4.1999. 135 pages, Bremen, 2000.

No. 150 **Schlünz, B. and G. Wefer**
Bericht über den 8. JGOFS-Workshop am 2. und 3.12.1999 in Bremen. Im Anhang: Publikationen zum deutschen Beitrag zur Joint Global Ocean Flux Study (JGOFS), Stand 1/ 2000. 95 pages, Bremen, 2000.

No. 151 **Schnack, K.**
Biostratigraphie und fazielle Entwicklung in der Oberkreide und im Alttertiär im Bereich der Kharga Schwelle, Westliche Wüste, SW-Ägypten. 142 pages, Bremen, 2000.

No. 152 **Karwath, B.**
Ecological studies on living and fossil calcareous dinoflagellates of the equatorial and tropical Atlantic Ocean. 175 pages, Bremen, 2000.

No. 153 **Moustafa, Y.**
Paleoclimatic reconstructions of the Northern Red Sea during the Holocene inferred from stable isotope records of modern and fossil corals and molluscs. 102 pages, Bremen, 2000.

No. 154 **Villinger, H. and cruise participants**
Report and preliminary results of SONNE-cruise 145-1 Balboa – Talcahuana, 21.12.1999 – 28.01.2000. 147 pages, Bremen, 2000.

No. 155 **Rusch, A.**
Dynamik der Feinfraktion im Oberflächenhorizont permeabler Schelfsedimente. 102 pages, Bremen, 2000.

No. 156 **Moos, C.**
Reconstruction of upwelling intensity and paleo-nutrient gradients in the northwest Arabian Sea derived from stable carbon and oxygen isotopes of planktic foraminifera. 103 pages, Bremen, 2000.

No. 157 **Xu, W.**
Mass physical sediment properties and trends in a Wadden Sea tidal basin. 127 pages, Bremen, 2000.

No. 158 **Meinecke, G. and cruise participants**
Report and preliminary results of METEOR Cruise M 45/1, Malaga (Spain) - Lissabon (Portugal), 19.05. - 08.06.1999. 39 pages, Bremen, 2000.

No. 159 **Vink, A.**
Reconstruction of recent and late Quaternary surface water masses of the western subtropical Atlantic Ocean based on calcareous and organic-walled dinoflagellate cysts. 160 pages, Bremen, 2000.

No. 160 **Willems, H. (Sprecher), U. Bleil, R. Henrich, K. Herterich, B.B. Jørgensen, H.-J. Kuß, M. Olesch, H.D. Schulz,V. Spieß, G. Wefer**
Abschlußbericht des Graduierten-Kollegs Stoff-Flüsse in marine Geosystemen. Zusammenfassung und Berichtszeitraum Januar 1996 - Dezember 2000. 340 pages, Bremen, 2000.

No. 161 **Sprengel, C.**
Untersuchungen zur Sedimentation und Ökologie von Coccolithophoriden im Bereich der Kanarischen Inseln: Saisonale Flussmuster und Karbonatexport. 165 pages, Bremen, 2000.

No. 162 **Donner, B. and G. Wefer**
Bericht über den JGOFS-Workshop am 18.-21.9.2000 in Bremen: Biogeochemical Cycles: German Contributions to the International Joint Global Ocean Flux Study. 87 pages, Bremen, 2000.

No. 163 **Neuer, S. and cruise participants**
Report and preliminary results of Meteor Cruise M 45/5, Bremen – Las Palmas, October 1 – November 3, 1999. 93 pages, Bremen, 2000.

No. 164 **Devey, C. and cruise participants**
Report and preliminary results of Sonne Cruise SO 145/2, Talcahuano (Chile) - Arica (Chile), February 4 – February 29, 2000. 63 pages, Bremen, 2000.

No. 165 **Freudenthal, T.**
Reconstruction of productivity gradients in the Canary Islands region off Morocco by means of sinking particles and sediments. 147 pages, Bremen, 2000.

No. 166 **Adler, M.**
Modeling of one-dimensional transport in porous media with respect to simultaneous geochemical reactions in CoTReM. 147 pages, Bremen, 2000.

No. 167 **Santamarina Cuneo, P.**
Fluxes of suspended particulate matter through a tidal inlet of the East Frisian Wadden Sea (southern North Sea). 91 pages, Bremen, 2000.

No. 168 **Benthien, A.**
Effects of CO2 and nutrient concentration on the stable carbon isotope composition of C37:2 alkenones in sediments of the South Atlantic Ocean. 104 pages, Bremen, 2001.

No. 169 **Lavik, G.**
Nitrogen isotopes of sinking matter and sediments in the South Atlantic. 140 pages, Bremen, 2001.

No. 170 **Budziak, D.**
Late Quaternary monsoonal climate and related variations in paleoproductivity and alkenone-derived sea-surface temperatures in the western Arabian Sea. 114 pages, Bremen, 2001.

No. 171 **Gerhardt, S.**
Late Quaternary water mass variability derived from the pteropod preservation state in sediments of the western South Atlantic Ocean and the Caribbean Sea. 109 pages, Bremen, 2001.

No. 172 **Bleil, U. and cruise participants**
Report and preliminary results of Meteor Cruise M 46/3, Montevideo (Uruguay) – Mar del Plata (Argentina), January 4 – February 7, 2000. Bremen, 2001.

No. 173 **Wefer, G. and cruise participants**
Report and preliminary results of Meteor Cruise M 46/4, Mar del Plata (Argentina) – Salvador da Bahia (Brazil), February 10 – March 13, 2000. With partial results of METEOR cruise M 46/2. 136 pages, Bremen, 2001.

No. 174 **Schulz, H.D. and cruise participants**
Report and preliminary results of Meteor Cruise M 46/2, Recife (Brazil) – Montevideo (Uruguay), December 2 – December 29, 1999. 107 pages, Bremen, 2001.

No. 175 **Schmidt, A.**
Magnetic mineral fluxes in the Quaternary South Atlantic: Implications for the paleoenvironment. 97 pages, Bremen, 2001.

No. 176 **Bruhns, P.**
Crystal chemical characterization of heavy metal incorporation in brick burning processes. 93 pages, Bremen, 2001.

No. 177 **Karius, V.**
Baggergut der Hafengruppe Bremen-Stadt in der Ziegelherstellung. 131 pages, Bremen, 2001.

No. 178 **Adegbie, A. T.**
Reconstruction of paleoenvironmental conditions in Equatorial Atlantic and the Gulf of Guinea Basins for the last 245,000 years. 113 pages, Bremen, 2001.

No. 179 **Spieß, V. and cruise participants**
Report and preliminary results of R/V Sonne Cruise SO 149, Victoria - Victoria, 16.8. - 16.9.2000. 100 pages, Bremen, 2001.

No. 180 **Kim, J.-H.**
Reconstruction of past sea-surface temperatures in the eastern South Atlantic and the eastern South Pacific across Termination I based on the Alkenone Method. 114 pages, Bremen, 2001.

No. 181 **von Lom-Keil, H.**
Sedimentary waves on the Namibian continental margin and in the Argentine Basin – Bottom flow reconstructions based on high resolution echosounder data. 126 pages, Bremen, 2001.

No. 182 **Hebbeln, D. and cruise participants**
PUCK: Report and preliminary results of R/V Sonne Cruise SO 156, Valparaiso (Chile) - Talcahuano (Chile), March 29 - May 14, 2001. 195 pages, Bremen, 2001.

No. 183 **Wendler, J.**
Reconstruction of astronomically-forced cyclic and abrupt paleoecological changes in the Upper Cretaceous Boreal Realm based on calcareous dinoflagellate cysts. 149 pages, Bremen, 2001.

No. 184 **Volbers, A.**
Planktic foraminifera as paleoceanographic indicators: production, preservation, and reconstruction of upwelling intensity. Implications from late Quaternary South Atlantic sediments. 122 pages, Bremen, 2001.

No. 185 **Bleil, U. and cruise participants**
Report and preliminary results of R/V METEOR Cruise M 49/3, Montevideo (Uruguay) - Salvador (Brasil), March 9 - April 1, 2001. 99 pages, Bremen, 2001.

No. 186 **Scheibner, C.**
Architecture of a carbonate platform-to-basin transition on a structural high (Campanian-early Eocene, Eastern Desert, Egypt) – classical and modelling approaches combined. 173 pages, Bremen, 2001.

No. 187 **Schneider, S.**
Quartäre Schwankungen in Strömungsintensität und Produktivität als Abbild der Wassermassen-Variabilität im äquatorialen Atlantik (ODP Sites 959 und 663): Ergebnisse aus Siltkorn-Analysen. 134 pages, Bremen, 2001.

No. 188 **Uliana, E.**
Late Quaternary biogenic opal sedimentation in diatom assemblages in Kongo Fan sediments. 96 pages, Bremen, 2002.

No. 189 **Esper, O.**
Reconstruction of Recent and Late Quaternary oceanographic conditions in the eastern South Atlantic Ocean based on calcareous- and organic-walled dinoflagellate cysts. 130 pages, Bremen, 2001.

No. 190 **Wendler, I.**
Production and preservation of calcareous dinoflagellate cysts in the modern Arabian Sea. 117 pages, Bremen, 2002.

No. 191 **Bauer, J.**
Late Cenomanian – Santonian carbonate platform evolution of Sinai (Egypt): stratigraphy, facies, and sequence architecture. 178 pages, Bremen, 2002.

No. 192 **Hildebrand-Habel, T.**
Die Entwicklung kalkiger Dinoflagellaten im Südatlantik seit der höheren Oberkreide. 152 pages, Bremen, 2002.

No. 193 **Hecht, H.**
Sauerstoff-Optopoden zur Quantifizierung von Pyritverwitterungsprozessen im Labor- und Langzeit-in-situ-Einsatz. Entwicklung - Anwendung – Modellierung. 130 pages, Bremen, 2002.

No. 194 **Fischer, G. and cruise participants**
Report and Preliminary Results of RV METEOR-Cruise M49/4, Salvador da Bahia – Halifax, 4.4.-5.5.2001. 84 pages, Bremen, 2002.

No. 195 **Gröger, M.**
Deep-water circulation in the western equatorial Atlantic: inferences from carbonate preservation studies and silt grain-size analysis. 95 pages, Bremen, 2002.

No. 196 **Meinecke,G. and cruise participants**
Report of RV POSEIDON Cruise POS 271, Las Palmas - Las Palmas, 19.3.-29.3.2001. 19 pages, Bremen, 2002.

No. 197 **Meggers, H. and cruise participants**
Report of RV POSEIDON Cruise POS 272, Las Palmas - Las Palmas, 1.4.-14.4.2001. 19 pages, Bremen, 2002. (out of print)

No. 198 **Gräfe, K.-U.**
Stratigraphische Korrelation und Steuerungsfaktoren Sedimentärer Zyklen in ausgewählten Borealen und Tethyalen Becken des Cenoman/Turon (Oberkreide) Europas und Nordwestafrikas. 197 pages, Bremen, 2002.

No. 199 **Jahn, B.**
Mid to Late Pleistocene Variations of Marine Productivity in and Terrigenous Input to the Southeast Atlantic. 97 pages, Bremen, 2002.

No. 200 **Al-Rousan, S.**
Ocean and climate history recorded in stable isotopes of coral and foraminifers from the northern Gulf of Aqaba. 116 pages, Bremen, 2002.

No. 201 **Azouzi, B.**
Regionalisierung hydraulischer und hydrogeochemischer Daten mit geostatistischen Methoden. 108 pages, Bremen, 2002.

No. 202 **Spieß, V. and cruise participants**
Report and preliminary results of METEOR Cruise M 47/3, Libreville (Gabun) - Walvis Bay (Namibia), 01.06 - 03.07.2000. 70 pages, Bremen 2002.

No. 203 **Spieß, V. and cruise participants**
Report and preliminary results of METEOR Cruise M 49/2, Montevideo (Uruguay) - Montevideo, 13.02 - 07.03.2001. 84 pages, Bremen 2002.

No. 204 **Mollenhauer, G.**
Organic carbon accumulation in the South Atlantic Ocean: Sedimentary processes and glacial/interglacial Budgets. 139 pages, Bremen 2002.

No. 205 **Spieß, V. and cruise participants**
Report and preliminary results of METEOR Cruise M49/1, Cape Town (South Africa) - Montevideo (Uruguay), 04.01.2001 - 10.02.2001. 57 pages, Bremen, 2003.

No. 206 **Meier, K.J.S.**
Calcareous dinoflagellates from the Mediterranean Sea: taxonomy, ecology and palaeoenvironmental application. 126 pages, Bremen, 2003.

No. 207 **Rakic, S.**
Untersuchungen zur Polymorphie und Kristallchemie von Silikaten der Zusammensetzung Me2Si2O5 (Me:Na, K). 139 pages, Bremen, 2003.

No. 208 **Pfeifer, K.**
Auswirkungen frühdiagenetischer Prozesse auf Calcit- und Barytgehalte in marinen Oberflächen-sedimenten. 110 pages, Bremen, 2003.

No. 209 **Heuer, V.**
Spurenelemente in Sedimenten des Südatlantik. Primärer Eintrag und frühdiagenetische Überprägung. 136 pages, Bremen, 2003.

No. 210 **Streng, M.**
Phylogenetic Aspects and Taxonomy of Calcareous Dinoflagellates. 157 pages, Bremen 2003.

No. 211 **Boeckel, B.**
Present and past coccolith assemblages in the South Atlantic: implications for species ecology, carbonate contribution and palaeoceanographic applicability. 157 pages, Bremen, 2003.

No. 212 **Precht, E.**
Advective interfacial exchange in permeable sediments driven by surface gravity waves and its ecological consequences. 131 pages, Bremen, 2003.

No. 213 **Frenz, M.**
Grain-size composition of Quaternary South Atlantic sediments and its paleoceanographic significance. 123 pages, Bremen, 2003.

No. 214 **Meggers, H. and cruise participants**
Report and preliminary results of METEOR Cruise M 53/1, Limassol - Las Palmas – Mindelo, 30.03.2002 - 03.05.2002. 81 pages, Bremen, 2003.

No. 215 **Schulz, H.D. and cruise participants**
Report and preliminary results of METEOR Cruise M 58/1, Dakar – Las Palmas, 15.04..2003 – 12.05.2003. Bremen, 2003.

No. 216 **Schneider, R. and cruise participants**
Report and preliminary results of METEOR Cruise M 57/1, Cape Town – Walvis Bay, 20.01. – 08.02.2003. 123 pages, Bremen, 2003.

No. 217 **Kallmeyer, J.**
Sulfate reduction in the deep Biosphere. 157 pages, Bremen, 2003.

No. 218 **Røy, H.**
Dynamic Structure and Function of the Diffusive Boundary Layer at the Seafloor. 149 pages, Bremen, 2003.

No. 219 **Pätzold, J., C. Hübscher and cruise participants**
Report and preliminary results of METEOR Cruise M 52/2&3, Istanbul – Limassol – Limassol, 04.02. – 27.03.2002. Bremen, 2003.

No. 220 **Zabel, M. and cruise participants**
Report and preliminary results of METEOR Cruise M 57/2, Walvis Bay – Walvis Bay, 11.02. – 12.03.2003. 136 pages, Bremen 2003.

No. 221 **Salem, M.**
Geophysical investigations of submarine prolongations of alluvial fans on the western side of the Gulf of Aqaba-Red Sea. 100 pages, Bremen, 2003.

No. 222 **Tilch, E.**
Oszillation von Wattflächen und deren fossiles Erhaltungspotential (Spiekerooger Rückseitenwatt, südliche Nordsee). 137 pages, Bremen, 2003.

No. 223 **Frisch, U. and F. Kockel**
Der Bremen-Knoten im Strukturnetz Nordwest-Deutschlands. Stratigraphie, Paläogeographie, Strukturgeologie. 379 pages, Bremen, 2004.

No. 224 **Kolonic, S.**
Mechanisms and biogeochemical implications of Cenomanian/Turonian black shale formation in North Africa: An integrated geochemical, millennial-scale study from the Tarfaya-LaAyoune Basin in SW Morocco. 174 pages, Bremen, 2004. Report online available only.

No. 225 **Panteleit, B.**
Geochemische Prozesse in der Salz- Süßwasser Übergangszone. 106 pages, Bremen, 2004.

No. 226 **Seiter, K.**
Regionalisierung und Quantifizierung benthischer Mineralisationsprozesse. 135 pages, Bremen, 2004.

No. 227 **Bleil, U. and cruise participants**
Report and preliminary results of METEOR Cruise M 58/2, Las Palmas – Las Palmas (Canary Islands, Spain), 15.05. – 08.06.2003. 123 pages, Bremen, 2004.

No. 228 **Kopf, A. and cruise participants**
Report and preliminary results of SONNE Cruise SO175, Miami - Bremerhaven, 12.11 - 30.12.2003. 218 pages, Bremen, 2004.

No. 229 **Fabian, M.**
Near Surface Tilt and Pore Pressure Changes Induced by Pumping in Multi-Layered Poroelastic Half-Spaces. 121 pages, Bremen, 2004.

No. 230 **Segl, M. , and cruise participants**
Report and preliminary results of POSEIDON cruise 304 Galway – Lisbon, 5. – 22. Oct. 2004.
27 pages, Bremen 2004

No. 231 **Meinecke, G. and cruise participants**
Report and preliminary results of POSEIDON Cruise 296, Las Palmas – Las Palmas, 04.04 – 14.04.2003. 42 pages, Bremen 2005.

No. 232 **Meinecke, G. and cruise participants**
Report and preliminary results of POSEIDON Cruise 310, Las Palmas – Las Palmas, 12.04 – 26.04.2004. 49 pages, Bremen 2005.

No. 233 **Meinecke, G. and cruise participants**
Report and preliminary results of METEOR Cruise 58/3, Las Palmas - Ponta Delgada, 11.06 - 24.06.2003. 50 pages, Bremen 2005.

No. 234 **Feseker, T.**
Numerical Studies on Groundwater Flow in Coastal Aquifers. 219 pages. Bremen 2004.

No. 235 **Sahling, H. and cruise participants**
Report and preliminary results of R/V POSEIDON Cruise P317/4, Istanbul-Istanbul ,
16 October - 4 November
2004. 92 pages, Bremen 2004.

No. 236 **Meinecke, G. und Fahrtteilnehmer**
Report and preliminary results of POSEIDON Cruise 305, Las Palmas (Spain) - Lisbon (Portugal), October 28th – November 6th, 2004. 43 pages, Bremen 2005.

No. 237 **Ruhland, G. and cruise participants**
Report and preliminary results of POSEIDON Cruise 319, Las Palmas (Spain) - Las Palmas (Spain), December 6th – December 17th, 2004. 50 pages, Bremen 2005.

No. 238 **Chang, T.S.**
Dynamics of fine-grained sediments and stratigraphic evolution of a back-barrier tidal basin of the German Wadden Sea (southern North Sea). 102 pages, Bremen 2005.

No. 239 **Lager, T.**
Predicting the source strength of recycling materials within the scope of a seepage water prognosis by means of standardized laboratory methods. 141 pages, Bremen 2005.

No. 240 **Meinecke, G.**
DOLAN - Operationelle Datenübertragung im Ozean und Laterales Akustisches Netzwerk in der Tiefsee. Abschlußbericht. 42 pages, Bremen 2005.

No. 241 **Guasti, E.**
Early Paleogene environmental turnover in the southern Tethys as recorded by foraminiferal and organic-walled dinoflagellate cysts assemblages. 203 pages, Bremen 2005.

No. 242 **Riedinger, N.**
Preservation and diagenetic overprint of geochemical and geophysical signals in ocean margin sediments related to depositional dynamics. 91 pages, Bremen 2005.

No. 243 **Ruhland, G. and cruise participants**
Report and preliminary results of POSEIDON cruise 320, Las Palmas (Spain) - Las Palmas (Spain), March 08th - March 18th, 2005. 57 pages, Bremen 2005.

No. 244 **Inthorn, M.**
Lateral particle transport in nepheloid layers – a key factor for organic matter distribution and quality in the Benguela high-productivity area. 127 pages, Bremen, 2006.

No. 245 **Aspetsberger, F.**
Benthic carbon turnover in continental slope and deep sea sediments: importance of organic matter quality at different time scales. 136 pages, Bremen, 2006.

No. 246 **Hebbeln, D. and cruise participants**
Report and preliminary results of RV SONNE Cruise SO-184, PABESIA, Durban (South Africa) – Cilacap (Indonesia) – Darwin (Australia), July 08th - September 13th, 2005. 142 pages, Bremen 2006.

No. 247 **Ratmeyer, V. and cruise participants**
Report and preliminary results of RV METEOR Cruise M61/3. Development of Carbonate Mounds on the Celtic Continental Margin, Northeast Atlantic. Cork (Ireland) – Ponta Delgada (Portugal), 04.06. – 21.06.2004. 64 pages, Bremen 2006.

No. 248 **Wien, K.**
Element Stratigraphy and Age Models for Pelagites and Gravity Mass Flow Deposits based on Shipboard XRF Analysis. 100 pages, Bremen 2006.

No. 249 **Krastel, S. and cruise participants**
Report and preliminary results of RV METEOR Cruise M65/2, Dakar - Las Palmas, 04.07. – 26.07.2005. 185 pages, Bremen 2006.

No. 250 **Heil, G.M.N.**
Abrupt Climate Shifts in the Western Tropical to Subtropical Atlantic Region during the Last Glacial. 121 pages, Bremen 2006.

No. 251 **Ruhland, G. and cruise participants**
Report and preliminary results of POSEIDON Cruise 330, Las Palmas – Las Palmas, November 21th – December 03rd, 2005. 48 pages, Bremen 2006.

No. 252 **Mulitza , S. and cruise participants**
Report and preliminary results of METEOR Cruise M65/1, Dakar – Dakar, 11.06.- 1.07.2005. 149 pages, Bremen 2006.

No. 253 **Kopf, A. and cruise participants**
Report and preliminary results of POSEIDON Cruise P336, Heraklion - Heraklion, 28.04. – 17.05.2006. 127 pages, Bremen, 2006.

No. 254 **Wefer, G. and cruise participants**
Report and preliminary results of R/V METEOR Cruise M65/3, Las Palmas - Las Palmas (Spain), July 31st - August 10th, 2005. 24 pages, Bremen 2006.

No. 255 **Hanebuth, T.J.J. and cruise participants**
Report and first results of the POSEIDON Cruise P342 GALIOMAR, Vigo – Lisboa (Portugal), August 19th – September 06th, 2006. Distribution Pattern, Residence Times and Export of Sediments on the Pleistocene/Holocene Galician Shelf (NW Iberian Peninsula). 203 pages, Bremen, 2007.

No. 256 **Ahke, A.**
Composition of molecular organic matter pools, pigments and proteins, in Benguela upwelling and Arctic Sediments. 192 pages, Bremen 2007.

No. 257 **Becker, V.**
Seeper - Ein Modell für die Praxis der Sickerwasserprognose. 170 pages, Bremen 2007.

No. 258 **Ruhland, G. and cruise participants**
Report and preliminary results of Poseidon cruise 333, Las Palmas (Spain) – Las Palmas (Spain), March 1st – March 10th, 2006. 32 pages, Bremen 2007.

No. 259 **Fischer, G., G. Ruhland and cruise participants**
Report and preliminary results of Poseidon cruise 344, leg 1 and leg 2, Las Palmas (Spain) – Las Palmas (Spain),
Oct. 20th –Nov 2nd & Nov. 4th – Nov 13th, 2006. 46 pages, Bremen 2007.

No. 260 **Westphal, H. and cruise participants**
Report and preliminary results of Poseidon cruise 346, MACUMA. Las Palmas (Spain) – Las Palmas (Spain), 28.12.2006 – 15.1.2007. 49 pages, Bremen 2007.

No. 261 **Bohrmann, G., T. Pape, and cruise participants**
Report and preliminary results of R/V METEOR Cruise M72/3, Istanbul – Trabzon – Istanbul, March 17th – April 23rd, 2007. Marine gas hydrates of the Eastern Black Sea. 130 pages, Bremen 2007.

No. 262 **Bohrmann, G., and cruise participants**
Report and preliminary results of R/V METEOR Cruise M70/3, Iraklion – Iraklion, 21 November – 8 December 2006. Cold Seeps of the Anaximander Mountains / Eastern Mediterranean. 75 pages, Bremen 2008.

No. 263 **Bohrmann, G., Spiess, V., and cruise participants**
Report and preliminary results of R/V Meteor Cruise M67/2a and 2b, Balboa -- Tampico -- Bridgetown, 15 March -- 24 April, 2006. Fluid seepage in the Gulf of Mexico. Bremen 2008.

No. 264 **Kopf, A., and cruise participants**
Report and preliminary results of Meteor Cruise M73/1: LIMA-LAMO (Ligurian Margin Landslide Measurements & Observatory), Cadiz, 22.07.2007 – Genoa, 11.08.2007. 170 pages, Bremen 2008.

No. 265 **Hebbeln, D., and cruise participants**
Report and preliminary results of RV Pelagia Cruise 64PE284. Cold-water Corals in the Gulf of Cádiz and on Coral Patch Seamount (NE Atlantic). Portimão - Portimão, 18.02. - 09.03.2008. 90 pages, Bremen 2008.

No. 266 **Bohrmann, G. and cruise participants**
Report and preliminary results of R/V Meteor Cruise M74/3, Fujairah – Male, 30 October - 28 November, 2007. Cold Seeps of the Makran subduction zone (Continental margin of Pakistan). 161 pages, Bremen 2008.

No. 267 **Sachs, O.**
Benthic organic carbon fluxes in the Southern Ocean: Regional differences and links to surface primary production and carbon export. 143 pages, Bremen, 2008.

No. 268 **Zonneveld, K. and cruise participants**
Report and preliminary results of R/V POSEIDON Cruise P339, Piräus - Messina, 16 June - 2 July 2006. CAPPUCCINO - Calabrian and Adriatic palaeoproductivity and climatic variability in the last two millenia. 61 pages, Bremen, 2008.

No. 269 **Ruhland, G. and cruise participants**
Report and preliminary results of R/V POSEIDON Cruise P360, Las Palmas (Spain) - Las Palmas (Spain), Oct. 29th - Nov. 6th, 2007. 27 pages, Bremen, 2008.

No. 270 **Ruhland, G., G. Fischer and cruise participants**
Report and preliminary results of R/V POSEIDON Cruise 365 (Leg 1+2). Leg 1: Las Palmas - Las Palmas, 13.4. - 16.4.2008. Leg 2: Las Palmas - Las Palmas, 18.4. - 29.4.2008. 40 pages, Bremen, 2009.

No. 271 **Kopf, A. and cruise participants**
Report and preliminary results of R/V POSEIDON Cruise P386: NAIL (Nice Airport Landslide), La Seyne sur Mer, 20.06.2009 – La Seyne sur Mer, 06.07.2009. 161 pages, Bremen, 2009.

No. 272 **Freudenthal, T., G. Fischer and cruise participants**
Report and preliminary results of Maria S. Merian Cruise MSM04/4 a & b, Las Palmas (Spain) – Las Palmas (Spain), Feb 27th – Mar 16th & Mar 19th – Apr 1st, 2007. 117 pages, Bremen 2009.

No. 273 **Hebbeln, D., C. Wienberg, L. Beuck, A. Freiwald, P. Wintersteller and cruise participants**
Report and preliminary results of R/V POSEIDON Cruise POS 385 "Cold-Water Corals of the Alboran Sea (western Mediterranean Sea)", Faro - Toulon, May 29 - June 16, 2009. 79 pages, Bremen 2009.

No. 274 **Zonneveld, K. and cruise participants**
Report and preliminary results of R/V Poseidon Cruises P 366-1 and P 366-2, Las Palmas - Las Palmas - Vigo, 03 -19 May 2008 and 22 -30 May 2008. PERGAMOM Proxy Education and Research cruise off Galicai, Morocco and Mauretania. 47 pages, Bremen 2010.

No. 275 **Wienberg, C. and cruise participants**
Report and preliminary results of RV POSEIDON cruise POS400 "CORICON - Cold-water corals along the Irish continental margin", Vigo - Cork, June 29 - July 15 2010. 46 pages, Bremen 2010.

No. 276 **Villinger, H. and cruise participants**
Report and preliminary results of R/V Sonne Cruise SO 207, Caldera-Caldera, 21 June -13 July, 2010. SeamountFlux: Efficient cooling in young oceanic crust caused by circulation of seawater through seamounts (Guatemala Basin, East Pacific Ocean). 161 pages, Bremen 2010.

No. 277 **Fischer, G. and cruise participants**
Report and preliminary results of RV POSEIDON Cruise POS 396, Las Palmas - Las Palmas (Spain), 24 February - 8 March 2010. 22 pages, Bremen 2011.

No. 278 **Bohrmann, G. and cruise participants**
Report and preliminary results of RV MARIA S. MERIAN Cruise MSM 15/2, Istanbul (Turkey) – Piraeus (Greece), 10 May - 2 June 2010. Origin and structure of methane, gas hydrates and fluid flows in the Black Sea. 130 pages, Bremen 2011.

No. 279 **Hebbeln, D. and cruise participants**
Report and preliminary results of RV SONNE Cruise SO-211, Valparaíso - Valparaíso, 2 November – 29 November 2010. ChiMeBo. Bremen 2011.

No. 280 **Bach, W. and cruise participants**
Report and preliminary results of RV SONNE Cruise SO 216, Townsville (Australia) - Makassar (Indonesia), June 14 – July 23, 2011. BAMBUS, Back-Arc Manus Basin Underwater Solfataras. 87 pages, Bremen 2011.

No. 281 **Bohrmann, G. and cruise participants**
Report and preliminary results of RV METEOR Cruise M84/2, Istanbul – Istanbul, 26 February – 02 April, 2011. Origin and Distribution of Methane and Methane Hydrates in the Black Sea. 164 pages, Bremen 2011.

No. 282 **Zonneveld, K. and cruise participants**
Report and preliminary results of R/V POSEIDON Cruise P398, Las Palmas – Lissabon, 1 – 16 April 2010. PAPOCA, Production and preservation of organic carbon in relationship to dust input and nepheloid layers in the upwelling area off NW Africa. 33 pages, Bremen 2011.

No. 283 **Hanebuth, T. J. J. and cruise participants**
Report and preliminary results of RV METEOR Cruise M84/4, GALIOMAR III, Vigo – Vigo, 1st – 28th May, 2011. 139 pages, Bremen 2012.

No. 284 **Kopf, A. and cruise participants**
Report and preliminary results of RV POSEIDON Cruise P410: MUDFLOW (Mud volcanism, Faulting and Fluid Flow on the Mediterranean Ridge Accretionary Complex), Heraklion / Greece, 12.03.2011 – Taranto / Italy, 01.04.2011. 128 pages, Bremen 2012.

No. 285 **Krastel, S., G. Wefer and cruise participants**
Report and preliminary results of RV METEOR Cruise M78/3. Sediment transport off Uruguay and Argentina: From the shelf to the deep sea. 19.05.2009 – 06.07.2009, Montevideo (Uruguay) – Montevideo (Uruguay). 79 pages, Bremen 2012.

No. 286 **Kopf, A. and cruise participants**
Report and preliminary results of RV POSEIDON Cruise P429. MEDFLUIDS: Slope Stability, Mud volcanism, Faulting and Fluid Flow in the Eastern Mediterranean Sea (Cretan Sea, Mediterranean Ridge) and Ligurian Margin (Nice slope), Heraklion / Greece, 22.03.2012 – La Seyne sur Mer / France, 06.04.2012. 80 pages, Bremen 2012.